This is to certify that the
dissertation entitled

BLIND SIGNAL DETECTION FOR DS-CDMA OVER
FREQUENCY-SELECTIVE FADING CHANNELS

presented by

Weiguo Liang

has been accepted towards fulfillment
of the requirements for the

Ph.D. degree in Electrical Engineering

Tongtong Li

Major Professor's Signature

12/9/2004

Date

BLIND SIGNAL DETECTION FOR DS-CDMA OVER FREQUENCY-SELECTIVE FADING CHANNELS

By

Weiguo Liang

A DISSERTATION

Submitted to
Michigan State University
in partial fulfillment of the requirements
for the degree of

DOCTOR OF PHILOSOPHY

Department of Electrical and Computer Engineering

2004

ABSTRACT

BLIND SIGNAL DETECTION FOR DS-CDMA OVER FREQUENCY-SELECTIVE FADING CHANNELS

By

Weiguo Liang

In conventional wireless communication systems, training sequences are transmitted periodically in order to track the time-varying channel environments. This is neither power efficient, nor spectrally efficient. As an effort to improve the spectral efficiency by reducing the overhead, this dissertation is focused on blind channel estimation and signal detection for direct sequence spread spectrum systems.

In literature, if the spreading sequences are periodic and repeat with every information symbol, the system is referred to as short-code CDMA, and if the spreading sequences are aperiodic or essentially pseudo-random, it is known as long-code CDMA. The time-varying nature of long-code CDMA significantly complicates the development of blind detectors, as needed statistics can no longer be obtained through time averaging of the observed data. For this reason, research on blind multiuser detection has largely been limited to short-code CDMA. On the other hand, long-code is widely used in virtually all operational and commercially proposed CDMA systems due to its inherent security features and performance stability in frequency fading environment.

In this dissertation, statistics based algorithms are developed for both short-code and long-code DS-CDMA systems, with emphasis on the long-code systems. The major contributions of the dissertation can be briefly summarized as: (i) Blind detectors based on the code-constrained super-exponential algorithm have been developed for multi-rate short-code CDMA systems, while only the spreading code of the desired user is assumed to be known. (ii) For long-code CDMA systems, consider-

ing the time variant nature of the spreading code, the chip-rate scrambled signal is taken as the system input, and the long-code CDMA is characterized using a time invariant model. (iii) In downlink long-code systems, after chip-level equalization, the descrambled signal is treated as the received signal of a short-code CDMA system, and super-exponential algorithm is applied to recover the information symbols. (iv) For uplink, two-stage approaches have been developed in this research. In the first stage, multi-step linear-prediction-based methods are developed to eliminate the inter-symbol interference. In the second stage, if the spreading codes are of nonconstant modulus, blind channel estimation is performed by exploiting the second-order statistics; if the spreading codes are of constant modulus, higher-order statistics based algorithms need to be applied to estimate the channels. (v) To further improve the transmission quality without increasing the transmission power or bandwidth, time-reversal space-time block coding (TR-STBC) scheme is applied at the base-station side in downlink CDMA, and blind signal detection algorithm based on the principal component analysis has been developed.

Throughout this research, computer simulations are carried out to illustrate the proposed approaches

Dedicated to my family

ACKNOWLEDGMENTS

I wish to express my gratitude to my advisor Professor Tongtong Li for her guidance, support and patience throughout the research work. It is Professor Li who gave me the key to the world of communications, taught me how to be a researcher, and made my studies in Michigan State University an unforgettable experience.

I would like to thank the members of my guidance committee: Professor John R. Deller, Professor Hayder Radha, Professor Ning Xi from the Department of Electrical and Computer Engineering, and Professor Chichia Chiu from the Department of Mathematics. Special thanks go to Professor Hayder Radha who gave me the chance to pursue my Doctorate Degree in Michigan State University.

Thanks also go to my lab-mates: Qi Ling and Huahui Wang. The discussions with them enriched my knowledge in the field of wireless communications.

I am grateful to all the teachers and friends who believe in my ability, and give me confidence during my life.

I wish to express my deepest thanks to my parents, who give me the support, teach me to be independent, and always let me make my own decision. They shape me into the person who I am today. I also thank my sister, who give me moral support throughout my study.

Finally, I especially thank my girlfriend Ying Yan, who has been sharing sweetness and bitterness with me in these years. It is her care, belief and love help me to overcome all the difficulties in my research work.

TABLE OF CONTENTS

LIST OF TABLES

LIST OF FIGURES

CHAPTER 1

Introduction

1.1 Evolution of Wireless Communications

The evolution of modern wireless communication networks is shown in Figure 1.1. The first generation (1G) cellular networks emerged in late 1970s and early 1980s, such as the U.S. Advanced Mobile Phone System (AMPS) and the European Total Access Cellular Systems (ETACS). They all used analog modulation, large cells and omnidirectional base station antennas. The number of users supported by these systems is very limited. To increase the system capacity and to improve call capabilities, second generation (2G) wireless systems were deployed in mid 1990s. 2G systems, such as the U.S. Digital Cellular Standard IS-136, IS-95 and the Pan-European Global System Mobile (GSM), use digital voice coding and digital modulation, and could provide at least a three-fold increase in the overall system capacity. While frequency modulation (FM) is used for radio transmission in AMPS standard, TDMA-based technologies are applied in most second generation standards.

Since 2G systems were designed before widespread utilization of the Internet, they mainly supported voice-centric services with very limited data services, like short messages, FAX, etc. In an effort to support modern Internet applications, new data-centric standards, known as 2.5G standards that can be overlaid upon existing 2G technologies were developed. With new base station add-ons and subscriber unit upgrades, these new standards (such as Enhanced Data Rate for GSM (EDGE), CDMAone) support higher data rate transmission for web browsing, e-mail traffic, mobile commerce (m-commerce) and location based mobile services. The third generation (3G) systems aim to support multi-megabit Internet access, and simultaneous

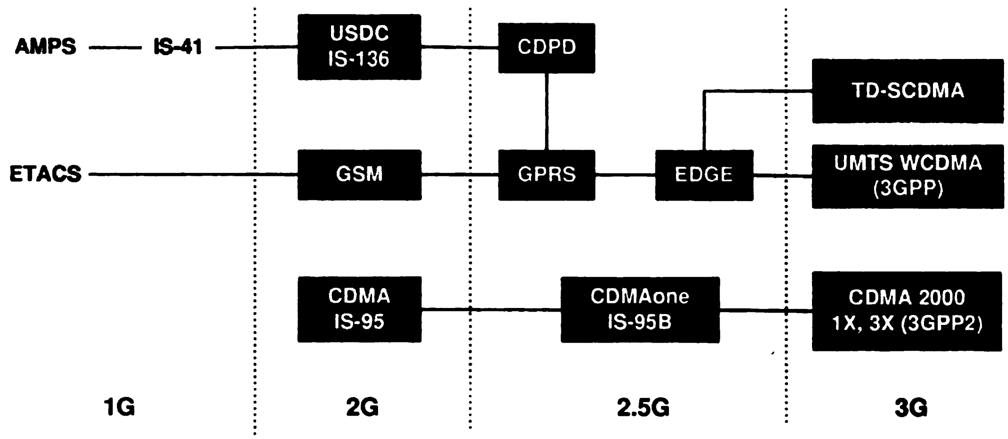

Figure 1.1. Evolution of modern wireless communication networks

voice and data access with multiple parties at the same time using a single mobile handset. 3G systems also allow seamless global roaming. Representative 3G standards include 3GPP (3rd generation partnership project) UMTS Wideband CDMA, 3GPP2 CDMA2000 3X, and 3G TD-SCDMA.

To support high-speed multimedia services, 3G networks use large bandwidths and rely on spread spectrum technologies. Code Division Multiple Access (CDMA) is the most popular spread spectrum technique applied in cellular systems. Compared with TDMA and FDMA, CDMA has a soft capacity limit. Besides, the inherent frequency diversity of CDMA can mitigate the effects of small scale fading, and make it robust to malicious narrow-band jamming.

1.2 CDMA Systems

Three basic multiple access schemes, FDMA, TDMA and CDMA, are illustrated in Figure 1.2. In TDMA and FDMA systems, the channels are separated in time domain and frequency domain respectively. In CDMA systems, the signals of different users can be transmitted simultaneously through the same frequency band. This is achieved by assigning each user a unique code sequence (known as spreading code or signature sequence), which is used to spread its information signal. The receiver recovers the symbols of the desired user by despreading the received signal with the its spreading

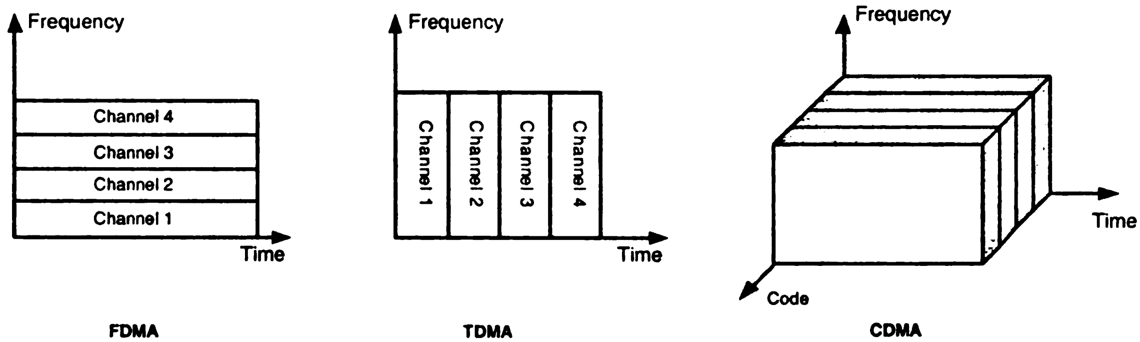

Figure 1.2. Basic multiple access schemes

code. To mitigate multiuser interference, spreading codes are generally orthogonal to each other, or have low cross-correlation. Because the bandwidth of the spread signal is chosen to be much larger than the original signal, the bandwidth of the signal is enlarged significantly by the spreading process.

In DS-CDMA (direct sequence CDMA), the data signal is directly multiplied by the spreading code. The principle of DS-CDMA is illustrated in Figure 1.3. The

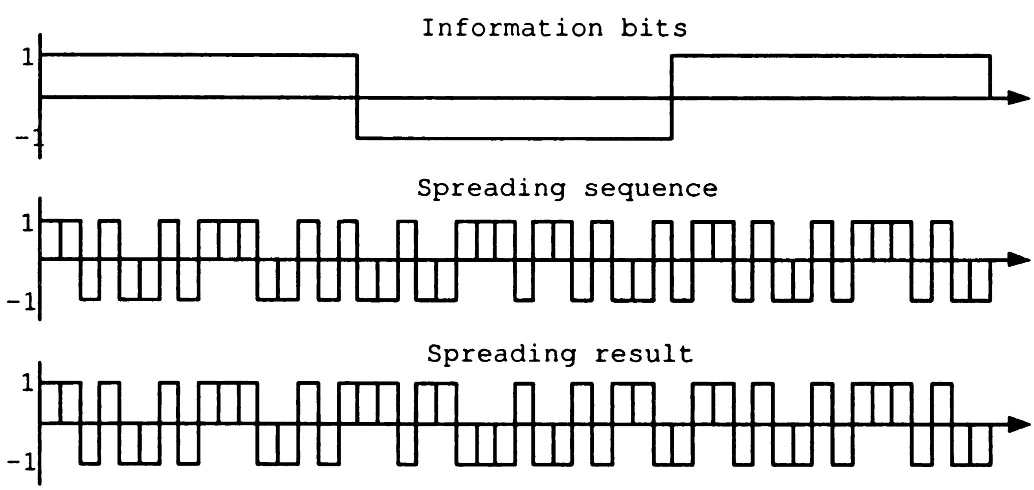

Figure 1.3. Principle of DS-CDMA

spreading code changes at chip rate, which is much higher than the symbol rate. The spreading gain (or processing gain) is equal to the ratio of chip rate to symbol rate.

In Figure 1.3, there are 16 chips per symbol period, that is the processing gain equals to 16.

Consider a DS-CDMA systems with M users. Let $u_i(n)$ denote the nth symbol of user i, and let the N-vector $\mathbf{c}_{i,n} = [c_{i,n}(0), c_{i,n}(1), \cdots, c_{i,n}(N-1)]$ denote the spreading sequence for symbol $u_i(n)$, where N is the spreading gain. The spreading result of $u_i(n)$ is simply given by

$$\mathbf{s}_i(n) = u_i(n)\mathbf{c}_{i,n}. \tag{1.1}$$

When the channels are ideal, and in the absence of noise, the received signal can be presented as

$$\mathbf{y}(n) = \sum_{i=1}^{M} \mathbf{s}_i(n) = \sum_{i=1}^{M} u_i(n)\mathbf{c}_{i,n}. \tag{1.2}$$

If the spreading sequences are chosen to be orthogonal, i.e. $\mathbf{c}_{i,n}\mathbf{c}_{j,n}^T = 0, \forall i \neq j$, and satisfy $\mathbf{c}_{i,n}\mathbf{c}_{i,n}^T = N$, then the nth symbol of user m can be recovered by the despreading process

$$u_m(n) = \frac{1}{N}\mathbf{y}(n)\mathbf{c}_{m,n}^T. \tag{1.3}$$

To perform the despreading operation, in addition to the knowledge of the spreading sequence of the desired user , the codes of the received signal and the locally generated codes have to be synchronized.

Because of the enlarged bandwidth and the simultaneous transmission through the same radio channel, CDMA has some properties that differ from other multiple access schemes. The major advantages of DS-CDMA systems are:

- *Soft capacity limit.* There is no absolute limit on the number of users in CDMA systems.

- *Privacy.* The transmitted signal can be recovered only if the the spreading code is known to the receiver.

- *Resistance to narrow band jamming.* In CDMA, the signal is spread over a large bandwidth. After despreading, the narrow band jamming is spread, making it appear as background noise compared with the despread signal.

- *Low probability of interception.* Because the signal is spread over a larger bandwidth, the power spectral density is low. Thus the signals can easily be concealed within the noise floor.

While CDMA systems have the noted advantages, at the same time they also face the following challenges:

- *Chip-level synchronization.* The synchronization of the locally generated code signal and the received signal has to be kept within a fraction of the chip period.

- *Frequency selective fading.* High chip rate implies that the signal bandwidth is larger than the coherent bandwidth of the channel, so different frequency components will experience different fading characteristics.

- *Multiuser interference.* Because multiple users transmit through the same frequency band simultaneously, multiuser interference occurs due to asynchronous transmission and multipath fading.

- *Near-far effect.* The power received by the base station from users close to it could be much higher than that received from users further away. As a result, the strongest user may capture the receiver, while the weaker users experience severe performance loss. To deal with this, tight power control is performed in practical CDMA systems.

1.3 Blind Equalization

Due to the time-varying nature of wireless environment, training sequences need to be sent periodically and frequently to obtain accurate channel estimation. Currently, all operational wireless communication systems are training based, and the channels are estimated based on the response of the known signals. For example, in GSM systems, each time slot has 156.25 bits, including a 26-bit training sequence [1]. In IS-95 systems, typically about 20% of the radiated power on the downlink is dedicated to the pilot signal [2]. Pilot channels are defined in W-CDMA and CDMA2000 standards to aid the channel estimation at the mobile devices [3]. It can be seen that training signals consume a lot of system resources. It is even worse in MIMO wireless systems, in which spatial diversity is exploited by employing multiple antennas at both the transmitter and receiver ends, and channels need to be estimated for each transmitter receiver antenna pair.

In the last few decades, wireless communications have seen explosive growth, and the number of worldwide subscribers has grown from less than 100 million to more than one billion. Since the frequency resource is limited, to increase the system capacity, the spectral efficiency has to be improved. By reducing or eliminating the training signal, blind signal detection has emerged as a promising technique, and has attracted more and more research attention.

Based on whether the channels are estimated explicitly, blind equalization methods can be divided into two groups: direct blind equalization and indirect blind equalization. For indirect blind equalization techniques, the channel is estimated first, and then equalizer is designed based on the estimated channel. A review of multichannel blind identification is presented in [4]. For direct equalization, the equalizer's parameters are extracted from the received data without explicit channel estimation.

Based on whether the statistical properties are exploited, the blind equalization methods can also be classified as statistical methods or deterministic methods. Our research is focused on the statistical methods, which again are generally split into two classes: SOS based and HOS based approaches.

1.3.1 Second-Order Statistics Based Methods

As presented in [5] and [6], when the channels are driven by cyclostationary processes, or can be modelled as single input and multiple outputs (SIMO) systems, it is possible to identify the channels blindly by exploiting only second-order statistics (SOS). In [7, 8], the cyclostationarity was introduced by modulating the input stream with a periodic sequence at the transmitter side. The SIMO structure can be obtained by applying multiple receive antennas, or by oversampling the received signal to generate multiple virtual channels (subchannels) [5,9]. While most SOS based approaches need to identify the channel first, some direct blind equalization methods were presented in [10–13].

Lots of existing second-order moment-based algorithms can be classified into one of the following categories: eigenstructure-based algorithms, correlation/spectrum fitting methods and linear prediction based approaches. Among eigenstructure-based algorithms, subspace methods [14, 15] are a class of most popular blind channel estimation techniques in recent years. The main idea is that the orthogonality between the signal space and the noise space can be exploited to estimate the channel vector up to a scalar factor. The major advantage of the subspace methods is that they can provide a closed-form solution, however, they could be sensitive to modelling errors.

The optimal weighted correlation fitting approach was proposed in [16], which achieved the performance bound of asymptotic normalized mean square error (ANMSE). A more practical suboptimal approach has been presented in [17]. Compared with eigenstructure-based approaches, correlation/spectrum fitting methods are robust to channel order selection and ill conditioning of the channels, but they are not easy to implement because of the local minima in the optimization. An approach combines the strength of both correlation fitting and subspace methods was proposed in [18], which is referred to as the joint optimization with subspace constraints (JOSC).

Multi-step linear prediction based method is an SOS based approach that eliminates the inter-symbol interference before channel identification, which was proposed in [19], and was extended to IIR channels with common zeros in [20]. Compared to subspace methods, the multi-step approach is more robust to order mismatches of the underlying FIR channel [19, 20].

1.3.2 Higher-Order Statistics Based Methods

Compared with second-order statistics, higher-order statistics can provide more information about random signals. While phase information is lost in the second-order statistics (SOS) of symbol rate sampled channel outputs, higher-order statistics (HOS) have the ability to preserve both magnitude and non-minimum phase information. Therefore, by applying higher order statistical methods, a much larger class of channel models can be identified. Another advantage is that for Gaussian signals, all cumulants of order greater than two are identically zero. If a non-Gaussian signal is received with additive Gaussian noise, higher-order cumulants can suppress the effect of Gaussian noise effectively. A review of the properties and applications of higher-order statistics can be found in [21]. Most higher-order statistical blind equalization methods are inverse filter criteria (IFC) based algorithms, which were initially proposed in [22–24], and were extended to MIMO systems in [25]. This kind of approaches find the optimal equalizer by searching for the maximum of a class of cumulant based cost functions either explicitly or implicitly. Two well known IFC based approaches are super-exponential algorithm (SEA) and constant modulus algorithm (CMA). Usually they have better performance than the SOS based methods, but require higher computational complexity. A short review can be found in [26].

Constant modulus algorithm (CMA) was first proposed by Godard in [27]. It is one of the earliest blind receiver designs, and is also one of most widely used blind equalization methods. A CMA receiver is obtained by minimizing a cost function which is defined by a constant modulus criterion. As in most IFC based methods, gradient search method is usually applied to find the minimum of the CM cost function. The receivers designed with CMA methods have similar MSE performance to the non-blind Wiener receivers [27]. Not only can the CMA approach recover source symbols possessing a constant modulus, but also can equalize signals characterized by source alphabets not possessing a constant modulus, like 16-QAM [28].

The SEA (super-exponential algorithm) is a class of iterative algorithms for solving the blind deconvolution problem, which was first proposed in [29], and has been extended for multichannel deconvolution in [30]. In [31], it is shown that SEA method is equivalent to a gradient search algorithm which minimizes an inverse filter criteria with dynamic step-size.

CMA and SEA algorithms both are special cases of IFC based algorithms, and they are closely related to each other. Actually, under certain circumstances, they are equivalent to each other [26, 31–34].

1.3.3 Blind Channel Estimation and Equalization in CDMA Systems

In CDMA systems, besides inter-symbol interference, the receivers have to combat multiuser interference (MUI). While the signals of the interfering users are treated as Gaussian noise in most commercial systems, significant gain can be achieved by modelling the MUI as part of the system explicitly. Some initial work of multiuser detection can be found in [35]. In this section, existing blind multiuser detection methods for both long-code and short-code CDMA systems are briefly reviewed.

A. Blind Signal Detection for Short-Code CDMA Systems

In short-code CDMA systems, a time-invariant MIMO model can be obtained when taking the symbol-rate signals as the system inputs. Therefore, by exploiting the code structure, the algorithms developed for single user systems can be applied to short-code CDMA systems. For this reason, most research works of blind equalization for DS-CDMA systems have been focused on short-code systems.

SOS based blind signal detection methods for DS-CDMA can be found in the following research works [36–49]. In [36], a blind multiuser detection method, which minimizes the output energy (MOE) of the receiver subject to a special constraint, was proposed for CDMA systems without multipath distortion. An extension to the multipath case was presented in [37]. This approach coincides with the MMSE solution in the constrained space, while the knowledge of the desired user's transmission delay is supposed to be known at the receiver. A general framework and the performance analysis of the MOE based approach were given in [38]. Subspace based blind channel estimation methods for DS-CDMA systems were proposed in [39–44], and a direct equalizer design approach was presented in [45]. The blind detection method developed in [44] is claimed to have lower computational complexity compared with the MOE detector, assuming the prior knowledge of the timing of the desired user. The research work of [41] has been extended to multi-rate DS-CDMA systems in [46]. In [47] and [48], moment matching methods was developed to estimate the channels blindly for single-rate and multirate DS-CDMA systems, respectively. In [49], multistep linear predictor based (MSLP) methods are presented for CDMA systems.

Higher-order inverse filter criterion based algorithms have been proposed in [50], [51] and [52]. The approaches presented in [51] and [52] have no control that which user is extracted first, and a user identification algorithm (UIA) was developed in [52] to identify the extracted signals. In [50], code-constrained IFC methods was developed so that only the code sequence of the desired user need to be known. CMA based approaches can be found in [53–56], and SEA based approaches have been proposed in [57–59].

B. Blind Signal Detection for Long-Code CDMA Systems

In long-code CDMA, the time-varying nature of the received signal model severely complicates the equalizer development approaches, since consistent estimation of the needed signal statistics can not be achieved by time-averaging over the received data record. More recently, both training based (e.g. [60–62]) and blind (e.g. [63–71]) multiuser detection methods targeted at the long code CDMA systems have been proposed. In this dissertation, we will focus on blind channel estimation and user separation for long code CDMA systems. Based on the channel model, most existing blind algorithms can roughly be divided into three classes:

- **Symbol-by-symbol approaches** As in long code systems, each user's spreading code changes for every information symbol, symbol-by-symbol approaches (see [68–71] for example) process each received symbol individually based on the assumption that channel is invariant in each symbol. In [68, 69, 71], channel estimation and equalization is carried out for each individual received symbol by taking instantaneous estimates of signal statistics based on the sample values of each symbol. In [70], based on the BCJR algorithm, an iterative Turbo multiuser detector was proposed.

- **Frame-by-frame approaches** Algorithms in this category (see [66, 72] for example) stack the total received signal corresponding to a whole frame or slot

into a long vector, and formulate a deterministic channel model. In [66], computational complexity is reduced by breaking the big matrix into small blocks and implementing the inversion "locally". As can be seen, the "localization" is similar to the process of the symbol-by-symbol approach. And the work is extended to fast fading channels in [72].

- **Chip-level equalization** By taking chip rate information as input, the time-varying effect of the pseudo-random sequence is absorbed into the input sequence. With the observation that channels remain approximately stationary over each time slot, the underlying channel, therefore, can be modelled as a time-invariant system, and at the receiver, chip-level equalization is performed. Please refer to [65, 73–75] and references therein.

In all these three categories, one way or another, the time-varying channel is "converted" or "decomposed" into *time-invariant* channels.

1.4 Space-Time Coding

To support multimedia services, high transmission data rates are required in the next generation wireless communication systems. Although the capacity can be improved by increasing the transmission power and bandwidth, they are not practical due to the limitations of devices, systems and available bandwidth. In addition, increasing the transmission power will introduce more co-channel interference. For these reasons, exploiting the spacial diversity has attracted a lot of research interest, and intensive research has been undertaken in this area. To apply spacial diversity, multiple antennas are equipped in either the transmitter, or the receiver side, and sometimes in both sides, which results in a so called MIMO (multiple-input multiple-output) system. A review of the MIMO systems is presented in [76].

In a cellular system, because of the limitation of the size and power of the mobile devices, it is more feasible to equip multiple antennas in the base stations than in the mobile devices. In the uplink, receiver diversity can be achieved by combing the output of each receive antenna, while in the downlink, space-time coding (STC) can be applied to provide transmission spacial diversity. In [77], space-time trellis codes (STTC) were developed to improve the reliability of communications. Although STTC can provide both spacial diversity gain and coding gain, the trellis complexity increases exponentially as a function of the spectrum efficiency and the diversity order [77]. Meanwhile, space-time block coding (STBC), first introduced by Alamouti in [78], has become a popular space-time coding scheme for its simplicity in decoding. The original Alamouti scheme was developed for systems with two transmission antennas. It is generalized to support arbitrary number of transmission antennas in [79]

The STBC schemes were originally designed for flat fading channels. While in the third generation (3G) communication systems, because of the high chip-rate of the transmitted signal, the systems suffer from frequency selective fading. The structure of the coding blocks is corrupted by the inter-symbol interference in this situation. To overcome this obstacle, MIMO equalizer (MIMO-EQ) was designed to mitigate the inter-symbol interference before space-time decoding in [80]. Although the diversity gain can be observed from the simulation results, the theoretical analysis is not addressed in the paper. Time-reversal space-time block coding (TR-STBC), which can provide full diversity gain, was designed specifically for frequency selective channels in [81]. The detailed coding structure and simulation examples were presented in [82]. A general coding scheme was proposed in [83], which achieves the maximum diversity gain in frequency fading channels, and includes the TR-STBC as a special case.

As CDMA has been identified as the major multiple access technique in 3G standards, researchers have been investigating space-time coding schemes for CDMA systems. In fact, the Alamouti scheme has been adopted in the W-CDMA standard. Recently, following [81] and [83], schemes combining TR-STBC and CDMA were proposed in [84] [85] to provide maximum diversity in downlink CDMA systems. In [84], equalization is carried out in time domain, while in [85], equalization is performed in frequency domain.

Existing blind and semiblind equalization approaches for space-time coded CDMA systems are mainly designed for Alamouti based coding schemes. Code constrained inverse filter criterion [86] and subspace based approach [87] have been proposed for ST coded short-code CDMA systems, and a semiblind approach is presented in [88] for STBC CDMA systems with aperiodic spreading codes. In [86] and [87], each user is assigned two short-codes, while only one spreading code is required for each user in [88].

1.5 Objectives

This dissertation is focused on blind channel estimation and signal detection for CDMA systems. Upon reviewing the research works in literature, we aim to achieve the following objectives:

- **Develop HOS based *fast* blind equalization approach for short-code *multi-rate* CDMA systems.** For short-code CDMA, most existing HOS based blind detection methods search for a global minimum/maximum of a cost function explicitly, or implicitly. Therefore the bottleneck is the convergence speed of the iteration procedure. In multi-rate short-code systems, a high-rate user is usually modelled as several basic-rate virtual users. Instead of extracting the signals of each virtual user independently, the correlations between different virtual users need to be exploited to speed up the iteration procedure. The first objective of this dissertation is to solve these problems, and to develop an efficient blind equalization algorithm for multi-rate systems.

- **Design novel *chip-level* blind equalization approaches for long-code CDMA systems.** As mentioned previously, research works about blind equalization are mainly focused on short-code CDMA systems. Blind detection of long-code CDMA signals remains a challenging topic due to its time-varying nature caused by aperiodic scrambling. As mentioned in Section 1.3.3 that, by taking the chip-rate signals as inputs, the system model can be characterized using a time-invariant model. Our second objective is to design novel chip-level blind equalizers for long-code systems.

- **Design blind equalizer for *space-time* coded long-code CDMA systems.** It is a trend to incorporate transmission diversity at base station to improve the downlink transmission quality. Notice that the main research works in this area consider systems combing short-code CDMA with STBC scheme which was originally designed for *flat fading* channels, in this dissertation, we aim to design a blind equalizer for space-time coded long-code CDMA systems with full transmission diversity in *frequency selective* environment.

1.6 Contributions

In this dissertation, statistics based blind equalization methods are developed for both short-code and long-code CDMA systems. Long-code CDMA systems with transmission space-time diversity are also considered. The main contributions of this dissertations are:

- *Blind equalization algorithm design for multi-rate short-code CDMA*

  A fast HOS based blind equalization approach – code-constrained super exponential algorithm (CSEA) is designed for multi-rate short-code systems [89]. Compared with existing IFC based algorithms, the proposed method has significantly faster convergence speed due to its dynamic step size.

- *Chip-rate blind equalizer design for long-code CDMA*

  Multistep linear prediction based two-step approaches are developed for both downlink and uplink long-code CDMA. In the first step, the convolutional mixture models are transformed to ISI free instantaneous mixture models. In the second step, the channels are identified using either SOS or HOS based methods, and the chip-rate equalizers are designed based on the estimated channels.

  - In the downlink, the novelty of this research resides in that, after descrambling, the chip sequence is treated as the output of a short-code system, and SEA can be applied to extract the signal of the desired user. By using this approach, the performance is improved significantly, and the spreading sequences are no longer required to be orthogonal to each other, which is a necessary condition for most downlink chip-rate equalizers.

  - In the uplink, for systems whose spreading codes are nonconstant modulus, transmitter induced cyclostationarity is exploited to identify the channels blindly [90]. The codes with special property in frequency domain are designed in order to apply Fourier analysis to identify the channels. By using matrix pencil method, requirements on the spreading codes can be relaxed. For systems whose spreading codes are constant modulus, JADE algorithm – a higher order statistics method is applied to solve the instantaneous mixture problem [91].

- *Blind equalizer design for space-time coded long-code CDMA systems*

  Downlink CDMA combining time-reversal space-time coding (TR-STBC) scheme is considered in this part. The major contribution is that the principal component analysis method is applied to perform blind channel estimation. The advantages of the proposed approach are that the ISI, MUI, and noise are completely suppressed in the channel estimation procedure, and only one spreading code is needed for each user.

1.7 Outline of the Dissertation

This dissertation is organized as follows. In Chapter 2, discrete system models for both short-code and long-code DS-CDMA are presented, along with the assumptions used through the dissertation. The difference of the symbol-rate model and chip-rate model are also discussed for long-code CDMA in this chapter. In Chapter 3, super-exponential algorithms (SEA) are introduced, and code-constrained SEA (CSEA) based approach is designed for multi-rate short-code CDMA. Both multi-code (MC) and variable sequence length (VSL) multi-rate schemes are discussed. Convergence analysis and identifiability aspects are provided, while the detailed proof is given in Appendix C. In Chapter 4, multi-step linear prediction based methods are developed for both downlink and uplink long-code CDMA systems. In the uplink, spreading codes with both constant and nonconstant modulus are considered. The methods developed for uplink can be used for downlink directly, since the downlink is a special case of the uplink. In Chapter 5, blind equalizer is designed for space-time coded long-code CDMA. Principal component analysis method is developed to perform channel estimation. Both zero padding and cyclic prefix/postfix are exploited to remove the inter-block interference. Conclusions and related future works are presented in Chapter 6.

CHAPTER 2

DS-CDMA System Models

In this Chapter, system models are presented for both uplink and downlink DS-CDMA systems, and the differences between short-code and long-code CDMA are explained. Without special notification, the discussions in the remaining part of the dissertation will follow the notations and models defined in this chapter.

2.1 Discrete-Time Uplink CDMA System Models

In short-code CDMA systems, spreading codes repeat symbol by symbol, while in long-code systems, every symbol in a given frame has a distinct spreading codes. This radical difference results in different characteristics of the system model and different statistical properties of the received signal. In this section, uplink system models of both short-code and long-code CDMA are introduced.

2.1.1 Short-Code CDMA

Consider an up-link DS-CDMA system with M users. For $m = 1, 2, \cdots, M$, let $u_m(k)$ denote the kth symbol transmitted by user m, and $c_m(n)$, $n = 0, 1, \ldots, N_m - 1$, denote the spreading code of user m, where N_m is the spreading gain for user m. As illustrated in Figure 1.3, the information sequence is spread with the signature sequence before transmission. Thus the spreading result of user m is given by

$$s_m(n) = \sum_{k=-\infty}^{\infty} u_m(k) c_m(n - kN_m), \tag{2.1}$$

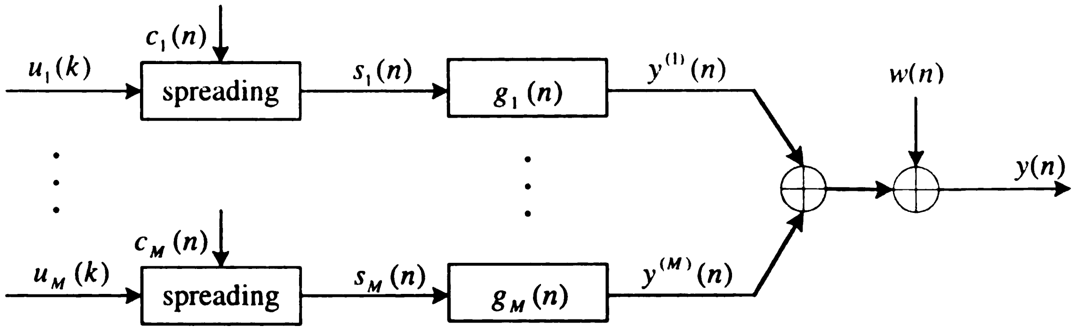

Figure 2.1. Block diagram of uplink short-code DS-CDMA system with single receive antenna

and the transmitted continuous time signal has the format

$$s'_m(t) = \sum_{k=-\infty}^{\infty} s_m(k)p(t - kT_c), \tag{2.2}$$

where $p(t)$ is the chip pulse shaping filter, and T_c is the chip duration. Let $\tau_{m,l}$ and $\alpha_{m,l}$ denote the delay and the complex gain of the lth ray respectively, then the linear time-invariant multipath channel for user m is given by

$$g'_m(t) = \sum_{l} \alpha_{m,l}\delta(t - \tau_{m,l}). \tag{2.3}$$

Therefore the component of the received signal due to user m can be obtained as

$$\begin{aligned} y^{(m)}(t) &= s'_m(t) * g'_m(t) \\ &= \sum_{k=-\infty}^{\infty} s_m(k)g_m(t - kT_c), \end{aligned} \tag{2.4}$$

where $*$ denotes the convolution operation, and $g_m(t) = g'_m(t) * p(t)$. Sampling $y^{(m)}(t)$ at the chip rate, it can be obtained that

$$y^{(m)}(n) = \sum_{k=-\infty}^{\infty} s_m(k)g_m(n - k) \tag{2.5}$$

where g_m is the effective channel impulse response of user m sampled at chip rate. The discrete time system diagram is shown in Figure 2.1. From (2.1) and (2.5), it can be obtained that

$$y^{(m)}(n) \quad = \quad \sum_{k=-\infty}^{\infty} u_m(k)h_m(n-kN_m), \tag{2.6}$$

where

$$h_m(n) \quad = \quad \sum_{l=-\infty}^{\infty} g_m(l)c_m(n-l) \tag{2.7}$$

represents the effective signature sequence of user m. The overall received signal at chip rate observed in additive white Gaussian noise $w(n)$ is given by

$$\begin{aligned} y(n) &= \sum_{m=1}^{M} y^{(m)}(n) + w(n) \\ &= \sum_{m=1}^{M} \sum_{k=-\infty}^{\infty} u_m(k)h_m(n-kN_m) + w(n). \end{aligned} \tag{2.8}$$

In a single rate DS-CDMA system, all users have the same spreading gain, that is $N_m = N$. The system can be represented with a multiple inputs multiple outputs (MIMO) model. Collect N samples of $y(n)$ into an N-vector

$$\mathbf{y}(k) := [y(kN), y(kN+1), \ldots, y(kN+N-1)]^T, \tag{2.9}$$

and define

$$\mathbf{h}_m(l) := [h_m(lN), h_m(lN+1), \ldots, h_m(lN+N-1)]^T, \tag{2.10}$$

then the symbol-rate MIMO model is given by

$$\mathbf{y}(k) = \sum_{m=1}^{M} \sum_{l=0}^{L_m-1} \mathbf{h}_m(l)u_m(k-l) + \mathbf{w}(k), \tag{2.11}$$

where $\mathbf{w}(k) = [w(kN), w(kN+1), \ldots, w(kN+N-1)]^T$. Because all symbols of a given user share the same spreading code, this is a time-invariant model.

Define the $N \times M$ matrix

$$\bar{\mathbf{H}}(l) := [\mathbf{h}_1(l), \mathbf{h}_2(l), \cdots, \mathbf{h}_M(l)], \tag{2.12}$$

and $M \times 1$ vector

$$\mathbf{u}(k) := [u_1(k), u_2(k), \cdots, u_M(k)]^T, \tag{2.13}$$

then the system model can be represented by

$$\mathbf{y}(k) = \sum_{l=0}^{L-1} \bar{\mathbf{H}}(l)\mathbf{u}(k-l) + \mathbf{w}(k), \tag{2.14}$$

where L is the maximum possible value of L_m.

2.1.2 Long-Code CDMA

Due to its better performance stability and information security, long-code CDMA systems are used in virtually all operational and commercially proposed DS-CDMA systems. As illustrated in Figure 2.2, in a commercial long code CDMA system, the user's symbols is first spread by user specified short code, then a pseudorandom long sequence is used to scramble the spread sequence. Therefore the overall spreading codes are aperiodic in each frame. This results in a time-variant symbol-rate system model. However, it can be observed that, if the channels remain unchanged in one frame, and the chip-rate scrambled signal is taken as the input, the system can be characterized using a time-invariant model. In this subsection, we consider a system with K receive antennas as shown in Figure 2.2.

Let $r_m(n)$ denote the spreading result of user m, which is given by

$$r_m(n) := \sum_{k=-\infty}^{\infty} u_m(k)c_m(n - kN_m). \tag{2.15}$$

Figu
ceiv

The

wh

th

st

w

and

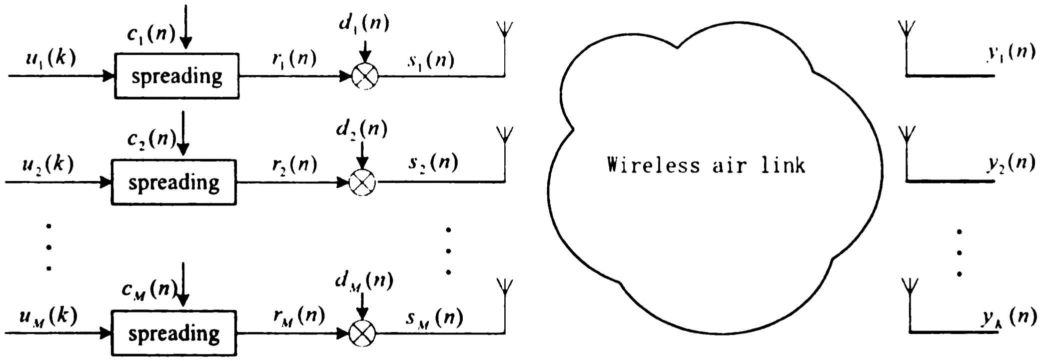

Figure 2.2. Block diagram of uplink long-code DS-CDMA system with multiple receive antennas

The chip-rate scrambled signal can be expressed as

$$s_m(n) = r_m(n)d_m(n), \tag{2.16}$$

where $d_m(n)$ is the pseudorandom scrambling sequence of user m. Let $g_m^{(p)}(l)$ represent the channel impulse response between user m and the pth receive antenna of the base station, then the received signal at antenna p can be represented as

$$y_p(n) = \sum_{m=1}^{M}\sum_{l=0}^{L-1} g_m^{(p)}(l)s_m(n-l) + w_p(n), \tag{2.17}$$

where $w_p(n)$ is the additive noise at pth antenna. Define

$$\mathbf{s}(n) := [s_1(n), s_2(n), \ldots, s_M(n)]^T, \tag{2.18}$$

and the received signal vector

$$\mathbf{y}(n) := [y_1(n), y_2(n), \ldots, y_K(n)]^T, \tag{2.19}$$

then the chip-rate time-invariant MIMO model can be obtained as

$$\begin{aligned} \mathbf{y}(n) &= \sum_{l=0}^{L-1} \mathbf{H}(l)\mathbf{s}(n-l) + \mathbf{w}(n) \\ &:= \mathbf{y}_s(n) + \mathbf{w}(n), \end{aligned} \tag{2.20}$$

where

$$\mathbf{H}(l) := \begin{bmatrix} g_1^{(1)}(l) & g_2^{(1)}(l) & \cdots & g_M^{(1)}(l) \\ g_1^{(2)}(l) & g_2^{(2)}(l) & \cdots & g_M^{(2)}(l) \\ \vdots & \vdots & \ddots & \vdots \\ g_1^{(K)}(l) & g_2^{(K)}(l) & \cdots & g_M^{(K)}(l) \end{bmatrix}, \tag{2.21}$$

and $\mathbf{w}(n) := [w_1(n), w_2(n), \dots, w_K(n)]^T$.

Note that N_m $(m = 1, \dots, M)$ could be different, therefore this model is suitable for both single-rate and multi-rate CDMA systems.

When the symbol-rate signals are taken as the system input, the spreading codes are implicitly part of the channel impulse response, resulting in a time-varying channel model. On the other hand, when taking the chip-rate signals as input, the underlying channel becomes time-invariant. For channel estimation and signal detection methods which are based on the cyclostationarity of the received signals, the time-variant model introduces significant complexity, as required statistics can not be estimated through time-averaging of the observed signals. This makes the chip-rate time-invariant model be more attractive for long-code CDMA systems.

2.2 Discrete-Time Downlink Long-Code CDMA System Models

In downlink CDMA, signals are transmitted from the base station to every user in the same cell as shown in Figure 2.3. Signal destined for each user is first spread using the user-specific channelization code, then signals from every users are added

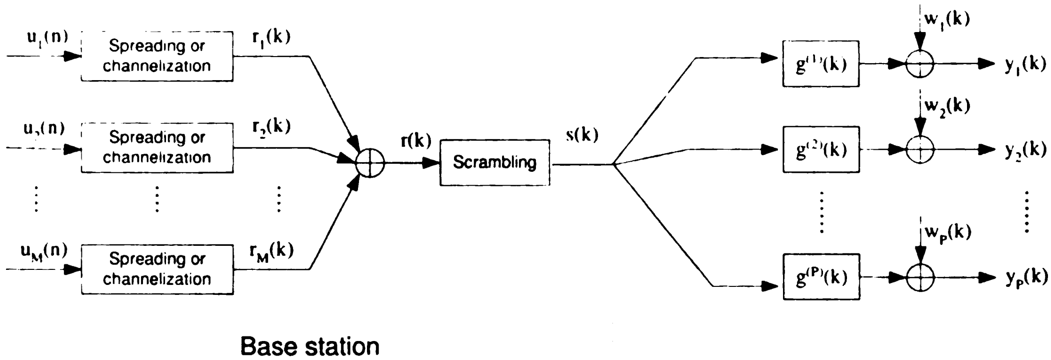

Figure 2.3. Illustration of downlink long-code CDMA with multiple receive antennas

together and scrambled using the same pseudorandom sequence.

When inter-cell interference is negligible, system model of downlink CDMA is just a special case of the uplink system. Consider a downlink long-code CDMA system with one transmission antenna at the base station, and P receive antennas at each mobile device. If we take the scrambled chip-rate signal $s(k)$ as the system input, the system model will be reduced to a single input multiple outputs (SIMO) model.

As shown in Figure 2.3, the transmitted chip-rate signal is given by

$$s(n) := r(n)d(n), \tag{2.22}$$

where

$$r(k) := \sum_{m=1}^{M} r_m(k) \tag{2.23}$$

is the sum of all spread signals, and $d(n)$ is the scrambling sequence. Let $g^{(p)}(l)$ represent the channel between the base station and the pth antenna of the desired user. The received signal at the antenna p of the desired user is given by

$$y_p(n) \;=\; \sum_{l=0}^{L-1} g^{(p)}(l)s(n-l) + w_p(n), \tag{2.24}$$

Define

$$\begin{aligned} \mathbf{g}(l) &:= [g^{(1)}(l), g^{(2)}(l), \ldots, g^{(P)}(l)]^T && (2.25) \\ \mathbf{w}(n) &:= [w_1(n), w_2(n), \ldots, w_P(n)]^T, && (2.26) \end{aligned}$$

then the received signal vector $\mathbf{y}(n) = [y_1(n), y_2(n), \cdots, y_P(n)]^T$ can be expressed as

$$\begin{aligned} \mathbf{y}(n) &= \sum_{l=0}^{L-1} \mathbf{g}(l)s(n-l) + \mathbf{w}(n) \\ &= \mathbf{y}_s(n) + \mathbf{w}(n), && (2.27) \end{aligned}$$

which is a time-invariant SIMO model.

2.3 General Assumptions

Without special indication, the algorithms presented in this dissertation are based on following assumptions:

(A1) The information sequences $\{u_m(k)\}, m = 1, \ldots, M$, are zero mean, mutually independent i.i.d, and are drawn from a finite alphabet with $E\{|u_m(k)|^2\} = 1$;

(A2) The scrambling sequences $\{d_m(k)\}$ are i.i.d. BPSK sequences, independent of the information sequences;

(A3) The noise sequence $\mathbf{w}(k)$ is zero mean Gaussian, independent of the information sequences, with $E\{\mathbf{w}(n+k)\mathbf{w}(n)\} = \sigma_w^2 I\delta(k)$.

(A4) $\bar{\mathcal{H}}(z)$, $\mathcal{H}(\mathbf{z})$ and $G(z)$ are FIR, and have full column rank for every z, including $z = \infty$ but excluding $z = 0$. ($\bar{\mathcal{H}}(z)$, $\mathcal{H}(\mathbf{z})$ and $G(z)$ denote the z-transform of $\bar{\mathbf{H}}(l)$, $\mathbf{H}(l)$ and $\mathbf{g}(l)$ respectively.) This last assumption is to ensure the existence of an FIR inverse filter (please refer to [25]).

Obviously, (A4) implies that we need $N \geq M$. That is, the processing gain is larger than or equal to the number of active users.

2.4 Summary

System models of both short-code and long-code CDMA systems are presented in this chapter. When the symbol-rate signals are taken as the input, short-code CDMA systems can be characterized using a time-invariant model, while long-code CDMA system results in a time variant model due to the chip-level pseudo-random scrambling. However, when the chip-rate signals are taken as the input, both short-code and long-code systems can be modelled as time invariant systems.

General assumptions which are used throughout the dissertation are also presented in this chapter.

CHAPTER 3

Blind Signal Detection for Short-Code DS-CDMA Systems

In this chapter, the super-exponential algorithm (SEA) is applied to short-code systems for its fast convergence speed. Code constrained SEA (CSEA) approach of blind detection of short-code DS-CDMA signals is presented first, then the CSEA approach is developed for *multi-rate* DS-CDMA systems.

3.1 Introduction to Super-Exponential Algorithms

The super-exponential algorithm (SEA), first proposed in [29], is a class of iterative algorithms for solving the blind deconvolution problem. In this section, we use a single-input single-output (SISO) system to introduce the basic idea of the SEA method. Consider a noise free SISO system

$$y(n) = \sum_{l=0}^{L-1} h(l)x(n-l), \tag{3.1}$$

where $h(l)$ is the channel impulse response, and $x(n)$ is the channel input. Let $f(n)$ denote the equalizer with length L_e, and $z(n)$ denote the equalizer output, then the overall response of the system is given by

$$\theta(n) = \sum_{l=0}^{L_e-1} h(l)f(n-l). \tag{3.2}$$

We want to find an equalizer $f(n)$ such that

$$\theta(n) = e^{j\phi}\delta(n-k), \tag{3.3}$$

where k stands for the equalization delay, and ϕ represents the phase shift. Consider the following two-step iterative procedure:

$$\begin{aligned} \theta'(n) &= \theta^p(n)(\theta^*(n))^q, & (3.4)\\ \theta''(n) &= \frac{\theta'(n)}{\sqrt{\sum_n |\theta'(n)|^2}}. & (3.5)\end{aligned}$$

Compared to other higher-order-statistics based blind deconvolution algorithms, the major advantage of SEA is that the above iteration forces $\theta(n)$ to converge exponentially to the desired response. More specifically, the leading tap converges to one, while all other taps converge to zero. Define the equalizer vector $\tilde{\mathbf{f}} = [f(0), f(1), \ldots, f(L_e-1)]^T$. It was shown in [29] that the above algorithm can be realized as:

$$\begin{aligned} \tilde{\mathbf{f}}' &= \mathbf{R}^{\#}\mathbf{d},\\ \tilde{\mathbf{f}}'' &= \frac{\tilde{\mathbf{f}}'}{\sqrt{(\tilde{\mathbf{f}}')^H\mathbf{R}\tilde{\mathbf{f}}'}}, \end{aligned} \tag{3.6}$$

where $\mathbf{R}$ is the $L_e \times L_e$ matrix whose (i,j)th element is

$$R_{ij} = \frac{E\{y(n-j)y^*(n-i)\}}{E\{x(n)x^*(n)\}}, \tag{3.7}$$

and $\mathbf{d}$ is the $L_e \times 1$ vector whose kth element is given by

$$d(n) = \frac{\text{cum}\{z(k):p, z^*(k):q, y^*(k-n\}}{\text{cum}\{x(k):p, x^*(k):q+1\}}, \tag{3.8}$$

where "cum" stands for "cumulant" (Please refer to Appendix B for the definition of cumulants). It has been proven in [31] that SEA is equivalent to a gradient search algorithm for cumulant maximization with an optimal time-varying step-size, which ensures the fast convergence of SEA.

3.2 Code Constrained Super-Exponential Methods for Blind Detection of Single-Rate Short-code DS-CDMA Signals

In this section, equation of combined channel-equalizer impulse response is derived first. Next, the unconstrained SEA approach is presented. Finally, code-constrained SEA approach is developed, and the convergence and identifiability aspect are analyzed.

3.2.1 Matrix Representation of the Combined Channel-equalizer Impulse Response

Recall that (please refer to Section 2.1.1) the chip-rate sampled channel output of an uplink short-code CDMA can be represented as

$$\mathbf{y}(k) = \sum_{m=1}^{M} \sum_{l=0}^{L_m-1} \mathbf{h}_m(l) u_m(k-l) + \mathbf{w}(k), \tag{3.9}$$

where $\mathbf{y}(k) = [y(kN), y(kN+1), \ldots, y(kN+N-1)]^T$ contains the chip signal observed in the kth symbol period.

Let $\{\mathbf{f}(i)\}_{N\times 1}, i = 0, 1, \ldots, L_e - 1$ denote the $N \times 1$ vector equalizer of length L_e symbols, then the equalizer output is given by

$$e(k) = \sum_{i=0}^{L_e-1} \mathbf{f}^H(i)\mathbf{y}(k-i). \tag{3.10}$$

It follows from (3.9) and (3.10) that

$$e(k) = \sum_{m=1}^{M} \sum_{l=0}^{L+L_e-2} \theta_m^*(l) u_m(k-l) + \sum_{i=0}^{L_e-1} \mathbf{f}^H(i)\mathbf{w}(k-i), \tag{3.11}$$

where $\theta^*_m(l) := \sum_{i=0}^{L_e-1} \mathbf{f}^H(i)\mathbf{h}_m(l-i)$. Let $\bar{L} = L + L_e - 2$, and define

$$\begin{aligned}\mathbf{\Theta} &:= [\theta_1(0), \theta_1(1), \cdots, \theta_1(\bar{L}), \theta_2(0), \theta_2(1), \cdots, \theta_2(\bar{L}), \\ &\quad \cdots, \theta_M(0), \theta_M(1), \cdots, \theta_M(\bar{L})]^T_{M(\bar{L}+1)\times 1}, \quad (3.12)\\ \mathbf{u}(k) &:= [u_1(k), u_1(k-1), \cdots, u_1(k-\bar{L}), u_2(k), u_2(k-1), \cdots, u_2(k-\bar{L}), \\ &\quad \cdots, u_M(k), u_M(k-1), \cdots, u_M(k-\bar{L})]^T_{M(\bar{L}+1)\times 1}, \quad (3.13)\end{aligned}$$

then (3.11) can be rewritten as

$$e(k) = \mathbf{\Theta}^H \mathbf{u}(k) + \tilde{\mathbf{f}}^H \tilde{\mathbf{w}}(k), \tag{3.14}$$

where

$$\begin{aligned}\tilde{\mathbf{f}} &:= [\mathbf{f}^H(0), \mathbf{f}^H(1), \cdots, \mathbf{f}^H(L_e-1)]^H, \quad (3.15)\\ \tilde{\mathbf{w}}(k) &:= [\mathbf{w}^H(k), \mathbf{w}^H(k-1), \cdots, \mathbf{w}^H(k-L_e+1)]^H. \quad (3.16)\end{aligned}$$

Define the block-Toeplitz matrix

$$\tilde{H}_m \triangleq \begin{bmatrix} \mathbf{h}_m^H(0) & 0 & \cdots & 0 \\ \mathbf{h}_m^H(1) & \mathbf{h}_m^H(0) & \cdots & 0 \\ \vdots & \vdots & \ddots & \vdots \\ \mathbf{h}_m^H(L-1) & \mathbf{h}_m^H(L-2) & \ddots & 0 \\ 0 & \mathbf{h}_m^H(L-1) & \ddots & \vdots \\ \vdots & \vdots & \ddots & \vdots \\ 0 & 0 & \cdots & \mathbf{h}_m^H(L-1) \end{bmatrix}_{[\bar{L}+1]\times[NL_e]}, \tag{3.17}$$

and

$$\tilde{\mathbf{H}} := [\tilde{H}_1^T, \tilde{H}_2^T, \cdots, \tilde{H}_M^T]^T, \tag{3.18}$$

then the combined channel-equalizer impulse response can be represented as

$$\mathbf{\Theta} = \tilde{\mathbf{H}}\tilde{\mathbf{f}}. \tag{3.19}$$

If the m_0th user is the desired user, the output of the ideal equalizer should satisfy

$$e(n) = \alpha u_{m_0}(n-d), \tag{3.20}$$

where d is the equalization delay, and α is a complex scaling factor. In other words, the combined impulse response should satisfy

$$\Theta = [\underbrace{0, 0, \cdots, 0}_{(m_0-1)(\bar{L}+1) \text{ zeros}}, \alpha^* \tilde{\mathbf{I}}_d, 0, 0, \cdots, 0]^T, \tag{3.21}$$

with

$$\tilde{\mathbf{I}}_d = [\underbrace{0, 0, \cdots, 0}_{d \text{ zeros}}, 1, 0, 0, \cdots, 0]_{1\times[\bar{L}+1]}. \tag{3.22}$$

3.2.2 Super-Exponential Approach

In this section, following [29] [92] [93], (unconstrained) SEA approach is presented for CDMA systems. Consider the following two-step iterations ($m = 1, 2, \cdots, M$ and $k = 0, 1, \cdots, \bar{L}$)

$$\theta_m^{(1)}(k) = (\theta_m(k))^p(\theta_m^*(k))^q, \tag{3.23}$$

$$\theta_m^{(2)}(k) = \theta_m^{(1)}(k)/\|\Theta^{(1)}\|_2, \tag{3.24}$$

where $\Theta^{(1)}$ is obtained by substituting $\theta_m(k)$ in (3.12) with $\theta_m^{(1)}(k)$, and p, q are positive integers that satisfy $p, q > 0$, $p+q \geq 2$. According to [29] and [93], as long as the "leading" (maximum magnitude) tap of the initial value of Θ is unique, the above iterations converge at a "super-exponential" rate to the combined channel-equalizer response

$$\Theta = [\underbrace{0, 0, \cdots, 0}_{(m-1)(\bar{L}+1) \text{ zeros}}, \alpha^* \tilde{\mathbf{I}}_d, 0, 0, \cdots, 0]^T, \tag{3.25}$$

for some m and d, where $1 \leq m \leq M$ and $0 \leq d \leq \bar{L}$. *For simplicity, we choose $p = 2$ and $q = 1$ through out this chapter.* Since Θ is not available, an algorithm in terms of the equalizer $\tilde{\mathbf{f}}$ and data is need to be developed.

Define

$$\vartheta(n) := (\theta_m(k))^2(\theta_m^*(k)), \tag{3.26}$$
$$(n = (m-1)(\bar{L}+1)+k,\ m = 1,2,\cdots,M,\ k = 0,1,\cdots,\bar{L}.)$$

and construct an $M(\bar{L}+1)$-column vector $\mathcal{G} = [\vartheta(1), \vartheta(2), \cdots, \vartheta(M(\bar{L}+1))]^T$. According to (3.23), we seek for $\tilde{\mathbf{f}}'$ to minimize $\|\tilde{\mathbf{H}}\tilde{\mathbf{f}}' - \mathcal{G}\|$. This is a linear least square problem whose solution is given by

$$\tilde{\mathbf{f}}' = (\tilde{\mathbf{H}}^H\tilde{\mathbf{H}})^{\#}\tilde{\mathbf{H}}^H\mathcal{G}. \tag{3.27}$$

The normalization operation in (3.24) can be carried out as

$$\tilde{\mathbf{f}}'' = \frac{\tilde{\mathbf{f}}'}{\sqrt{\tilde{\mathbf{f}}'^H\tilde{\mathbf{H}}^H\tilde{\mathbf{H}}\tilde{\mathbf{f}}'}}. \tag{3.28}$$

Projecting the $\mathbf{f}$-domain (equalizer domain) algorithm back to $\boldsymbol{\Theta}$-domain (combined channel-equalizer domain) following (3.19), we obtain

$$\boldsymbol{\Theta}' = \tilde{\mathbf{H}}(\tilde{\mathbf{H}}^H\tilde{\mathbf{H}})^{\#}\tilde{\mathbf{H}}^H\mathcal{G}, \tag{3.29}$$
$$\boldsymbol{\Theta}'' = \frac{\boldsymbol{\Theta}'}{\|\boldsymbol{\Theta}'\|}. \tag{3.30}$$

As $\tilde{\mathbf{H}}$ and $\mathcal{G}$ are unknown, the algorithm given by (3.27) and (3.28) is still cannot be implemented directly. Next, this algorithm will be converted into a realizable algorithm in terms of joint cumulants of the input and the output of the equalizer. Define

$$\mathbf{Y}_s^T(k) := [\mathbf{y}_s^T(k), \mathbf{y}_s^T(k-1), \cdots, \mathbf{y}_s^T(k-L_e+1)]^T, \tag{3.31}$$

where

$$\mathbf{y}_s(k) = \sum_{m=1}^{M}\sum_{l=0}^{L_m-1}\mathbf{h}_m(l)u_m(k-l) \tag{3.32}$$

is the noise-free channel output. Under assumption (**A1**), it follows that the correlation matrix of the noise-free channel output is given by

$$\mathcal{R}_{ss} := E\{\mathbf{Y}_s(k)\mathbf{Y}_s^H(k)\} = \tilde{\mathbf{H}}^H\tilde{\mathbf{H}}. \tag{3.33}$$

Consider the noise-free equalizer output

$$e_s(k) = \sum_{m=1}^{M}\sum_{l=0}^{\bar{L}} \theta_m^*(l)u_m(k-l), \tag{3.34}$$

then the iterations (3.23)(3.24) can be realized as

$$\tilde{\mathbf{f}}' = \mathcal{R}_{ss}^{\#}\mathbf{d}, \tag{3.35}$$

$$\tilde{\mathbf{f}}'' = \frac{\tilde{\mathbf{f}}'}{\sqrt{\tilde{\mathbf{f}}'^H\mathcal{R}_{ss}\tilde{\mathbf{f}}'}}, \tag{3.36}$$

where

$$\mathbf{d} := \frac{\mathrm{cum}\{e_s^*(k), e_s^*(k), e_s(k), \mathbf{Y}_s(k)\}}{\mathrm{cum}_4\{u_m(k)\}}. \tag{3.37}$$

(3.38)

In the presence of the additive noise, define

$$\mathbf{Y}^T(k) := [\mathbf{y}^T(k), \mathbf{y}^T(k-1), \cdots, \mathbf{y}^T(k-L_e+1)]^T, \tag{3.39}$$

if follows (3.9) and (3.32) that $\mathbf{Y}(k) = \mathbf{Y}_s(k) + \mathbf{W}(k)$, where $\mathbf{W}(k)$ is the $[NL_e] \times 1$ noise vector defined in the same manner as $\mathbf{Y}(k)$ and $\mathbf{Y}_s(k)$. The correlation matrix of the channel output is given by

$$\mathcal{R}_{yy} := E\{\mathbf{Y}(k)\mathbf{Y}^H(k)\} = \mathcal{R}_{ss} + \sigma_w^2\mathbf{I}_{NL_e}. \tag{3.40}$$

Since all cumulants of order greater than two are zero for Gaussian random variables, th

In
b
[3
p

3

In
b
t

e

It

the SEA in the presence of noise can be obtained as

$$\tilde{\mathbf{f}}' = \mathcal{R}_{yy}^{\#}\mathbf{d}, \tag{3.41}$$

$$\tilde{\mathbf{f}}'' = \frac{\tilde{\mathbf{f}}'}{\sqrt{\tilde{\mathbf{f}}'^H \mathcal{R}_{yy} \tilde{\mathbf{f}}'}}. \tag{3.42}$$

In the limit of iterations, the equalizer obtained from the super-exponential algorithm blindly converges to a solution which is approximately the non-blind Wiener filter [34, 92, 94, 95] which extracts user m with delay d for some $m \in \{1, 2, \cdots, M\}$. The problem is: *there is no control over which user the system will converge to.*

3.2.3 Code-Constrained Super-Exponential Algorithm

In this section, to ensure that the system will extract the desired user, a constraint based on the knowledge of the desired user's spreading code is formulated first, and then the code-constrained super-exponential approach is briefly presented.

From Section 3.2.1, it can be observed that to extract the desired user m_0 with equalization delay d, the inverse filter equalizer should satisfy

$$\begin{aligned} \tilde{\mathbf{H}}\tilde{\mathbf{f}} &= [\underbrace{0, 0, \cdots, 0}_{(m_0-1)(\bar{L}+1)\text{ zeros}}, \alpha^* \tilde{\mathbf{I}}_d, 0, 0, \cdots, 0]^T \\ \Longleftrightarrow\quad \tilde{\mathbf{f}}^H \mathbf{Y}_s(k) &= e_s(k) = \alpha u_{m_0}(k-d). \end{aligned} \tag{3.43}$$

Multiplying both sides by $\tilde{\mathbf{H}}^H$, we obtain

$$\begin{aligned} \tilde{\mathbf{H}}^H \tilde{\mathbf{H}}\tilde{\mathbf{f}} &= \alpha^* [\mathbf{h}_{m_0}^H(d), \mathbf{h}_{m_0}^H(d-1), \cdots, \mathbf{h}_{m_0}^H(0), 0, \cdots, 0]^H \\ &:= \alpha^* \tilde{\mathbf{h}}_{m_0}^{(d)}. \end{aligned} \tag{3.44}$$

It then follows from (3.33) that

$$\mathcal{R}_{ss}\tilde{\mathbf{f}} = \alpha^* \tilde{\mathbf{h}}_{m_0}^{(d)}. \tag{3.45}$$

According to the orthogonal projection theorem [96], (3.45) is a necessary and sufficient condition for $\tilde{\mathbf{f}}$ to satisfy (3.43).

For any desired equalization delay d, define

$$\mathbf{h}_m^{(d)} := [\mathbf{h}_m^T(0), \mathbf{h}_m^T(1), \cdots, \mathbf{h}_m^T(d)]^T = \mathbf{C}_m^{(d)}\mathbf{g}_m, \tag{3.46}$$

where

$$\mathbf{C}_m^{(d)} := \begin{bmatrix} c_m(0) & 0 & \cdots & 0 \\ c_m(1) & c_m(0) & \ddots & \vdots \\ \vdots & c_m(1) & \ddots & 0 \\ c_m(N-1) & \vdots & \ddots & c_m(0) \\ 0 & c_m(N-1) & \ddots & c_m(1) \\ \vdots & 0 & \ddots & \vdots \\ 0 & \vdots & \ddots & c_m(N-1) \\ \vdots & \vdots & \cdots & \vdots \\ 0 & 0 & \cdots & 0 \end{bmatrix}_{[(d+1)N]\times[LN]} \tag{3.47}$$

and

$$\mathbf{g}_m := [g_m(0), g_m(1), \cdots, g_m(LN-1)]^T. \tag{3.48}$$

Define an $[N(d+1)] \times [N(d+1)]$ matrix $\mathcal{T}_d$ as

$$\mathcal{T}_d := \begin{bmatrix} 0 & \cdots & 0 & I_N \\ 0 & \cdots & I_N & 0 \\ \vdots & \ddots & \vdots & \vdots \\ I_N & \cdots & 0 & 0 \end{bmatrix}, \tag{3.49}$$

then from (3.46), we have

$$\mathbf{h}_{m_0}^{(d)} = \mathcal{T}_d[\mathbf{h}_{m_0}^H(d), \mathbf{h}_{m_0}^H(d-1), \cdots, \mathbf{h}_{m_0}^H(0)]^H. \tag{3.50}$$

Further define an $[NL_e] \times [NL_e]$ matrix $\mathcal{T}^{(d)}$ as

$$\mathcal{T}^{(d)} := \begin{bmatrix} \mathcal{T}_d & 0 \\ 0 & I_{N(L_e-1-d)} \end{bmatrix}. \tag{3.51}$$

Thus, from (3.45)-(3.51), we have

$$\mathcal{T}^{(d)}\mathcal{R}_{ss}\tilde{\mathbf{f}} = \alpha^* \mathcal{T}^{(d)}\tilde{\mathbf{h}}_{m_0} = \alpha^* \mathcal{C}_{m_0}^{(d)}\mathbf{g}_{m_0}, \tag{3.52}$$

where

$$\mathcal{C}_{m_0}^{(d)} := \begin{bmatrix} \mathbf{C}_{m_0}^{(d)} \\ 0 \end{bmatrix}_{[L_e N]\times[\bar{L}N]}. \tag{3.53}$$

Let the columns of $\mathcal{U}_{m_0}^{(d)}$ denote an orthonormal basis for the orthogonal complement of $\mathcal{C}_{m_0}^{(d)}$. Because $\mathcal{C}_{m_0}^{(d)}$ is of full column rank, $\mathcal{U}_{m_0}^{(d)}$ is an $[NL_e] \times [NL_e - N\bar{L}]$ matrix. This leads to

$$\mathcal{U}_{m_0}^{(d)H}\mathcal{T}^{(d)}\mathcal{R}_{ss}\tilde{\mathbf{f}} = 0. \tag{3.54}$$

In the absence of noise, we have $\mathcal{R}_{yy} = \mathcal{R}_{ss}$, therefore it can be obtained that

$$\mathcal{U}_{m_0}^{(d)H}\mathcal{T}^{(d)}\mathcal{R}_{yy}\tilde{\mathbf{f}} := \mathcal{A}^{(m_0)}\tilde{\mathbf{f}} = 0, \tag{3.55}$$

where $\mathcal{A}^{(m_0)}$ is an $[N(L_e - \bar{L})] \times [NL_e]$ matrix. Thus, in order to extract the desired user, a necessary condition is that $\tilde{\mathbf{f}}$ belongs to the null space of $\mathcal{A}^{(m_0)}$. Assume the effective rank of $\mathcal{A}^{(m_0)}$ is r, and carry out an SVD of $\mathcal{A}^{(m_0)}$

$$\mathcal{A}^{(m_0)} = \begin{bmatrix} U_1 & U_2 \end{bmatrix} \begin{bmatrix} \Sigma_r & 0 \\ 0 & \Sigma_\varepsilon \end{bmatrix} \begin{bmatrix} V_1^H \\ V_2^H \end{bmatrix}, \tag{3.56}$$

where Σ_r is the diagonal $r \times r$ matrix containing the effective non-zero singular values of $\mathcal{A}^{(m_0)}$, and Σ_ε contains the insignificant singular values of $\mathcal{A}^{(m_0)}$. Therefore, in the absence of noise, (3.55) is equivalent to

$$V_1^H \tilde{\mathbf{f}} = 0. \tag{3.57}$$

With the existence of noise, V_1 is determined by the effective rank of $\mathcal{A}^{(m_0)}$.

Recall that $\tilde{\mathbf{f}}'$ was chosen to minimize $\|\tilde{\mathbf{H}}\tilde{\mathbf{f}}' - \mathcal{G}\|$. This requirement is now modified as: choose $\tilde{\mathbf{f}}'$ to minimize $\|\tilde{\mathbf{H}}\tilde{\mathbf{f}}' - \mathcal{G}\|$ subject to $V_1^H \tilde{\mathbf{f}}' = 0$. The minimum-norm solution to this problem is given by

$$\tilde{\mathbf{f}}' = (\tilde{\mathbf{H}}\Pi^{\perp}_{\mathcal{A}^{(m_0)}})^{\#}\mathcal{G}, \tag{3.58}$$

where

$$\Pi^{\perp}_{\mathcal{A}^{(m_0)}} := V_2 V_2^H \tag{3.59}$$

is the $[NL_e] \times [NL_e]$ projection matrix onto the null space of $\mathcal{A}^{(m_0)}$. Note that $\Pi^{\perp}_{\mathcal{A}^{(m_0)}}(\tilde{\mathbf{H}}\Pi^{\perp}_{\mathcal{A}^{(m_0)}})^{\#} = (\tilde{\mathbf{H}}\Pi^{\perp}_{\mathcal{A}^{(m_0)}})^{\#}$, from (3.58), we have $\Pi^{\perp}_{\mathcal{A}^{(m_0)}}\tilde{\mathbf{f}}' = \tilde{\mathbf{f}}'$. Then the combined response is given by

$$\Theta = (\tilde{\mathbf{H}}\Pi^{\perp}_{\mathcal{A}^{(m_0)}})\tilde{\mathbf{f}}. \tag{3.60}$$

Therefore, mimicking the development in Section 3.2.2, the code-constrained algorithm is given by

$$\tilde{\mathbf{f}}' = (\Pi^{\perp}_{\mathcal{A}^{(m_0)}}\mathcal{R}_{yy}\Pi^{\perp}_{\mathcal{A}^{(m_0)}})^{\#}\Pi^{\perp}_{\mathcal{A}^{(m_0)}}\mathbf{d}, \tag{3.61}$$

$$\tilde{\mathbf{f}}'' = \frac{\tilde{\mathbf{f}}'}{\sqrt{\tilde{\mathbf{f}}'^H \mathcal{R}_{yy}\tilde{\mathbf{f}}'}}, \tag{3.62}$$

which are the counterparts to (3.35) and (3.36).

Convergence and Identifiability Aspects

Proposition 3.1 *Define space $\mathcal{S}_{CA} = range(\tilde{\mathbf{H}}\Pi^{\perp}_{\mathcal{A}^{(m_0)}})$, and let $\mathcal{P}_{CA}$ represent the orthogonal projection operator on to the space $\mathcal{S}_{CA}$, then iteration procedure given in*

(3.61) and (3.62) is equivalent to the gradient search algorithm defined by

$$\begin{aligned}\Theta' &= \Theta^{(n)} + \frac{1}{2\mathbf{F}_4(\Theta^{(n)})}\mathcal{P}_{CA}\nabla_{\Theta^*}\mathbf{F}_4(\Theta^{(n)})\\ \Theta^{(n+1)} &= \frac{\Theta'}{\|\Theta'\|_2},\end{aligned}$$

which maximizes the cost function

$$F_4(\Theta) = \left\{\frac{\|\Theta\|_4}{\|\Theta\|_2}\right\}^4,$$

subject to $\Theta \in \mathcal{S}_{CA}$.

Please refer to Appendix C for the proof of Proposition 3.1.

For unconstrained case, the restriction is in a larger subspace $\mathcal{S}$, which is the range space of $\tilde{\mathbf{H}}$. According to the assumption (A1) in Chapter 2, we have $E\{|u_m(k)|^2\} = 1$. In absence of noise, we have

$$F_4(\Theta) = \tilde{J}_{42}(\Theta)/|\text{cum}_4(u_m(k))|, \tag{3.63}$$

where

$$\tilde{J}_{42}(\Theta) := J_{42}(\tilde{\mathbf{f}}) := \frac{|\text{cum}_4(e(k))|}{[E|e(k)|^2]^2}. \tag{3.64}$$

Consider the unconstrained case under the sufficient order condition of $\mathcal{P}_A = I$. In this case, Θ is unrestricted (except for $\Theta \neq 0$) and the global maxima of $ln\mathbf{F}_4(\Theta)$ and $\mathbf{F}_4(\Theta)$ coincide. Let $\tilde{\mathbf{f}}$ be a subequalizer for which $J_{42}(\tilde{\mathbf{f}})$ achieves the global maxima $|\gamma_{4s}|$, corresponding to $max_\Theta ln\mathbf{F}_4(\Theta) = 0$, where $|\gamma_{4s}| := \text{cum}_4\{u_m(k)\}$. The corresponding output is given by $e(n) = \alpha u_{m_d}(n - d_0)$. Thus $\tilde{\mathbf{f}}$ leads to the extraction of user m_d with delay d_0. Then, by construction, $\mathcal{A}^{(m_d)}\tilde{\mathbf{f}} = 0$. Therefore, for code-constrained SEA, $max_{\Theta\in\mathcal{S}_{CA}} ln\mathbf{F}_4(\Theta) = 0$. If $J_{42}(\tilde{\mathbf{f}}) \neq |\gamma_{4s}|$, (3.43) cannot hold true. Therefore, constrained global maxima of $J_{42}(\tilde{\mathbf{f}})$ are given by those $\tilde{\mathbf{f}}$'s for which $J_{42}(\tilde{\mathbf{f}}) = \gamma_{4s}$ and $\mathcal{A}\tilde{\mathbf{f}} = 0$, equivalently, for which (3.43) and (3.55) hold true.

Next we consider the identifiability aspect of the algorithm. Consider the following condition:

C 3.1 *The* $[NL_e] \times [\bar{L}N+1]$ *matrix* $[\mathcal{C}_{m0}^{(d)} \vdots \mathcal{T}^{(d)}\tilde{\mathbf{h}}_m^{(d_0)}]$ *has full column rank for every* $m \neq m_0$ *and every* $d_0 \in \{d-\bar{L}+1, d-\bar{L}+2, \ldots, d\}$ *where* $L_e \geq d+1$ *and* $d \geq 2$.

Proposition 3.2 *Under Condition 3.1, any solution that satisfies (3.55) and (3.52) corresponds to* $m = m_0$ *and* $d_0 \in \{d-L+1, d-L+2, \cdots, d\}$, *where* $L_e \leq d+1$ *and* $d \leq L$.

Please refer to [53] for the proof. From the above discussion, under the condition C3.1, all constrained global maxima of $lnF_4(\Theta)$ in $\mathcal{S}_{CA}$ are specified by the solutions given in Proposition 3.2.

3.3 CSEA Based Blind Equalization of Multirate Asynchronous CDMA Systems

As is well known, the third generation wireless system aims to provide multimedia services with high data rate and variable quality of service. Multirate design is therefore required to map different data rates into the allocated bandwidth. For CDMA systems, two basic multirate schemes are multicode (MC) transmission and variable sequence length (VSL) (also known as variable spreading factor). In MC systems, the information sequence of a high-rate user are subsampled to obtain several symbol streams, and each stream is spread using a distinct signature sequence. In VSL systems, users requiring different rates are assigned signature sequences of different lengths. For both schemes, the signal of a high-rate user can be treated as the superposition of several basic-rate virtual users' signals.

In this section, motivated by the previous works in [97] and [57], we consider blind detection of the desired user's signal in multirate CDMA systems using super-exponential algorithm. *Compared with the single-rate case, the major challenge of the multirate case lies in that the signals of different virtual users corresponding to the same high-rate user have to be extracted synchronously and in correct order.*

3.3.1 System Model for Multirate DS-CDMA Systems

In this section, an equivalent baseband system model is presented for both VSL and MC systems. In the following discussion, R denotes the basic symbol rate, and the pair (i, j) is used to denote user j at rate R_i, where $R_i = p_i R$ (p_i is an integer). K stands for the number of different user rates, and assume there are Q_i users at rate R_i. N represents the processing gain of the basic rate users. In MC systems, all users have the same processing gain, while in VSL systems, the processing gain of users at rate R_i is given by $N_i = N/p_i$.

A. VSL Systems

In VSL systems, users at different rates have different processing gains. Let the signature sequence of user j at rate R_i be denoted by $\mathbf{c}_{ij} := [c_{ij}(0), c_{ij}(1), \cdots, c_{ij}(N_i - 1)]^T$. Then the effective signature waveform of user (i, j) is given by

$$h_{ij}(n) = \sum_{k=0}^{N_i-1} c_{ij}(k) g_{ij}(n-k), \tag{3.65}$$

where $g_{ij}(n)$ is the effective channel impulse response with respect to user (i, j). A high rate user at rate p_i times basic rate can be converted to p_i basic rate virtual users. The symbols of the mth ($m = 0, 1, \ldots, p_i - 1$) virtual user $u_{ij}^{(m)}(l)$ can be extracted by subsampling:

$$u_{ij}^{(m)}(l) := u_{ij}(p_i l + m), \ (m = 0, 1, \ldots, p_i - 1). \tag{3.66}$$

where $\{u_{ij}(k)\}$ is the symbol sequence of user (i, j) drawn from a finite alphabet, and is independently and identically distributed (i.i.d). Let x_{ij} denote the received signal component due to user (i, j). If we stack x_{ij} into an $N \times 1$ column vector $\mathbf{x}_{ij}(n) := [x_{ij}(nN), \ldots, x_{ij}(nN + N - 1)]^T$, then we have

$$\mathbf{x}_{ij}(n) = \sum_{m=0}^{p_i-1} \sum_{l=0}^{L_h-1} \mathbf{h}_{ij}^{(m)}(l) u_{ij}^{(m)}(n-l), \tag{3.67}$$

where $\mathbf{h}_{ij}^{(m)}(l) := [h_{ij}(lN - d_{ij} - mN_i), \ldots, h_{ij}(lN - d_{ij} - mN_i + N - 1)]^T$, d_{ij} is the transmission delay of user (i, j), and L_h is the maximum length of the channel impulse response of each virtual user of user (i, j) in terms of basic rate symbols. Thus, $\mathbf{x}_{ij}$ can be considered as the superposition of p_i virtual users derived from user (i, j). The spreading code for the mth virtual user is given by [97]

$$\mathbf{c}_{ij}^{(m)} := [\mathbf{0}_{1\times[mN_i]} \quad \mathbf{c}_{ij}^T \quad \mathbf{0}_{1\times[(p_i-1-m)N_i]}]^T. \tag{3.68}$$

B. MC Systems

In MC systems, high rate user (i, j) can also be converted to p_i basic rate virtual users. The symbol stream of each virtual user is derived by the same way as (3.66). Those virtual users have their own spreading codes $\mathbf{c}_{ij}^{(m)}$, $(m = 0, 1, \ldots, p_i - 1)$. The effective signature waveform of the mth virtual user of user (i, j) is given by

$$h_{ij}^{(m)}(n) = \sum_{l=0}^{N-1} c_{ij}^{(m)}(l) g_{ij}(n - l). \tag{3.69}$$

If we stack $h_{ij}^{(m)}(n)$ into an $N \times 1$ vector, and define $\mathbf{h}_{ij}^{(m)}(l) := [h_{ij}^{(m)}(lN - d_{ij}), \ldots, h_{ij}^{(m)}(lN - d_{ij} + N - 1)]^T$, then the received signal from user (i, j) can also be represented by (3.67).

C. Unified Model

Based on the above derivation and take the received signals from all users into consideration, we can obtain an MIMO model for both VSL and MC systems:

$$\mathbf{y}(k) = \sum_{i=1}^{K} \sum_{j=1}^{Q_i} \sum_{m=0}^{p_i-1} \sum_{l=0}^{L_h-1} \mathbf{h}_{ij}^{(m)}(l) u_{ij}^{(m)}(k - l) + \mathbf{w}(k), \tag{3.70}$$

where $\mathbf{y}(k) := [\tilde{x}(kN), \tilde{x}(kN+1), \ldots, \tilde{x}(kN + N - 1)]^T$, and $\tilde{x}(n)$ is the total received signal. $\mathbf{w}(k)$ is the Gaussian noise defined in a manner similar to $\mathbf{y}(k)$. In other words, the total received signal can be represented by the superposition of total $\sum_{i=1}^{K} Q_i p_i$

virtua

then,

C

d i

ba

3.

A.

Le

the

virtual users plus the additive white Gaussian noise. Define

$$\mathbf{h}_{ij}^{(m,d)} := [\mathbf{h}_{ij}^{(m)H}(0), \mathbf{h}_{ij}^{(m)H}(1), \ldots, \mathbf{h}_{ij}^{(m)H}(d)]^H, \tag{3.71}$$

$$\mathbf{g}_{ij} := [g_{ij}(-d_{ij}), \ldots, g_{ij}(-d_{ij} - 1 + N\bar{L}_g)]^T, \tag{3.72}$$

then, for both VSL and MC systems, we have $\mathbf{h}_{ij}^{(m,d)} = \mathbf{C}_{ij}^{(m,d)} \mathbf{g}_{ij}$, where

$$\mathbf{C}_{ij}^{(m,d)} := \begin{bmatrix} c_{ij}^{(m)}(0) & 0 & \cdots & 0 \\ c_{ij}^{(m)}(1) & c_{ij}^{(m)}(0) & \ddots & \vdots \\ \vdots & \ddots & \ddots & 0 \\ c_{ij}^{(m)}(N-1) & \ddots & \ddots & c_{ij}^{(m)}(0) \\ 0 & c_{ij}^{(m)}(N-1) & \ddots & \vdots \\ \vdots & \ddots & \ddots & \vdots \\ 0 & 0 & \cdots & c_{ij}^{(m)}(N-1) \\ \vdots & \vdots & \cdots & \vdots \\ 0 & 0 & \cdots & 0 \end{bmatrix}_{[(d+1)N]\times[\bar{L}_g N]}, \tag{3.73}$$

d is the desired equalizer delay, and $\bar{L}_g$ is the maximum length of $\{g_{ij}\}$ in terms of basic rate symbols. According to the definition of L_h, $L_h = \bar{L}_g + 1$.

3.3.2 Code-Constrained Super-Exponential Algorithms for Multirate CDMA Systems

A. The Combined Channel-Equalizer System

Let $\{\mathbf{f}^{(m_0)}(k)\}_{k=0}^{L_e-1}$ denote the $N \times 1$ vector subequalizer for virtual user (i_0, j_0, m_0), the m_0th virtual user of the desired user (i_0, j_0). Then its output is given by

$$e^{(m_0)}(n) = \sum_{k=0}^{L_e-1} [\mathbf{f}^{(m_0)}(k)]^H \mathbf{y}(n-k) := [\tilde{\mathbf{f}}^{(m_0)}]^H \mathbf{Y}(n), \tag{3.74}$$

where

$$\begin{aligned}
\tilde{\mathbf{f}}^{(m_0)} &:= [(\mathbf{f}^{(m_0)}(0))^H, \ldots, (\mathbf{f}^{(m_0)}(L_e-1))^H]^H, \\
\mathbf{Y}(n) &:= [\mathbf{y}^T(n), \ldots, \mathbf{y}^T(n-L_e+1)]^T.
\end{aligned}$$

Defining $\mathbf{u}_{ij}^{(m)}(n) = [u_{ij}^{(m)}(n), \cdots, u_{ij}^{(m)}(n-L_e-L_h+2)]^T$, and collect all $\{\mathbf{u}_{ij}^{(m)}(n)\}$s to a vector $\mathbf{u}(n)$. Following (3.70), we get

$$\mathbf{Y}(n) = \tilde{\mathbf{H}}^H \mathbf{u}(n) + \tilde{\mathbf{w}}(n), \tag{3.75}$$

where $\tilde{\mathbf{H}}$ is the transpose of the signature matrix, and $\tilde{\mathbf{w}}(n) := [\mathbf{w}^H(n), \cdots, \mathbf{w}^H(n-L_e+1)]^H$. Therefore, (3.74) can be rewritten as

$$e^{(m_0)}(n) = \Theta^H \mathbf{u}(n) + [\tilde{\mathbf{f}}^{(m_0)}]^H \tilde{\mathbf{w}}(n), \tag{3.76}$$

where

$$\Theta = \tilde{\mathbf{H}}\tilde{\mathbf{f}}^{(m_0)} \tag{3.77}$$

is the combined channel-equalizer impulse response.

Assuming that user (i_0, j_0) is the desired user, we wish to design subequalizer $\tilde{\mathbf{f}}^{(m_0)}$ such that

$$\theta_{ij}^{(m)}(l) = \begin{cases} \alpha^* \delta(l-d) & \text{if } (i,j,m) = (i_0, j_0, m_0) \\ 0 & \text{otherwise.} \end{cases} \tag{3.78}$$

In the absence of noise, this leads to

$$e^{(m_0)}(n) = \alpha u_{i_0 j_0}^{(m_0)}(n-d). \tag{3.79}$$

That is, the equalizer output is a scaled and shifted version of the signal of the virtual user (i_0, j_0, m_0). After we get all the subequalizers, their outputs are interleaved to get the equalized output of the high rate user (i_0, j_0)

$$\ldots, e^{(0)}(n), e^{(1)}(n), \ldots, e^{(p_{i_0}-1)}(n), e^{(0)}(n+1),$$

$$e^{(1)}(n+1)\ldots,e^{(p_{i_0}-1)}(n+1),\ldots \tag{3.80}$$

B. Multirate CSEA (MR-CSEA)

In this subsection, the CSEA method presented in [57] is extended to multirate systems.

Following [57], we define an $[N(d+1)] \times [N(d+1)]$ matrix $\mathcal{T}_d$ as

$$\mathcal{T}_d \triangleq \begin{bmatrix} 0 & \cdots & 0 & I_N \\ 0 & \cdots & I_N & 0 \\ \vdots & \ddots & \vdots & \vdots \\ I_N & \cdots & 0 & 0 \end{bmatrix}, \tag{3.81}$$

and an $[NL_e] \times [NL_e]$ matrix $\mathcal{T}^{(d)}$ as

$$\mathcal{T}^{(d)} \triangleq \begin{bmatrix} \mathcal{T}_d & 0 \\ 0 & I_{N(L_e-1-d)} \end{bmatrix}. \tag{3.82}$$

In the absence of noise, following [97] and [57], if the equalizer output has the format given in (3.79), it can be shown that the equalizer should satisfy the following equation:

$$\mathcal{T}^{(d)}\mathcal{R}_{yy}\tilde{\mathbf{f}}^{(m_0)} = \alpha^*\mathcal{T}^{(d)}\tilde{\mathbf{h}}_{i_0j_0}^{(m_0,d)} = \alpha^*\mathcal{C}_{i_0j_0}^{(m_0,d)}\mathbf{g}_{i_0j_0}, \tag{3.83}$$

where $\mathcal{R}_{yy} \triangleq E\{\mathbf{Y}(k)\mathbf{Y}^H(k)\}$, and

$$\mathcal{C}_{i_0j_0}^{(m_0,d)} \triangleq \begin{bmatrix} \mathbf{C}_{i_0j_0}^{(m_0,d)} \\ 0 \end{bmatrix}_{[L_eN]\times[\bar{L}_gN]}, \tag{3.84}$$

$$\tilde{\mathbf{h}}_{i_0j_0}^{(m_0,d)} \triangleq [\mathbf{h}_{i_0j_0}^{(m_0)H}(d),\ldots,\mathbf{h}_{i_0j_0}^{(m_0)H}(0),0,\ldots,0]^H. \tag{3.85}$$

Let $\mathcal{U}_{i_0j_0}^{(m_0,d)}$ denote an orthonormal basis for the orthogonal complement of $\mathcal{C}_{i_0j_0}^{(m_0,d)}$. Because $\mathcal{C}_{i_0j_0}^{(m_0,d)}$ is of full column rank, $\mathcal{U}_{i_0j_0}^{(m_0,d)}$ is an $[NL_e] \times [NL_e - N\bar{L}_g]$ matrix. This leads to

$$\mathcal{U}_{i_0j_0}^{(m_0,d)H}\mathcal{T}^{(d)}\mathcal{R}_{yy}\tilde{\mathbf{f}}^{(m_0)} \triangleq \mathcal{A}^{(m_0)}\tilde{\mathbf{f}}^{(m_0)} = 0. \tag{3.86}$$

Thus, in order to extract the desired virtual user, a necessary condition is that $\tilde{\mathbf{f}}^{(m_0)}$ belongs to the null space of $\mathcal{A}^{(m_0)}$. Let $\Pi^{\perp}_{\mathcal{A}^{(m_0)}}$ denote the $[NL_e] \times [NL_e]$ projection matrix onto the null space of $\mathcal{A}^{(m_0)}$. Thus the combined response is given by

$$\Theta = (\tilde{\mathbf{H}}\Pi^{\perp}_{\mathcal{A}^{(m_0)}})\tilde{\mathbf{f}}^{(m_0)}. \tag{3.87}$$

Then the subequalizer $\tilde{\mathbf{f}}^{(m_0)}$ can be calculated using the following two-step iterative procedure similar to that of [57]:

$$\tilde{\mathbf{f}}' = (\Pi^{\perp}_{\mathcal{A}^{(m_0)}}\mathcal{R}_{yy}\Pi^{\perp}_{\mathcal{A}^{(m_0)}})^{\#}\Pi^{\perp}_{\mathcal{A}^{(m_0)}}\mathbf{d} \tag{3.88}$$

$$\tilde{\mathbf{f}}^{(n+1)} = \frac{\tilde{\mathbf{f}}'}{\sqrt{\tilde{\mathbf{f}}'^H\mathcal{R}_{yy}\tilde{\mathbf{f}}'}}, \tag{3.89}$$

where

$$\mathbf{d} = \frac{\mathrm{cum}\{e^{*(m_0)}(k), e^{*(m_0)}(k), e^{(m_0)}(k), \mathbf{Y}(k)\}}{\mathrm{cum}_4\{u_{i_0j_0}(k)\}}, \tag{3.90}$$

with

$$\begin{aligned}\mathrm{cum}(x_1, x_2, x_3, x_4) &= E\{x_1x_2x_3x_4\} - E\{x_1x_2\}E\{x_3x_4\} \\ &\quad -E\{x_1x_3\}E\{x_2x_4\} - E\{x_1x_4\}E\{x_2x_3\}\end{aligned}$$

(x_1, x_2, x_3 and x_4 are zero-mean random variables), and $e^{(m_0)}(k)$ is the equalization output of the nth iteration. As in [57], the code-constrained SEA is followed by unconstrained SEA (without the projection operator) to enhance the system performance.

MC System

Consider the following condition (the counterpart to the condition **C**3.1):

C 3.2 *The $[NL_e] \times [\bar{L}_gN + 1]$ matrix $[C^{(m_0,d)}_{i_0j_0} : \mathcal{T}^{(d)}\tilde{\mathbf{h}}^{(m,d_0)}_{ij}]$ has full column rank for every $(i, j, m) \neq (i_0, j_0, m_0)$ and every $d_0 \in \{d - \bar{L}_g + 1, d - \bar{L}_g + 2, \ldots, d\}$ where $L_e \geq d + 1$ and $d \geq 2$.*

As proved in [50], under condition **C**3.2, any solution that satisfies (3.79) with the constrain (3.86) corresponds to $(i, j, m) = (i_0, j_0, m_0)$ and $d_0 \in \{d - \bar{L}_g + 1, d - \bar{L}_g + 2, \ldots, d\}$. In MC systems, condition **C**3.2 is easy to be satisfied, since each virtual user is assigned a distinct spreading code.

Because all virtual users corresponding to a high rate user share the same channel, the equalizer $\hat{\bar{\mathbf{f}}}^{(m_0)}$, which is obtained from the iteration (3.88)-(3.89), can be used to set the initial values of subequalizers for all other virtual users. To ensure different virtual users which correspond to one high-rate user have the same equalizer delay and scale factor, the initialization method of [97] is adopted. For MC systems, we then get the initial guess for $\bar{\mathbf{f}}^{(m)}$, $m \neq m_0$, from (3.83) as

$$\hat{\bar{\mathbf{f}}}^{(m)} := [\mathcal{T}^{(d)}\mathcal{R}_{yy}]^{\#}\mathcal{C}_{i_0 j_0}^{(m,d)}[\mathcal{C}_{i_0 j_0}^{(m_0,d)}]^{\#}\mathcal{T}^{(d)}\mathcal{R}_{yy}\hat{\bar{\mathbf{f}}}^{(m_0)}. \tag{3.91}$$

This initial guess is used to initialize the SEA procedure to extract virtual user m, $\forall m \neq m_0$.

VSL System

In VSL systems, the spreading codes of virtual users corresponding to the same user are simply shifted version of each other, so the condition **C**3.2 is not necessarily satisfied. An example is given in [97]. Therefore, **C**3.2 has to be modified as

C 3.3 *For VSL systems, the* $[NL_e] \times [\bar{L}_g N + 1]$ *matrix* $[\mathcal{C}_{i_0 j_0}^{(m_0,d)} \ \vdots \ \mathcal{T}^{(d)}\tilde{\mathbf{h}}_{ij}^{(m,d_0)}]$ *has full column rank for every* $(i, j) \neq (i_0, j_0)$*, every* $m \in \{0, 1, \ldots, p_i - 1\}$*, every* $m_0 \in \{0, 1, \ldots, p_{i_0} - 1\}$*, and every* $d_0 \in \{d - \bar{L}_g + 1, d - \bar{L}_g + 2, \ldots, d\}$ *where* $L_e \geq d + 1$ *and* $d \geq 2$.

Under condition **C**3.3, the solution that yields (3.79) and satisfies (3.86) corresponds to $(i, j) = (i_0, j_0)$, $m \in \{0, 1, \ldots, p_{i_0} - 1\}$, and $d_0 \in \{d - \bar{L}_g + 1, d - \bar{L}_g + 2, \ldots, d\}$. This indicates that the two step iteration (3.88)-(3.89) will converge to an equalizer corresponding to a virtual user of high rate user (i_0, j_0), but it is not guaranteed that (i_0, j_0, m_0) will be extracted.

Due to the fact that the VSL spreading codes $\mathbf{c}_{ij}^{(m)}$ for $m = 0, 1, \ldots, p_i - 1$ share the same $\mathbf{c}_{ij}$, special care needs to be taken in order to extract the virtual users in correct order. Define

$$\mathcal{X}_c := \begin{bmatrix} \mathbf{0}_{N_{i_0} \times [NL_e - N_{i_0}]} & \mathbf{0}_{N_{i_0} \times N_{i_0}} \\ \mathbf{I}_{[NL_e - N_{i_0}]} & \mathbf{0}_{[NL_e - N_{i_0}] \times N_{i_0}} \end{bmatrix} \tag{3.92}$$

then it can be proved that [97]

$$\mathcal{X}_c^{(p_{i_0} - m_0)} \mathcal{T}^{(d)} \tilde{\mathbf{h}}_{i_0 j_0}^{(m_0, d_0)} = \mathcal{T}^{(d)} \tilde{\mathbf{h}}_{i_0 j_0}^{(0, d_0 - 1)}. \tag{3.93}$$

Let $\tilde{\mathbf{f}}_{d_0}^{(m)}$ denote the subequalizer of virtual user (i_0, j_0, m) with equalization delay d_0. In the absence of noise, it follows from (3.83) and (3.93) that

$$\mathcal{T}^{(d)} \mathcal{R}_{yy} \tilde{\mathbf{f}}_{d_0 - 1}^{(0)} = \mathcal{X}_c^{(p_{i_0} - m_0)} \mathcal{T}^{(d)} \mathcal{R}_{yy} \tilde{\mathbf{f}}_{d_0}^{(m_0)}. \tag{3.94}$$

Therefore, instead of (3.91), once the system converges to a virtual user (i_0, j_0, m_0) with delay d_0, i.e. $\hat{\tilde{\mathbf{f}}}_{d_0}^{(m_0)}$ is obtained, we use following method to initialize the subequalizers for virtual user (i_0, j_0, m):

$$\begin{aligned} \hat{\tilde{\mathbf{f}}}_{d_0}^{(m)} &:= (\mathcal{T}^{(d)} \mathcal{R}_{yy})^{\#} \mathcal{X}_c^{(m - m_0)} \mathcal{T}^{(d)} \mathcal{R}_{yy} \hat{\tilde{\mathbf{f}}}_{d_0}^{(m_0)} \quad (\text{for } m_0 < m < p_i), & (3.95) \\ \hat{\tilde{\mathbf{f}}}_{d_0 - 1}^{(m)} &:= (\mathcal{T}^{(d)} \mathcal{R}_{yy})^{\#} \mathcal{X}_c^{(p_i + m - m_0)} \mathcal{T}^{(d)} \mathcal{R}_{yy} \hat{\tilde{\mathbf{f}}}_{d_0}^{(m_0)} \quad (\text{for } 0 \le m < m_0). & (3.96) \end{aligned}$$

The interleaved subequalizer output will be

$$\begin{gathered} \ldots, \alpha u_{i_0 j_0}^{(m_0)}(n - d_0), \ldots, \alpha u_{i_0 j_0}^{(p_{i_0} - 1)}(n - d_0), \\ \alpha u_{i_0 j_0}^{(0)}(n + 1 - d_0), \ldots, \alpha u_{i_0 j_0}^{(m_0 - 1)}(n + 1 - d_0), \\ \alpha u_{i_0 j_0}^{(m_0)}(n + 1 - d_0), \alpha u_{i_0 j_0}^{(m_0 + 1)}(n + 1 - d_0), \ldots \end{gathered} \tag{3.97}$$

From (3.97), we can see that, even it is not sure which virtual user is extracted first, the interleaved output is still in correct order.

3.3.3 Summary of the Multirate CSEA Approach

The Multirate CSEA algorithm for both MC and VSL systems can be summarized as:

1) Take $m_0 = 0$, and use multirate CSEA method to extract virtual user (i_0, j_0, m_0). The iteration is considered converged if $\|\tilde{\mathbf{f}}^{(n+1)} - \tilde{\mathbf{f}}^{(n)}\| < \varepsilon$ (where ε is a small positive number, such as 10^{-3}). For MC system, when the algorithm converges, it will converge to user $(i_0, j_0, 0)$. For VSL system, the algorithm may converge to (i_0, j_0, m_0), with $m_0 \neq 0$, since the spreading codes of all the virtual users corresponding to one high rate user are highly correlated (please refer to equation (3.68). However, in this case, even if $m_0 \neq 0$, the resulted output (see equation (3.97)) will only be a shift version compared to that of $m_0 = 0$.

2) For MC systems, use (3.91) to initialize the subequalizers for all other virtual users (i_0, j_0, m), $m \in \{0, 1, \ldots, p_{i_0} - 1\}$, and $m \neq m_0$. For VSL systems, use the initialization (3.95) and (3.96). Then use SEA procedure to extract virtual users (i_0, j_0, m), $m \in \{0, 1, \ldots, p_{i_0} - 1\}$, and $m \neq m_0$.

3) Interleave the outputs of the subequalizers to obtain the output of user (i_0, j_0) according to (3.80).

Remark 3.1 *Please refer to Section 3.2.3 and Appendix C for the convergence and identifiability analysis.*

Remark 3.2 *Another possibility is to use $\mathcal{P}_A = \mathcal{R}_{yy}^{-1}\mathcal{T}^{(d)}\mathcal{C}_{i_0j_0}^{(m_0,d)}[\mathcal{T}^{(d)}\mathcal{C}_{i_0j_0}^{(m_0,d)}]^T\mathcal{R}_{yy}^{-1}$ to project the equalizer onto the weighted null space of $\mathcal{A}^{m_0}$ as suggested in [98]. In the absence of noise or when SNR is high, $\mathcal{R}_{yy}$ may not be full rank or tend to be ill-conditioned, therefore $\mathcal{R}_{yy}^{-1}$ has to be replaced with the pseudoinverse of $\mathcal{R}_{yy}$. In this case, $\mathcal{P}_A$ is no longer a projection matrix onto the null space of $\mathcal{A}^{m_0}$. Simulation results indicate that when $\mathcal{P}_A$ is used, the system still converges, but loses control of which user the system is extracting, so we stick to the projection matrix $\Pi^{\perp}_{\mathcal{A}^{(m_0)}}$ in this research.*

3.3.4 Simulation Examples

In this section, simulation examples are explored to illustrate the proposed approaches and compare the performance with that of MR-CC-IFC in [97] and MMSE method with known channels. For both VSL and MC schemes, we consider DS-CDMA systems with two different symbol rates. Each user transmits 4-QAM signals. The symbol rate of a high rate user is 4 times that of a low rate user. The basic rate processing gain is 32. Thus, each high rate user can be converted to 4 virtual users. The spreading codes were randomly generated binary (± 1 with equal probability) sequences. The multi-path channels for each users have 4 paths. The transmission delays are uniformly distributed over one basic rate symbol (32 chips), and the remaining 3 paths have delays (w.r.t. the first arrival) uniformly distributed over one basic rate symbol. The multi-path amplitudes are mutually independent, complex Gaussian with zero mean and unit variance. The channels for each user were generated randomly for each Monte Carlo run. The subequalizers of length $L_e = 5$ and delay $d = 3$ were designed based on a record length of 1024 symbols. Then they were applied to an independent record of 3072 symbols for calculating the normalized equalization mean-square error (NEMSE) (normalized by the desired user's information sequence power). NEMSE was averaged over 100 Monte Carlo runs to evaluate the performance of the equalizers. In the equal power case, a symbol of a high rate user is transmitted with the same energy as a symbol of a low rate user. In the near far case, the power of the desired user is 10dB below that of other users at the same rate. SNR refers to the chip signal-noise-ratio with respect to the desired user. For MR-CC-IFC approach, we set $\mu_{\mathcal{A}} = \mu_{\mathcal{B}} = \mu_{\mathcal{D}} = 2$, where $\mu_{\mathcal{A}}$, $\mu_{\mathcal{B}}$, and $\mu_{\mathcal{D}}$ are the scaling factors for certain penalty functions. Please refer to [97] for the meaning of those coefficients. For both MR-CSEA and MR-CC-IFC methods, $\varepsilon = 10^{-3}$ was used in the simulations, and the iterative procedure is ended either when this criterion is met, or 30 iterations have been performed.

SNR (dB)	0	5	10	15	20	25
MR-CC-IFC (s)	20.2	14.5	14.0	19.8	20.4	19.8
MR-CSEA (s)	28.5	24.08	17.4	3.7	3.9	3.7
MR-CSEA (without enhancement) (s)	21.3	17.4	13.0	2.4	2.3	2.3

Table 3.1. Example 1 - VSL system, average time per run, equal power case, same condition as in Fig.3.1.

A. Example 1

In this simulation example, we consider a DS-CDMA system with 3 users (two basic rate users and a high rate user). The high rate user is the desired user. The results for VSL systems are shown in Fig. 3.1 and Fig. 3.2, and the results for MC systems are shown in Fig. 3.3 and Fig. 3.4. It can be observed that, when both methods converge, the MR-CSEA approach has better performance than that of the MR-CC-IFC approach. At high SNRs, we can get comparable results with MR-CC-IFC by calculating the subequalizers using (3.91) for MC systems and (3.95)-(3.96) for VSL systems directly. In the meantime, due to the existence of noise, we can get better results if we enhance each subequalizer individually as in this research.

Table 3.1 shows the average time in seconds per Monte Carlo run for both algorithms in the equal power case in the VSL system. The model of the computer used in this simulation is Dell Dimension 4550, P4 2.8GHz, 1G RAM. From the table, we can see that, when SNR$\geq$ 15dB, the MR-CSEA method converges much faster than the MR-CC-IFC method.

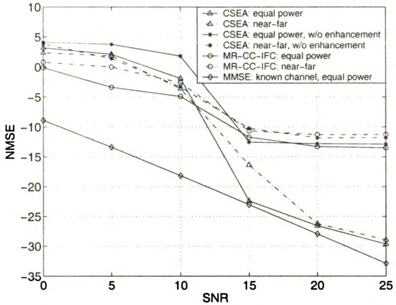

Figure 3.1. VSL system - Normalized MSE for the high rate user: 8 chips/symbol for the high rate (HR) user, 32 chips/symbol for basic rate (BR) users, 1 HR and 2 BR users, record length = 1024 BR symbols, evaluation length = 3072 BR symbols, 100 Monte Carlo runs. ("without enhancement" means that the subequalizers are calculated from (3.95)-(3.96) directly.)

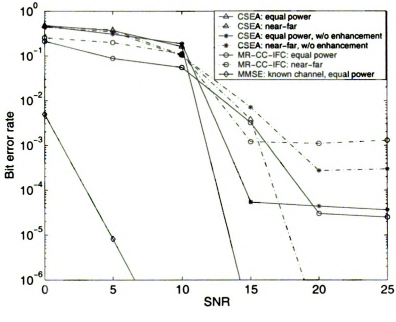

Figure 3.2. VSL system - BER of the high rate user, same condition as Figure 3.1

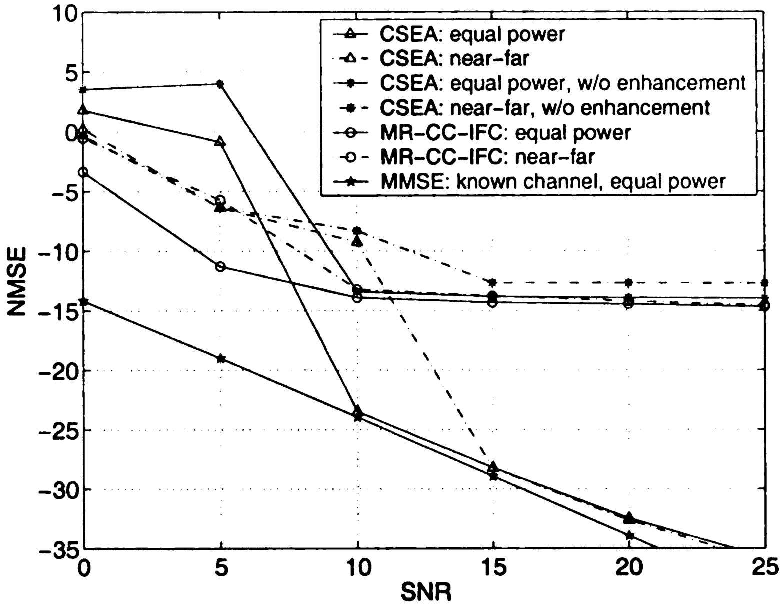

Figure 3.3. MC system - Normalized MSE for the high rate user: 32 chips/symbol for each symbol stream of the high rate (HR) user, 32 chips/symbol for basic rate (BR) users, 1 HR and 2 BR users, record length = 1024 BR symbols, evaluation length = 3072 BR symbols, 100 Monte Carlo runs. ("without enhancement" means that the subequalizers are calculated from (3.91) directly)

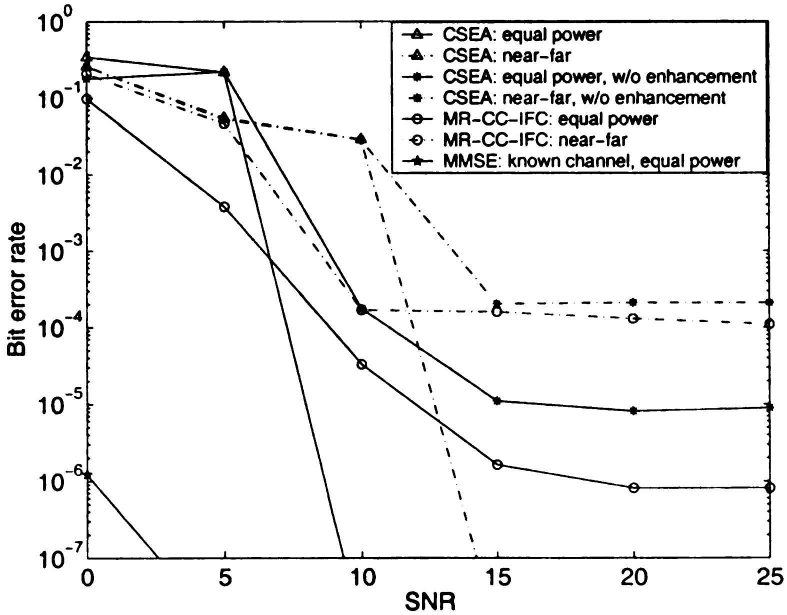

Figure 3.4. MC system - BER of the high rate user, same condition as Figure 3.3

B. Example 2

In this example, we study the performance of both approaches for different loads in both VSL and MC systems. We fixed the desired user's SNR at 20dB and vary the number of active users. In VSL systems, let the pair (HR users, LR users)=(1,1), (1,2), (1,3), (1,4), (2,1), which corresponds to 5 $\sim$ 9 virtual users. In MC systems, the number of users (8, 10, 12, 14, 16, 18) corresponds to the pair sequence (HR users, LR users)=(1,4), (2,2), (2,4), (3,2), (3,4), (4,2). The desired user is the first high rate user. The simulation results of MC and VSL systems are shown in Fig. 3.5 and Fig. 3.6, respectively.

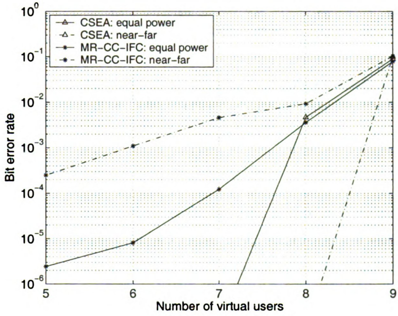

Figure 3.5. Load test of VSL systems. Bit error rate of different loads at SNR = 20dB. Totally 100 Monte Carlo runs. The sequence (5, 6, 7, 8, 9) of virtual users corresponds to the pair sequence (number of HR users, number of BR users) = (1,1), (1,2), (1,3), (1,4), (2,1).

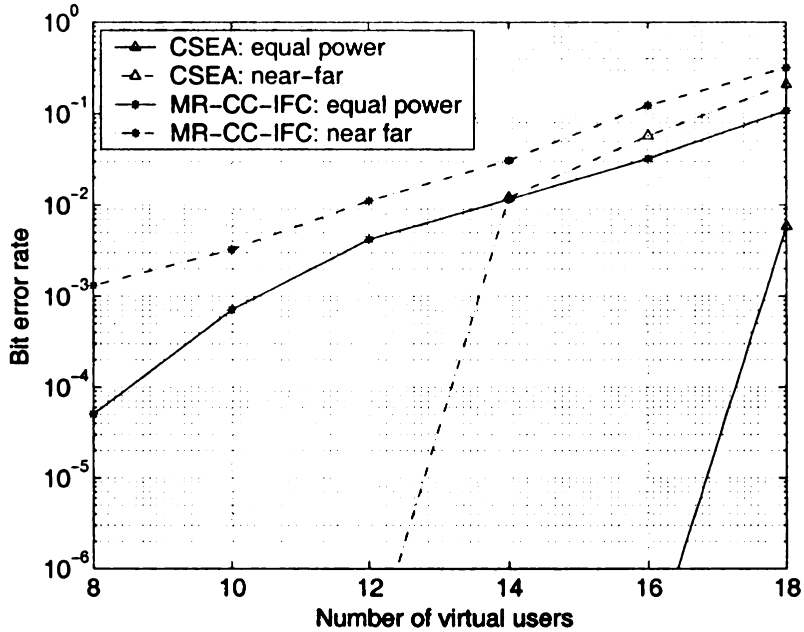

Figure 3.6. Load test of MC systems. Bit error rate of different loads at SNR = 20dB. Totally 100 Monte Carlo runs. The sequence (8, 10, 12, 14, 16, 18) corresponds to the pair sequence (1,4), (2,2), (2,4), (3,2), (3,4), (4,2).

3.4 Summary

In this chapter, code-constrained super-exponential approach is developed for blind equalization of multirate DS-CDMA signals. Both multicode and variable sequence length are considered. Simulation examples demonstrate that, when the algorithm actually converges (SNR$\geq$ 15dB), MR-CSEA delivers better results with faster convergence speed compared with existing cumulant maximization blind detectors.

CHAPTER 4

Blind Equalization for Long-Code CDMA Systems

In this chapter, we consider blind detection of long-code CDMA signals. Multistep linear prediction based blind channel estimation methods are developed for both downlink and uplink DS-CDMA, and the equalizers can readily be designed based on the estimation results. For downlink CDMA, the scrambled chip-rate signal is recovered first. *The descrambled signal is then regarded as the output of a short-code CDMA system*, and SEA approach is applied to extract the symbol-rate signal. For uplink CDMA, first, based on multistep linear prediction methods, *convolutive mixtures are reduced to instantaneous mixtures.* Secondly, for systems with nonconstant modulus spreading codes, the channels can be identified by exploiting only the second-order statistics of the signal. While if the spreading codes are constant modulus, higher-order statistics approaches should be utilized to perform blind channel identification.

4.1 Blind Equalization For Downlink Long-Code CDMA Systems

In downlink long-code CDMA, the signals destined for all users are transmitted synchronously. Therefore, at each mobile device, the received signal components corresponding to different users share the same channel impulse response. For this reason, chip-level equalization can be performed to restore the signals transmitted from the base station, and then the orthogonality between different data streams can be exploited to recover the signals of the desired user (see [99–103]). In this section, inspired by [20] and [104], multistep linear predictor based (MSLP) algorithms are applied to perform blind channel estimation, then MMSE equalizer is designed to extract the chip-rate signal.

4.1.1 Multistep Linear Prediction Based Blind Channel Estimation

The system model presented in Section 2.2 is applied in this section. Consider a downlink CDMA system with M users, and each user has P receive antennas, then the received signal vector is given by (2.27):

$$\begin{aligned} \mathbf{y}(n) &= \sum_{l=0}^{L-1} \mathbf{g}(l)s(n-l) + \mathbf{w}(n) \\ &:= \mathbf{y}_s(n) + \mathbf{w}(n). \end{aligned} \tag{4.1}$$

Following [20], $\mathbf{y}_s(n)$ can be decomposed in the following format:

$$\mathbf{y}_s(n) = \hat{\mathbf{y}}_s(n|n-l) + \mathbf{e}(n|n-l), \quad (l = 1, 2, ...) \tag{4.2}$$

where $\hat{\mathbf{y}}_s(n|n-l)$ is the l-step (ahead) linear predictor of $\mathbf{y}_s(n)$ given $\{\mathbf{y}_s(k), k \leq n-l\}$, and has the following presentation

$$\hat{\mathbf{y}}_s(n|n-l) = \sum_{i=l}^{L_l} \mathbf{A}_i^{(l)} \mathbf{y}_s(n-i). \tag{4.3}$$

for some $L_l \leq L + l - 2$. The prediction error $\mathbf{e}(n|n-l)$ is given by

$$\mathbf{e}(n|n-l) = \sum_{i=0}^{l-1} \mathbf{g}(i)s(n-i). \tag{4.4}$$

satisfying

$$E\{\mathbf{e}(n|n-l)\mathbf{y}_s^H(n-m)\} = 0, \quad \forall m \geq l. \tag{4.5}$$

From (4.2)-(4.5), we can get

$$
\begin{aligned}
\mathbf{R}_{y_s}(m) &:= E\{\mathbf{y}_s(n)\mathbf{y}_s^H(n-m)\} \\
&= \sum_{i=l}^{L_l} \mathbf{A}_i^{(l)} E\{\mathbf{y}_s(n-i)\mathbf{y}_s^H(n-m)\} \\
&= \sum_{i=l}^{L_l} \mathbf{A}_i^{(l)} \mathbf{R}_{y_s}(m-i) \\
&= [\mathbf{A}_l^{(l)}, \mathbf{A}_{l+1}^{(l)}, \ldots, \mathbf{A}_{L_l}^{(l)}] \begin{bmatrix} \mathbf{R}_{y_s}(m-l) \\ \mathbf{R}_{y_s}(m-l-1) \\ \vdots \\ \mathbf{R}_{y_s}(m-L_l) \end{bmatrix}.
\end{aligned} \tag{4.6}
$$

Define

$$
\mathcal{R}_{y_s} := \begin{bmatrix} \mathbf{R}_{y_s}(0) & \mathbf{R}_{y_s}(1) & \cdots & \mathbf{R}_{y_s}(L_l-l) \\ \mathbf{R}_{y_s}(-1) & \mathbf{R}_{y_s}(0) & \cdots & \mathbf{R}_{y_s}(L_l-l+1) \\ \vdots & \vdots & \cdots & \vdots \\ \mathbf{R}_{y_s}(l-L_l) & \mathbf{R}_{y_s}(l+1-L_l) & \cdots & 0 \end{bmatrix}. \tag{4.7}
$$

It follows from (4.6)-(4.7) that

$$
[\mathbf{A}_l^{(l)}, \mathbf{A}_{l+1}^{(l)}, \ldots, \mathbf{A}_{L_l}^{(l)}]\mathcal{R}_{y_s} = [\mathbf{R}_{y_s}(l), \mathbf{R}_{y_s}(l+1), \ldots, \mathbf{R}_{y_s}(L_l)]. \tag{4.8}
$$

A minimum norm solution to (4.8) can be obtained as [105]

$$
[\mathbf{A}_l^{(l)}, \mathbf{A}_{l+1}^{(l)}, \ldots, \mathbf{A}_{L_l}^{(l)}] = [\mathbf{R}_{y_s}(l), \mathbf{R}_{y_s}(l+1), \ldots, \mathbf{R}_{y_s}(L_l)]\mathcal{R}_{y_s}^{\#}. \tag{4.9}
$$

From (4.2) and (4.3), we have

$$
\mathbf{e}(n|n-l) = \sum_{i=0}^{\bar{L}} \bar{\mathbf{A}}_i^{(l)} \mathbf{y}_s(n-i), \quad \forall l \geq 1, \tag{4.10}
$$

where $\tilde{L} = L_l - l + 1 + d$, and

$$\bar{\mathbf{A}}_i^{(l)} = \begin{cases} \mathbf{I}_K & i = 0 \\ 0 & 1 \leq i \leq l-1 \\ -\mathbf{A}_i^{(l)} & l \leq i \leq L_l \\ 0 & L_l \leq i \leq \tilde{L} \end{cases} . \tag{4.11}$$

Define

$$\bar{\mathbf{e}}_l(n) := \mathbf{e}(n|n-l) - \mathbf{e}(n|n-l+1), \tag{4.12}$$

and

$$\mathbf{E}(n) = [\bar{\mathbf{e}}_{d+1}^T(n+d), \bar{\mathbf{e}}_d^T(n+d-1), \dots, \bar{\mathbf{e}}_2^T(n+1), \mathbf{e}^T(n|n-1)]^T, \tag{4.13}$$

then it can be derived from (4.2)-(4.4) that

$$\mathbf{E}(n) = \begin{bmatrix} \mathbf{g}(d) \\ \mathbf{g}(d-1) \\ \vdots \\ \mathbf{g}(0) \end{bmatrix} s(n) := \tilde{\mathbf{g}} s(n). \tag{4.14}$$

According to (A1), we have $E\{s(n)s(n)^*\} = 1$, then it can be obtained that

$$\mathbf{R}_{EE} := E\{\mathbf{E}(n)\mathbf{E}^H(n)\} = \tilde{\mathbf{g}}\tilde{\mathbf{g}}^H. \tag{4.15}$$

Note that $\mathbf{R}_{EE}$ is a rank one matrix, in the noise free case, the channel impulse response vector $\tilde{\mathbf{g}}$ (which contains the channel impulse response from the signal source to every receive antenna) can be obtained up to a scalar from (4.15).

4.1.2 MMSE Equalization and SEA Enhancement

In this section, MMSE equalizer is designed based on the channel estimation result to recover the chip-rate signal transmitted from the base station. Next, the descrambled chip sequence is treated as the channel output of an unknown short-code CDMA system, and SEA approach is applied to extract the symbol-rate information sequence of the desired user.

Let $\{\mathbf{f}_d(k)\}_{k=0}^{L_e-1}$ denote the $K \times 1$ vector equalizer with equalization delay d. The equalizer output is then given by

$$\hat{s}(n-d) = \sum_{i=0}^{L_e-1} \mathbf{f}_d^H(i)\mathbf{y}(n-i). \tag{4.16}$$

The mean square error between $\{s(n)\}$ and its estimate value is

$$E\{|e(n)|^2\} = E\left\{|\hat{s}(n) - s(n)|^2\right\}. \tag{4.17}$$

Define

$$\tilde{\mathbf{f}}_d := [\mathbf{f}_d^T(0), \mathbf{f}_d^T(1), \ldots, \mathbf{f}_d^T(L_e-1)]^T, \tag{4.18}$$

$$\mathbf{Y}(n) := [\mathbf{y}^T(n), \mathbf{y}^T(n-1), \ldots, \mathbf{y}^T(n-L_e+1)]^T, \tag{4.19}$$

then, the MMSE solution which minimizes (4.17) is given by [106]

$$\tilde{\mathbf{f}}_d = R_Y^{\#}\mathbf{g}_d. \tag{4.20}$$

where $R_Y = E\{\mathbf{Y}(n)\mathbf{Y}(n)^H\}$, and $\mathbf{g}_d = [\mathbf{g}^T(d), \mathbf{g}^T(d-1), \mathbf{g}^T(0), 0, \ldots, 0]^T$.

In downlink, signals of all users are synchronous. According to (2.22), the de-scrambling process $\hat{r}(n) = \hat{s}(n)d(n)$ results in an estimate of $r(n)$. At this stage, the desired user's signal can be extracted directly using correlators. That is

$$\hat{u}_m(k) = \frac{1}{N}\mathbf{c}_m^T(k)\hat{\mathbf{r}}(k). \tag{4.21}$$

where

$$\hat{\mathbf{r}}(k) := [\hat{r}(kN), \hat{r}(kN+1), \cdots, \hat{r}(KN+N-1)]^T. \tag{4.22}$$

Instead of depreading the descrambled signal $\hat{r}(n)$ directly, here we choose to model it as an MIMO short-code CDMA system

$$\hat{\mathbf{r}}(k) = \sum_{m=1}^{M}\sum_{l=0}^{L_0-1}\bar{\mathbf{h}}_m(l)u_m(k-l), \tag{4.23}$$

where the channel responses $\{\bar{\mathbf{h}}_m(l)\}$, $m = 1, \ldots, M$, are unknown. Therefore, existing blind multiuser detection methods for short-code CDMA system can be applied to eliminate the multiuser interference. In this work, super exponential algorithm (SEA) is chosen to extract the signal of the desired user from $\{\hat{r}(k)\}$. Suppose user 1 is the desired user. Our goal is to design an $N \times 1$ vector equalizer $\{\mathbf{f}'(i)\}_{i=0}^{Le'-1}$

$$u_1(n-d') = \sum_{i=0}^{L'_e-1}\mathbf{f}'^H(i)\hat{\mathbf{r}}(n-i). \tag{4.24}$$

Comparing (4.24) with (4.21), $\mathbf{c}_1$ can be used to initialize $\mathbf{f}'^{(0)}$ to carry out the following two-stage iteration [58]:

$$\begin{aligned}\breve{\mathbf{f}}'^{(n+1)} &= R_r^{\#}\mathbf{v},\\ \mathbf{f}'^{(n+1)} &= \frac{\breve{\mathbf{f}}'^{(n+1)}}{\sqrt{\breve{\mathbf{f}}'^{(n+1)H}R_r\breve{\mathbf{f}}'^{(n+1)}}},\end{aligned} \tag{4.25}$$

where

$$\begin{aligned}R_r &= E\{\hat{\mathbf{r}}(n)\hat{\mathbf{r}}^H(n)\},\\ \mathbf{v} &= \frac{\text{cum}\{e^*(k), e^*(k), e(k), \hat{\mathbf{r}}(k)\}}{\text{cum}_4\{u_1(k)\}},\end{aligned}$$

and $\{e(k)\}$ is the equalization result using $\mathbf{f}'^{(n)}$

$$e(k) = \sum_{i=0}^{L'_e-1}[\mathbf{f}'^{(n)}(i)]^H\hat{\mathbf{r}}(k-i). \tag{4.26}$$

The iteration is quit once $|\mathbf{f}'^{(n+1)} - \mathbf{f}'^{(n)}| < \varepsilon$, where ε is a small positive number. Please refer to Chapter 3 for more details.

4.1.3 Simulation Examples

In the simulations, it is assumed that the base station transmits QPSK signals to each mobile user with equal power. The spreading gain is $N = 16$, and the spreading sequences were randomly generated. Gold sequence with period $(2^{18} - 1)$ is used to scramble the spread signals. The downlink channel corresponding to each receive antenna has 4 paths, and the first path is the dominant path. The initial transmission delay and the delay spread are unknown, only assumed to be uniformly distributed over one symbol period. The noise is white Gaussian with zero mean, and SNR refer to the chip rate signal to noise ratio with respect to the desired user. The channels were randomly generated. Channel estimation and equalizer design were based only on a blocksize of 256 symbols. MSE of channel estimation (CHMSE) and MSE of input-output symbols (SMSE) were calculated over 100 Monte Carlo runs. In the simulations, by "w/o SEA enhancement", we mean using $\mathbf{c}_1$ as the correlator to extract user 1 directly after we get $\{\hat{\mathbf{r}}(n)\}$.

In Example 1, the number of users is assumed to be 8. Both one and two receive antennas were considered. The proposed approach is compared with MMSE equalizer with known channel, which is not enhanced with SEA. The CHMSE is shown in Fig.4.1, while the performance of the equalizer is shown in Fig.4.2 and Fig.4.3. It can be seen that, compared with direct correlation based user extraction, SEA enhancement delivers much better results. Meanwhile, as expected, the space diversity provided by applying multiple receive antennas (2 in our case) results in significant performance improvement. Because of the superior performance of the channel estimation algorithm, the equalization results (without enhancement) using the estimated channels are very close to those of using known channel parameters.

In Example 2, SNR was fixed at 15dB, and the proposed approach was tested under different loads. The results are shown in Fig.4.4 and Fig. 4.5. It can be seen that SEA enhancement can increase the system capacity significantly.

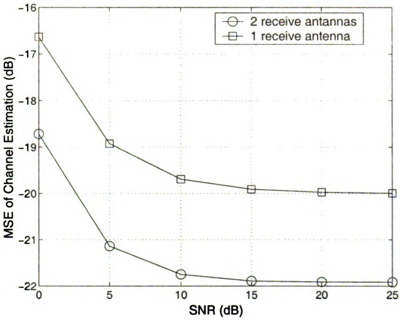

Figure 4.1. Example 1. MSE of channel estimation for 8 users, N=16, channel estimation was based on 256 symbols, MSE was averaged over 100 Monte Carlo runs.

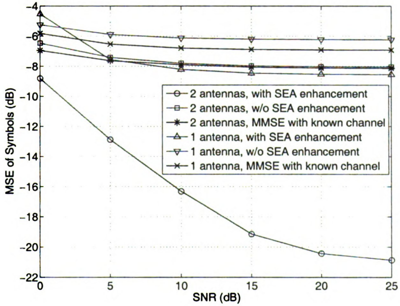

Figure 4.2. Example 1. MSE of equalization for 8 users, N=16, 100 Monte Carlo runs and 1024 symbols per run.

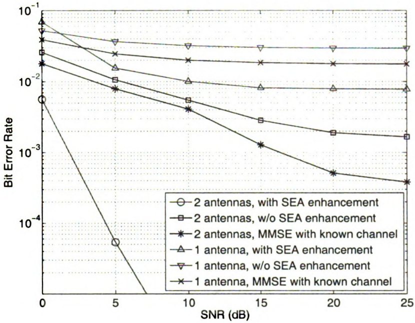

Figure 4.3. Example 1. BER performance, same condition as that in Figure 4.2.

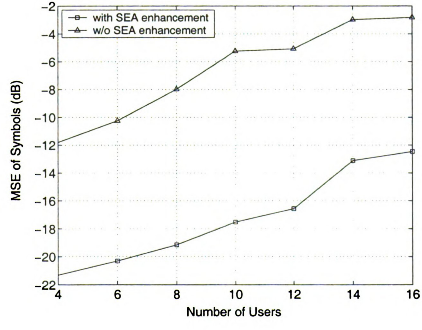

Figure 4.4. Example 2. Symbol MSE under different loads, SNR = 15dB, 2 receive antennas, N=16, 100 Monte Carlo runs and 1024 symbols per run.

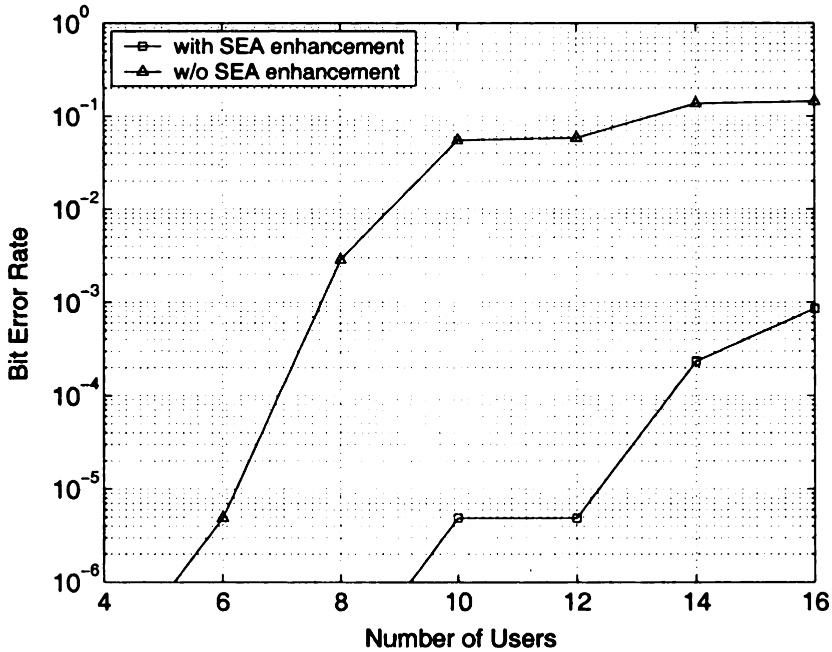

Figure 4.5. Example 2. BER under different loads, SNR = 15dB, 2 receive antennas, N=16,100 Monte Carlo runs and 1024 symbols per run.

4.2 Blind Equalization for Uplink Long-Code CDMA with Non-Constant Modulus Spreading Sequences

In this section, the long-code CDMA system is characterized as a time-invariant MIMO system as in Section 2.1.2. Actually, the received signals and MUIs can be modeled as cyclostationary processes with modulation induced cyclostationarity, and we consider blind channel estimation and signal separation for long code CDMA systems using multistep linear predictors. Linear prediction-based approach for MIMO model was first proposed by Slock in [107], and developed by others in [20, 104, 108–110]. It has been reported [104, 109] that compared with subspace methods, linear prediction methods can deliver more accurate channel estimates and are more robust to overmodeling in channel order estimate. In this section, multistep linear prediction method is used to separate the intersymbol interference introduced by multipath channel, and channel estimation is then performed using non-constant modulus precoding technique both with and without the matrix pencil approach [111, 112]. The channel estimation algorithm without the matrix pencil approach relies on the Fourier transform, and requires additional constraint on the code sequences other than being non-constant modulus. It is found that by introducing a random linear transform, the matrix pencil approach can remove (with probability one) the extra constraint on the code sequences. After channel estimation, equalization is carried out using a cyclic Wiener filter. Finally, since chip-level equalization is performed, the proposed approach can readily be extended to multirate cases, either with multicode or variable spreading factor. Simulation results show that compared with the approach using the Fourier transform, the matrix pencil based approach can significantly improve the accuracy of channel estimation, therefore the overall system performance.

4.2.1 System Model

Consider a DS-CDMA system with M users and K receive antennas, and the same notations as in section 2.1.2 are adopted in this section. Assume the processing gain is N, and the channelization code sequence extends over L_c symbols. The spreading code for user m is denoted by

$$\mathbf{c}_m := [c_m(0), c_m(1), \cdots, c_m(L_c N - 1)]. \tag{4.27}$$

The spreading process can be carried out as

$$\begin{aligned} & [r_m(kN), r_m(kN+1), \cdots, r_m(kN + L_c N - 1)] \\ = \; & [u_m(k)c_m(0), u_m(k)c_m(1), \cdots, u_m(k)c_m(N-1), \ldots, \\ & u_m(k+L_c-1)c_m((L_c-1)N), u_m(k+L_c-1)c_m((L_c-1)N+1), \cdots, \\ & u_m(k+L_c-1)c_m(L_c N - 1)], \end{aligned} \tag{4.28}$$

where k is equal to an integer times of L_c. The successive scrambling processing is achieved by

$$\begin{aligned} & [s_m(kN), s_m(kN+1), \cdots, s_m((k+L_c)N-1)] \\ = \; & [r_m((kN)d_m(kN), r_m((kN+1)d_m(kN+1), \cdots, \\ & r_m((k+L_c)N-1)d_m((k+L_c)N-1)], \end{aligned} \tag{4.29}$$

where $d_m(n)$ is the scrambling sequence of user m. Define

$$\begin{aligned} & [v_m(kN), \cdots, v_m((k+L_c)N-1)] \\ = \; & [u_m(k)d_m(kN), \cdots, u_m(k)d_m(kN+N-1), \\ & \ldots, u_m(k+L_c-1)d_m((k+L_c-1)N), \\ & \cdots, u_m(k+L_c-1)d_m((K+L_c)N-1)], \end{aligned} \tag{4.30}$$

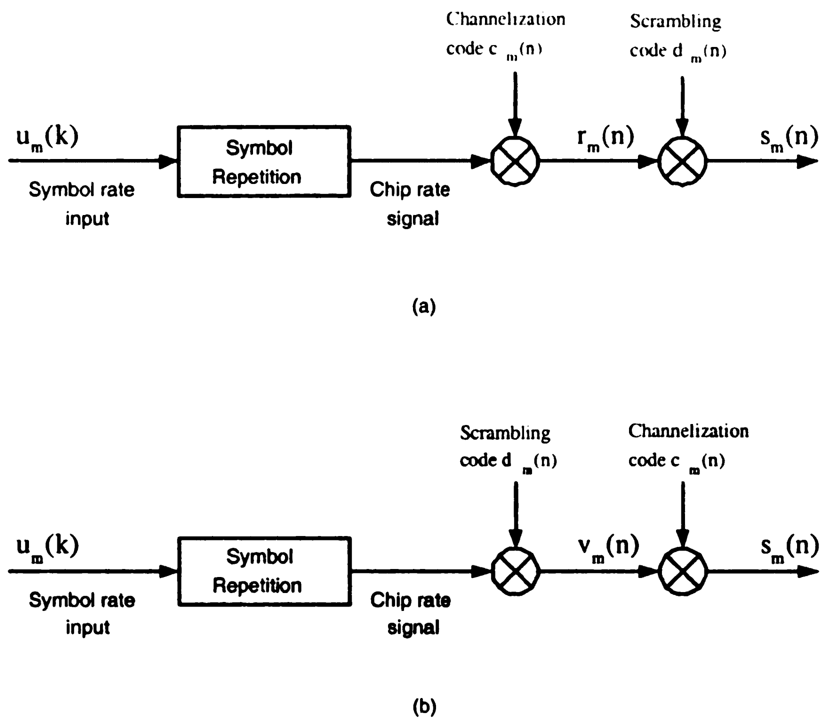

Figure 4.6. Two equivalent representation of the spreading and scrambling procedures

then it can be obtained that

$$\begin{aligned} & [s_m(kN), s_m(kN+1), \cdots, s_m((k+L_c)N-1)] \\ = & [v_m(kN)c_m(0), v_m(kN+1)c_m(1), \\ & \cdots, v_m((k+L_c)N-1)c_m(L_cN-1)], \end{aligned} \tag{4.31}$$

or in brief

$$s_m(n) = v_m(n)c_m(n). \tag{4.32}$$

Here $c_m(n) = c_m(n + L_cN)$ serves as a periodic precoding sequence with period L_cN. This is illustrated in Fig. 4.6. After symbol repetition, the chip-rate sequence can be multiplied with either the channelization code $c_m(n)$ or the scrambling code $d_m(n)$ first. They are just two equivalent procedures. Please note that, this form of periodic precoding (4.32) has been proposed in [7] to introduce cyclostationarity in the transmitted signal, therefore making blind channel estimation based on the second-order statistics of the channel outputs possible for SISO systems.

Following section 2.1.2, the channel output still can be represented as

$$\begin{aligned} \mathbf{y}(n) &= \sum_{l=0}^{L-1} \mathbf{H}(l)\mathbf{s}(n-l) + \mathbf{w}(n) \\ &= \mathbf{y}_s(n) + \mathbf{w}(n), \end{aligned} \tag{4.33}$$

where $\mathbf{H}(l)$ is defined in (2.21), and $\mathbf{y}_s(n)$ is the noiseless channel output.

4.2.2 ISI Reduction and Separation Based on Multistep Linear Predictors

In this section, multistep linear prediction method is used to resolve the intersymbol interference introduced by multipath channel. Following [20] and [104], the noiseless channel output $\mathbf{y}_s(n)$ has the following canonical representation:

$$\mathbf{y}_s(n) = \sum_{i=l}^{L_l} A_{n,i}^{(l)} \mathbf{y}_s(n-i) + \mathbf{e}(n|n-l), \quad l = 1, 2, \cdots \tag{4.34}$$

for some $L_l \leq M(L-1) + l - 1$. The l-step ahead linear prediction error $\mathbf{e}(n|n-l)$ is given by

$$\mathbf{e}(n|n-l) = \sum_{i=0}^{l-1} \mathbf{H}(i)\mathbf{s}(n-i). \tag{4.35}$$

which satisfies

$$E\{\mathbf{e}(n|n-l)\mathbf{y}_s^H(n-m)\} = 0, \ \ \forall m \geq l. \tag{4.36}$$

From (4.34) and (4.36), it can be obtained that

$$E\{\mathbf{y}_s(n)\mathbf{y}_s^H(n-m)\} = \sum_{i=l}^{L_l} A_{n,i}^{(l)} E\{\mathbf{y}_s(n-i)\mathbf{y}_s^H(n-m)\}, \forall m \geq l. \tag{4.37}$$

Define

$$\mathbf{R}_{y_s}(n,k) := E\{\mathbf{y}_s(n)\mathbf{y}_s^H(n-k)\}, \tag{4.38}$$

then we have

$$
\begin{aligned}
\mathbf{R}_{y_s}(n,m) &= \sum_{i=l}^{L_l} A_{n,i}^{(l)} \mathbf{R}_{y_s}(n-i,m-i) \\
&= [A_{n,l}^{(l)}, A_{n,l+1}^{(l)}, \cdots, A_{n,L_l}^{(l)}] \begin{bmatrix} \mathbf{R}_{y_s}(n-l,m-l) \\ \mathbf{R}_{y_s}(n-l-1,m-l-1) \\ \vdots \\ \mathbf{R}_{y_s}(n-L_l,m-L_l) \end{bmatrix}. \qquad (4.39)
\end{aligned}
$$

It follows (4.39) that

$$
\begin{aligned}
& [\mathbf{R}_{y_s}(n,l), \mathbf{R}_{y_s}(n,l+1), \cdots, \mathbf{R}_{y_s}(n,L_l)] \\
= \; & [A_{n,l}^{(l)}, A_{n,l+1}^{(l)}, \cdots, A_{n,L_l}^{(l)}] \mathcal{R}_{y_s}(n,l,L_l), \qquad (4.40)
\end{aligned}
$$

where

$$
\mathcal{R}_{y_s}(n,l,L_l) =
\begin{bmatrix}
\mathbf{R}_{y_s}(n-l,0) & \mathbf{R}_{y_s}(n-l,1) & \cdots & \mathbf{R}_{y_s}(n-l,L_l-l) \\
\mathbf{R}_{y_s}(n-l-1,-1) & \mathbf{R}_{y_s}(n-l-1,0) & \cdots & \mathbf{R}_{y_s}(n-l-1,L_l-l-1) \\
\vdots & \vdots & \ddots & \vdots \\
\mathbf{R}_{y_s}(n-L_l,l-L_l) & \mathbf{R}_{y_s}(n-L_l,l-L_l+1) & \cdots & \mathbf{R}_{y_s}(n-L_l,0)
\end{bmatrix}. \qquad (4.41)
$$

A solution to (4.40) is given by

$$
\begin{aligned}
& [A_{n,l}^{(l)}, A_{n,l+1}^{(l)}, \cdots, A_{n,L_l}^{(l)}] \\
= \; & [\mathbf{R}_{y_s}(n,l), \mathbf{R}_{y_s}(n,l+1), \cdots, \mathbf{R}_{y_s}(n,L_l)] \mathcal{R}_{y_s}(n,l,L_l)^{\#}. \qquad (4.42)
\end{aligned}
$$

Following (4.33), we have

$$
\begin{aligned}
\mathbf{R}_{y_s}(n,k) &= E\left\{ \sum_{l=0}^{L-1} \sum_{m=0}^{L-1} \mathbf{H}(l)[\mathbf{s}(n-l)\mathbf{s}^H(n-k-m)]\mathbf{H}^H(m) \right\} \\
&= \sum_{l=0}^{L-1} \sum_{m=0}^{L-1} \mathbf{H}(l) E\{\mathbf{s}(n-l)s^H(n-k-m)\}\mathbf{H}^H(m)
\end{aligned}
$$

$$= \sum_{l=0}^{L-1}\sum_{m=0}^{L-1}\mathbf{H}(l)\mathbf{R}_s(n-l,k+m-l)\mathbf{H}^H(m), \tag{4.43}$$

where

$$\begin{aligned}\mathbf{R}_s(n,k) &:= E\{\mathbf{s}(n)\mathbf{s}^H(n-k)\} \\ &= \mathrm{diag}[|c_1(n)|^2, |c_2(n)|^2, \cdots, |c_M(n)|^2]\delta(k).\end{aligned} \tag{4.44}$$

Obviously, $\mathbf{R}_s(n,k) = \mathbf{R}_s(n+L_cN,k)$, since $c_m(n) = c_m(n+L_cN)$. Note that $\mathbf{R}_s(n,k) = 0, \forall k \neq 0$, define

$$\mathbf{R}_s(n) := \mathbf{R}_s(n,0), \tag{4.45}$$

Then

$$\mathbf{R}_{y_s}(n,k) = \sum_{l=0}^{L-1}\mathbf{H}(l)\mathbf{R}_s(n-l)\mathbf{H}^H(l-k). \tag{4.46}$$

From the above equation, it can be observed that $\mathbf{R}_{y_s}(n,k)$ has the period L_cN. Therefore, according to (4.42), $A_{n,i}^{(l)}$ also has a period of L_cN. Define $\mathbf{E}(n)$ and $\bar{\mathbf{e}}(l)$ as in Section 4.1.1. It follows (4.35) that

$$\mathbf{E}(n) = \begin{bmatrix} \mathbf{H}(d) \\ \mathbf{H}(d-1) \\ \vdots \\ \mathbf{H}(0) \end{bmatrix} \mathbf{s}(n) := \tilde{\mathbf{H}}\mathbf{s}(n), \tag{4.47}$$

where

$$\tilde{\mathbf{H}} := \begin{bmatrix} \mathbf{H}(d) \\ \mathbf{H}(d-1) \\ \vdots \\ \mathbf{H}(0) \end{bmatrix}. \tag{4.48}$$

This is an instantaneouse mixture model. Since $\mathbf{E}(n)$ is only determined by the channel and the current chip-rate channel input, this model is ISI free.

4.2.3 Channel Estimation through the Fourier Analysis

In this section, we present that, by designing the precoding sequences properly, the channels can be determined up to a complex scalar based on only the second order statistics of the chip-rate sampled channel outputs. First, consider the correlation matrix of $\mathbf{E}(n)$. From (4.47), we have

$$\begin{aligned} \mathbf{R}_E(n) &:= E\{\mathbf{E}(n)\mathbf{E}^H(n)\} = \tilde{\mathbf{H}}\mathbf{R}_s(n)\tilde{\mathbf{H}}^H \\ &= \tilde{\mathbf{H}}\mathrm{diag}\{|c_1(n)|^2, |c_2(n)|^2, \cdots, |c_M(n)|^2\}\tilde{\mathbf{H}}^H. \end{aligned} \tag{4.49}$$

Since $c_m(n) = c_m(n + L_cN), j = 1, 2, \cdots, M$, $\mathbf{R}_E(n)$ is has a period of L_CN. The discrete Fourier transform (DFT) of $\mathbf{R}_E(n)$ is given by

$$\mathbf{S}_E(k) = \sum_{n=0}^{L_cN-1} \mathbf{R}_E(n)e^{-i\frac{\pi nk}{N}} = \tilde{\mathbf{H}}\mathbf{C}_s(k)\tilde{\mathbf{H}}^H, \tag{4.50}$$

where

$$\begin{aligned} \mathbf{C}_s(k) &= \mathrm{diag}\{\sum_{n=0}^{L_cN-1} |c_1(n)|^2 e^{-i\frac{\pi nk}{N}}, \cdots, \sum_{n=0}^{L_cN-1} |c_M(n)|^2 e^{-i\frac{\pi nk}{N}}\} \\ &= \mathrm{diag}\{C_{s_1}(k), \cdots, C_{s_M}(k)\}. \end{aligned}$$

Design the precoding sequences $\{c_j(n)\}_{n=0}^{L_cN-1}$ in such a way that for a given $k = k_j$, $C_{s_j}(k_j) \neq 0$ and $C_{s_i}(k_j) = 0, \forall i \neq j$. Therefore only one entry in $\mathbf{C}_s(k)$ is nonzero, which is located in the diagonal of $\mathbf{C}_s(k)$. Without loss of generality, assume the first user is the desired user. Based on the design of the code sequences and following (4.50), it can be obtained that

$$\begin{aligned} \mathbf{S}_E(k_1) &= \tilde{\mathbf{H}}\mathrm{diag}\{C_{s_1}(k_1), 0, \cdots, 0\}\tilde{\mathbf{H}}^H \\ &= \alpha\mathbf{g}_1\mathbf{g}_1^H, \end{aligned} \tag{4.51}$$

where

$$\mathbf{g}_i = [g_i^{(1)}(d), \cdots, g_i^{(K)}(d), \cdots, g_i^{(1)}(0), \cdots, g_i^{(K)}(0)]^T, \tag{4.52}$$

and $\alpha = C_{s_1}(k_1)$. Thus the channel of user 1 can be determined up to a complex scalar from (4.51).

4.2.4 Channel Estimation Based on the Matrix Pencil Approach

If $\{c_m(n)\}_{m=1}^{M}$ are non-constant modulus, the period of $\mathbf{R}_E(n)$ is L_cN. Define random sequences $\{\beta(n)\}_{i=1,2}$, which are uniformly distributed in the interval $(0,1)$, then a matrix pencil $\{\mathbf{S}_1, \mathbf{S}_2\}$ can be formed by defining

$$\begin{aligned}
\mathbf{S}_i &:= \sum_{n=0}^{L_cN-1} \beta_i(n)\mathbf{R}_E(n) \\
&= \tilde{\mathbf{H}}\text{diag}\{\sum_{n=0}^{L_cN-1} \beta_i(n)|c_1(n)|^2, \cdots, \sum_{n=0}^{L_cN-1} \beta_i(n)|c_M(n)|^2\}\tilde{\mathbf{H}}^H \\
&:= \tilde{\mathbf{H}}\Gamma_i\tilde{\mathbf{H}}^H, \qquad (i = 1,2),
\end{aligned} \tag{4.53}$$

where

$$\Gamma_i := \text{diag}\{\sum_{n=0}^{L_cN-1} \beta_i(n)|c_1(n)|^2, \cdots, \sum_{n=0}^{L_cN-1} \beta_i(n)|c_M(n)|^2\} \qquad (i = 1,2). \tag{4.54}$$

Consider the generalized eigenvalue problem

$$\begin{aligned}
&\mathbf{S}_1\mathbf{x} = \lambda\mathbf{S}_2\mathbf{x} \\
\Longleftrightarrow\ &\tilde{\mathbf{H}}(\Gamma_1 - \lambda\Gamma_2)\tilde{\mathbf{H}}^H\mathbf{x} = 0.
\end{aligned} \tag{4.55}$$

According to assumption (A4), $\tilde{\mathbf{H}}$ is of full column rank, then it can be obtained from (4.55) that

$$(\Gamma_1 - \lambda\Gamma_2)\tilde{\mathbf{H}}^H\mathbf{x} = 0. \tag{4.56}$$

Thus the generalized eigenvalue is given by

$$\lambda_j = \frac{\sum_{n=0}^{L_cN-1} \beta_1(n)|c_j(n)|^2}{\sum_{n=0}^{L_cN-1} \beta_2(n)|c_j(n)|^2}, \qquad j = 1, 2, \cdots, M. \tag{4.57}$$

Note that $\beta_i(n)_{i=1,2}$ are generated randomly. $\lambda_j, j = 1, \cdots, M$ are distinct eigenvalues with probability 1. Let $\mathbf{x}_j$ denote the generalized eigenvector corresponding to eigenvalue λ_j. Because $(\Gamma_1 - \lambda\Gamma_2)$ is a diagonal matrix, $\mathbf{x}_j$ has to satisfy

$$\tilde{\mathbf{H}}^H \mathbf{x}_j = \gamma_j \mathcal{I}_j, \tag{4.58}$$

where γ_j is an unknown scalar, and $\mathcal{I}_j$ is an M-vector given by

$$\mathcal{I}_j = [\underbrace{0, 0, \cdots, 0}_{j-1 \text{ zeros}}, 1, 0, \cdots, 0]^T.$$

From (4.53)(4.58), it can be derived that

$$\mathbf{S}_i \mathbf{x}_j = \tilde{\mathbf{H}} \Gamma_i \tilde{\mathbf{H}}^H \mathbf{x}_j = \gamma_j \sum_{n=0}^{L_c N-1} \beta_i(n) |c_j(n)|^2 \mathbf{g}_j. \tag{4.59}$$

Therefore, $\mathbf{g}_j$ can be determined up to a scalar $\gamma_j \sum_{n=0}^{L_c N-1} \beta_i(n)|c_j(n)|^2$.

Remark 4.1 *It should be noticed that the channel estimation algorithm based on the Fourier analysis requires an additional condition on the coding sequences, which actually implies that for a given cycle, all but only one antennas are nulled out. More specifically, this constraint on the code sequences implies that for each user, there exists at least one narrow frequency band over which no other user is transmitting. When using the matrix pencil approach, on the other hand, random weights, hence a random linear transform, is introduced instead of the Fourier transform, resulting in that the condition on the code sequences can be relaxed to any non-constant modulus sequences which make λ_j's in (4.57) be distinct from each other for $j = 1, 2, \cdots, M$.*

4.2.5 Channel Equalization using the Cyclic Wiener Filter

Once the estimated channels are available, MMSE cyclic Wiener filter can be designed to extract the signal of the desired user. Assuming that user 1 is the desired user, we want to design a $K \times 1$ MMSE equalizer $\{\mathbf{f}_d(n,i)\}_{i=0}^{L_e-1}$ of length L_e which satisfies

$\mathbf{f}_d(n,i) = \mathbf{f}_d(n + L_c N, i)$, $i = 0, 1, \ldots, L_e - 1$. The output of the equalizer is

$$\hat{s}_1(n-d) = \sum_{i=0}^{L_e-1} \mathbf{f}_d^H(n,i)\mathbf{y}(n-i), \tag{4.60}$$

where $\hat{s}_1(n)$ is the estimate of $s_1(n)$, which is given by (4.32), and d is the equalization delay. The mean square error (MSE) between the input signal and the equalizer output is given by

$$E\{|e(n)|^2\} = E\left\{\left|\sum_{i=0}^{L_e-1} \mathbf{f}_d^H(n,i)\mathbf{y}(n-i) - s_1(n-d)\right|^2\right\}. \tag{4.61}$$

Applying the orthogonality principle, we have

$$E\left\{\left[\sum_{i=0}^{L_e-1} \mathbf{f}_d^H(n,i)\mathbf{y}(n-i) - s_1(n-d)\right] \mathbf{y}^H(n-k)\right\} = 0,$$
$$(k = 0, 1, \ldots, L_e - 1). \tag{4.62}$$

Define

$$Y(n) = [\mathbf{y}^T(n), \mathbf{y}^T(n-1), \ldots, \mathbf{y}^T(n - L_e + 1)]^T, \tag{4.63}$$
$$S(n) = [\mathbf{s}^T(n), \mathbf{s}^T(n-1), \cdots, \mathbf{s}^T(n - L_e - L + 2)]^T, \tag{4.64}$$

and

$$\mathcal{H} = \begin{bmatrix} H(0) & \cdots & H(L-1) & \cdots & 0 \\ \vdots & \ddots & \vdots & \ddots & \vdots \\ 0 & \cdots & H(0) & \cdots & H(L-1) \end{bmatrix}_{KL_e \times [(L+L_e-1)M]}, \tag{4.65}$$

then it follows (4.33) that

$$Y(n) = \mathcal{H}S(n) + W(n), \tag{4.66}$$

where $W(n)$ is define in the same manner as $Y(n)$ and $S(n)$. From (A1)-(A3), we have

$$\begin{aligned} \mathbf{R}_{s_1Y}(n) &:= E\{s_1(n-d)Y^H(n)\} \\ &= E\{s_1(n-d)[S(n)^H\mathcal{H}^H + W^H(n)]\} \\ &= |c_1(n-d)|^2 I_d^H \mathcal{H}^H \end{aligned} \tag{4.67}$$

where $I_d = [\mathbf{0}, \ldots, \mathbf{0}, \underbrace{1, 0, \ldots, 0}_{(d+1)'s\ M\times 1\ block}, \ldots, \mathbf{0}]^H$.

Define $\tilde{\mathbf{f}}_d(n) = [\mathbf{f}_d(n,0)^H, \mathbf{f}_d(n,1)^H, \ldots, \mathbf{f}_d(n, L_e-1)^H]^H$, then (4.62) can be rewritten as

$$\mathbf{R}_{YY}(n)\tilde{\mathbf{f}}_d(n) = |c_1(n-d)|^2\mathcal{H}I_d. \tag{4.68}$$

One solution of (4.68) is given by

$$\begin{aligned} \tilde{\mathbf{f}}_d(n) &= |c_1(n-d)|^2\mathbf{R}_{YY}^{\#}(n)\mathcal{H}I_d \\ &= |c_1(n-d)|^2\mathbf{R}_{YY}^{\#}(n)[\mathbf{h}_1(d)^H, \mathbf{h}_1(d-1)^H, \ldots, \mathbf{h}_1(0)^H, 0, \cdots, 0]^H \end{aligned} \tag{4.69}$$

where $\mathbf{h}_1(l) = [g_1^{(1)}(l), g_1^{(2)}(l), \ldots, g_1^{(k)}(l)]^T$.

Instead of recover the transmitted chip sequence $s_1(n)$, the equalizer can also be designed to recover $v_1(n)$ directly. Actually, the MSE given by (4.61) can be rewritten as

$$\begin{aligned} E\{|e(n)|^2\} &= E\left\{\left|\sum_{i=0}^{L_e-1}\mathbf{f}_d^H(n,i)\mathbf{y}(n-i) - c_1(n-d)v_1(n-d)\right|^2\right\} \\ &= |c_1(n-d)|^2 E\left\{\left|\sum_{i=0}^{L_e-1}\frac{\mathbf{f}_d^H(n,i)}{c_1(n-d)}\mathbf{y}(n-i) - v_1(n-d)\right|^2\right\}. \end{aligned} \tag{4.70}$$

Therefore, to minimize $E\{|e(n)|^2\}$ is equivalent to minimize the following error function

$$E\{|e'(n)|^2\} = E\left\{\left|\sum_{i=0}^{L_e-1}(\mathbf{f}'_d(n,i))^H\mathbf{y}(n-i) - v_1(n-d)\right|^2\right\}, \tag{4.71}$$

where

$$\mathbf{f}'_d(n,i)) = \frac{\mathbf{f}_d(n,i))}{c_1(n-d)} \tag{4.72}$$

is the equalizer used to restore the signal $v_1(n)$. Define $\tilde{\mathbf{f}}'_d(n)$ in the same way as $\tilde{\mathbf{f}}_d(n)$, then from (4.69) and (4.78), we have

$$\tilde{\mathbf{f}}'_d(n) = c_1(n-d)\mathbf{R}^{\#}_{YY}(n)[\mathbf{h}_1(d)^H, \mathbf{h}_1(d-1)^H, \ldots, \mathbf{h}_1(0)^H, 0, \cdots, 0]^H, \tag{4.73}$$

which is the same result as presented in [90].

After the channel equalization, descrambling and despreading process can be carried out as an inverse procedure of (4.28) and (4.29).

4.2.6 Extension to Multirate CDMA Systems

Since chip-level channel modeling and equalization are performed, the proposed approach can readily be extended to multirate case. As an MC system with high rate users is equivalent to a single rate system with more users, extension of the proposed approaches to MC multirate CDMA systems is therefore trivial. For VSL (variable sequence length) systems, let N be the smallest processing gain and let $L_{c,m}N$ denote the length of the mth user's spreading code. Define

$$L_c = \mathrm{LCM}(L_{c,1}, L_{c,2}, \cdots, L_{c,M}),$$

as the least common multiple of $\{L_{c,1}, L_{c,2}, \cdots, L_{c,M}\}$, the generalization of the proposed algorithm to VSL systems is then straightforward.

4.2.7 Simulation Examples (Nonconstant Modulus)

We consider the case of two users and four receive antennas. Each user transfers QPSK signals. The spreading gain is either $N = 16$ or $N = 8$. Three cases were considered: (1) Both users have spreading gain $N = 8$; (2) Both users have spreading gain $N = 16$; (3) Two users have different data rates, the spreading gain for the low rate user is $N = 16$, and that for the high rate user is $N = 8$.

The length of the channelization codes was chosen to be 32 chips, i.e. 2 to 4 symbols depending on the user's spreading gain. Both randomly generated codes and codes which satisfy the constrained given in 4.2.3 were considered. For the method presented in Section 4.2.3, the channelization codes were chosen to be:

$$\begin{aligned}
\mathbf{c}_1 &= [0.6857, 0.7145, 0.6356, 0.6849, 0.8433, 0.8036, 0.7597, 0.5856, \\
&\quad 0.7488, 0.5641, 0.7300, 0.7542, 0.7482, 0.5870, 0.7902, 0.6172, \\
&\quad 0.5409, 0.5474, 0.6425, 0.7834, 0.7520, 0.6743, 0.6904, 0.8114, \\
&\quad 0.5829, 0.6913, 0.5939, 0.7339, 0.8608, 0.6380, 0.8207, 0.8808], \qquad (4.74) \\
\mathbf{c}_2 &= [0.6670, 0.7275, 0.8540, 0.6100, 0.7518, 0.6363, 0.5545, 0.6887, \\
&\quad 0.7092, 0.6143, 0.6313, 0.7625, 0.5210, 0.8036, 0.7582, 0.6979, \\
&\quad 0.8136, 0.6944, 0.6902, 0.6660, 0.6536, 0.6908, 0.6010, 0.8078, \\
&\quad 0.7622, 0.5486, 0.6005, 0.6395, 0.6176, 0.8070, 0.6382, 0.8265]. \qquad (4.75)
\end{aligned}$$

The multipath channels have 3 rays, whose amplitudes are Gaussian with zero mean and identical variance. The transmission delays uniformly spread over 4 chip intervals. Complex zero mean white Gaussian noise was added to the received signals. The normalized mean-square-error of channel estimation (CHMSE) for the desired user is defined as

$$CHMSE = \frac{1}{KIL} \sum_{i=1}^{I} \sum_{p=1}^{K} \frac{\| \hat{\mathbf{g}}_1^{(p)} - \mathbf{g}_1^{(p)} \|^2}{\| \mathbf{g}_1^{(p)} \|^2} \qquad (4.76)$$

where I stands for the number of Monto Carlo runs, and K is the number of receive antennas. SNR refers to the chip level signal-to-noise ratio with respect to the desired user, and is chosen to be the same value at each receive antenna. The normalized mean square error of symbol estimation and the bit error rate (BER) were used to evaluate the performance of the equalizer. The result was averaged over $I = 100$ Monto Carlo runs. The channel was generated randomly in each run, and was estimated based on a record of 256 symbols. In the case of multirate, we mean 256 lower rate symbols. The equalizer with length $L_e = 6$ was constructed according to the

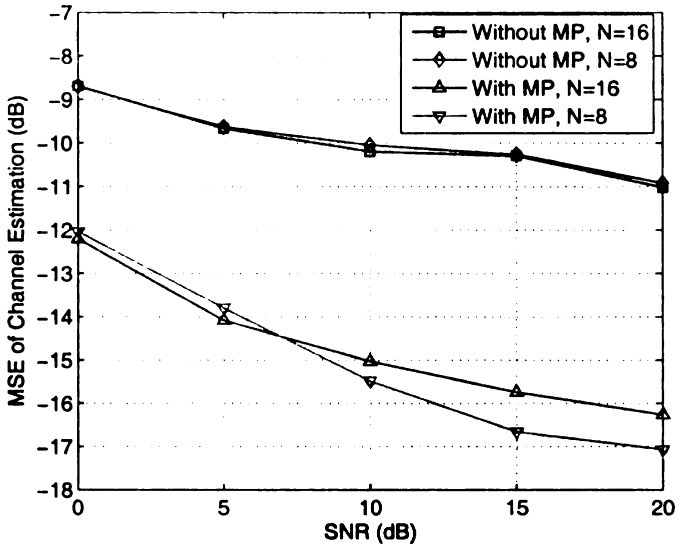

Figure 4.7. Normalized MSE of channel estimation versus SNR, single rate cases with N=16 and N=8 respectively

estimated channel, and is applied to a set of 1024 independent symbols in order to calculate the symbol MSE and BER for each Monto Carlo run. Channel estimation based on nonconstant modulus precoding was carried out both with and without the matrix pencil approach. Without matrix pencil approach, the channel estimation was obtained directly through the second-order statistics of $\mathbf{E}(n)$ based on the non-constant precoding technique. Figure 4.7 and Figure 4.8 correspond to the single rate cases, where both users have spreading gain $N = 8$ or $N = 16$, and the channelization codes are given by (4.74-4.75). Figure 4.9 and Figure 4.10 compared the performance of the matrix pencil based approach when different codes were used. In the figures, "codes with constraint" denotes the codes in (4.74-4.75), and we choose $N = 8$ for the higher rate user and $N = 16$ for the low rate user. The simulation results show that, by introducing a random linear transform, the matrix pencil approach delivers significantly better results for both single rate and multirate systems.

Table 4.1 shows the average time in seconds per Monte Carlo run for both with and without matrix pencil approach while the processing gain of both users is 16. The computer used in this simulation is a Dell Dimension 4550, P4 2.8GHz, 1G RAM.

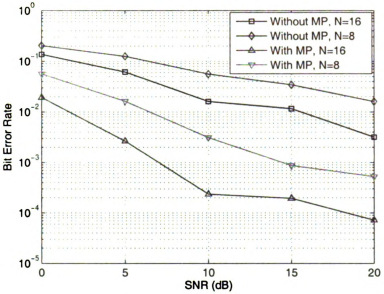

Figure 4.8. Comparison of BER versus SNR, single rate cases with N=16 and N=8 respectively

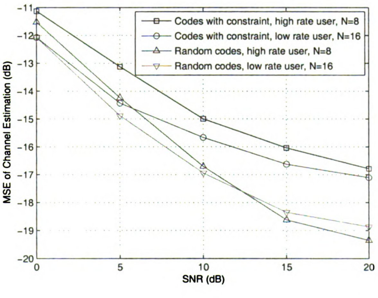

Figure 4.9. Normalized MSE of channel estimation versus SNR for matrix pencil based approach with different codes, multirate configuration with $N = 8$ for the high rate user, and $N = 16$ for the low rate user.

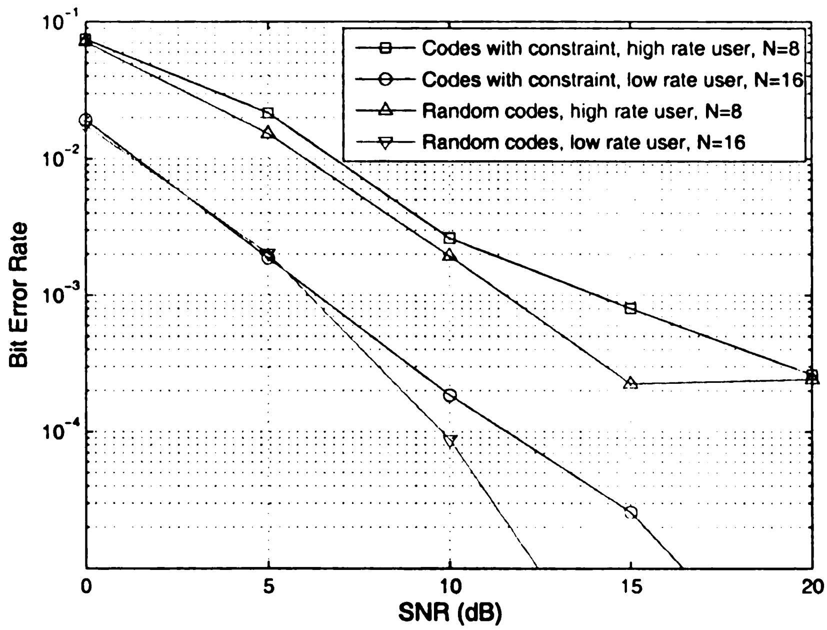

Figure 4.10. Comparison of BER versus SNR for matrix pencil based approach with different codes, multirate configuration with $N = 8$ for the high rate user, and $N = 16$ for the low rate user.

Channel Order	5		9	
Number of receive antennas	4	3	4	3
With MP (second)	15.59	13.11	34.86	26.86
Without MP (second)	15.57	12.99	34.06	26.79

Table 4.1. Average time per run

4.3 Blind Equalization for Uplink Long-Code CDMA Spreading Sequences with Constant Modulus

The drawback of the approaches presented in section 4.2.3 and section 4.2.4 is that the spreading codes need to be non-constant modulus, which causes inconvenience for practical design. To overcome this obstacle, instead of using only second-order statistics as in [75, 113], in this work, higher-order statistics are exploited as in [104] so that multiuser separation no longer requires the spreading code be non-constant modulus. In this section, after the system model is transformed to the instantaneous mixture mode, as in [104, 114], joint approximate diagonalization of eigen-matrices (JADE) algorithm is used to estimate the channels. MMSE equalizer is designed to recover the input signals. In the third generation wireless systems, multi-rate transmission is required to support variable quality of service. Because the chip level MIMO model is applied in this research, the proposed method supports multi-rate transmission inherently.

4.3.1 Blind Channel Identification using JADE Algorithm

In this section, $\{c_m(n)\}_{m=1}^{M}$ are assumed to satisfy $|c_m(n)| = 1$. From (4.44), we have $\mathbf{R}_s(n,k) = I_M\delta(k)$. Therefore, from (4.40) and (4.46), $\mathbf{R}_{y_s}(n,k)$ and $A_{n,i}^{(l)}$ are independent of n. It can be obtained from (4.49) that

$$\mathbf{R}_E(n) = \tilde{\mathbf{H}}\tilde{\mathbf{H}}^H. \tag{4.77}$$

Since $\mathbf{R}_E(n)$ is independent of n, we define $\mathbf{R}_E = \tilde{\mathbf{H}}\tilde{\mathbf{H}}^H$. Except for the one user case, $\tilde{\mathbf{H}}$ cannot be uniquely determined from (4.77), since $\tilde{\mathbf{H}}\tilde{\mathbf{H}}^H = \tilde{\mathbf{H}}\mathbf{B}\mathbf{B}^H\tilde{\mathbf{H}}^H$ for any unitary $\mathbf{B}$. Thus, higher order statistics has to be exploited. Consider the following instantaneous mixture problem:

$$\mathbf{E}(n) = \tilde{\mathbf{H}}\mathbf{s}(n). \tag{4.78}$$

JADE algorithm [114] is a higher-order-statistics based method used to separate $\tilde{\mathbf{H}}$ and $\mathbf{s}(n)$ blindly based on the following assumptions:

(H1) The processes $\{s_1(n)\}$, $\{s_2(n)\}$, $\cdots$, $\{s_M(n)\}$ are jointly stationary.

(H2) There is at most one signal source has a zero kurtosis.

(H3) The columns of $\tilde{\mathbf{H}}$ are linearly independent.

(H4) The variables $s_1(n)$, $s_2(n)$, $\cdots$, $s_M(n)$ are statistically independent for each n.

(H1), (H2) and (H4) can be satisfied with the general assumptions (A1)-(A3) given in Chapter 2, while (H3) requires that the channels corresponding to different users be independent.

First, find an $M \times (KL)$ whitening matrix $\mathbf{W}$ which satisfies $\mathbf{I}_M = \mathbf{W}\mathbf{R}_E\mathbf{W}^H = \mathbf{W}\tilde{\mathbf{H}}\tilde{\mathbf{H}}^H\mathbf{W}^H$. Let λ_i $(i = 1, \ldots, M)$ denote the eigenvalues of $\mathbf{R}_E$, and $\mathbf{v}_i$ $(i = 1, \ldots, M)$ denote the corresponding orthonormal eigenvectors. We choose $\mathbf{W} = \mathbf{\Gamma}^{-1}\mathbf{V}^H$, where $\mathbf{\Gamma} = \mathrm{diag}(\sqrt{\lambda_1}, \ldots, \sqrt{\lambda_M})$ and $\mathbf{V} = [\mathbf{v}_1, \ldots, \mathbf{v}_M]$. Then the whitening process is carried out as

$$\mathbf{z}(n) := \mathbf{W}\mathbf{E}(n) = \mathbf{W}\tilde{\mathbf{H}}\mathbf{s}(n) = \mathbf{U}\mathbf{s}(n), \tag{4.79}$$

where $\mathbf{U} := \mathbf{W}\tilde{\mathbf{H}}$. Let $Q_z(B)$ denote the $M \times M$ cumulant matrix associated with a $M \times M$ matrix B. The (i, j)th entry of $Q_z(B)$ is defined by

$$q_{ij} = \sum_{k,l=1,M} \mathrm{cum}(z_i, z_j^*, z_k, z_l^*) b_{lk}, \tag{4.80}$$

where z_m is the mth entry of vector $\mathbf{z}$, and b_{lk} is the (l, k)th entry of B. Let $\mathbf{a}_i$ denote the $M \times 1$ vector with 1 in the ith position and 0 elsewhere. Define the set of parallel cumulant slice as

$$\mathcal{S} := \{Q_z(\mathbf{a}_l\mathbf{a}_k^T)|1 \leq k, l \leq M\}. \tag{4.81}$$

A joint diagonaliser of set $\mathcal{S}$ is defined as the a unitary matrix which maximizes the criterion

$$C(V) = \sum_{1\leq k,l\leq M} |\text{diag}(V^H Q_z(\mathbf{a}_l\mathbf{a}_k^T)V)|^2. \tag{4.82}$$

As proved in [114], a joint diagonaliser of set $\mathcal{S}$ is *essentially equal* to $\mathbf{U}$ (Matrix A and C are said to be essentially equal when $A = CP$, where P is a permutation matrix).

Let $\hat{\mathbf{U}}$ denote a matrix that is essentially equal to $\mathbf{U}$, then the estimate of $\tilde{\mathbf{H}}$ can be obtained as $\hat{\tilde{\mathbf{H}}} = \mathbf{W}^{\#}\hat{\mathbf{U}}$. If we select the equalizer length $L_e = d$, the MMSE equalizer with delay d is given by

$$\mathbf{F}_e := [F_e^H(0), F_e^H(1), \ldots, F_e^H(L_e - 1)]^H = R_{yL_e}^{\#}\hat{\tilde{\mathbf{H}}} \tag{4.83}$$

where $R_{yL_e} := E\{[\mathbf{y}^T(n), \ldots, \mathbf{y}^T(n - L_e + 1)]^T[\mathbf{y}(n), \ldots, \mathbf{y}(n - L_e + 1)]\}$. The equalization output is given by

$$\hat{\mathbf{s}}(n - d) = \sum_{k=0}^{L_e-1} F_e^H(k)\mathbf{y}(n - k). \tag{4.84}$$

Because $\hat{\mathbf{U}}$ is essentially equal to $\mathbf{U}$, $\hat{\tilde{\mathbf{H}}}$ is also only essentially equal to $\tilde{\mathbf{H}}$. That means we have no knowledge about which entry of $\hat{\mathbf{s}}$ belongs to a specified user. By calculating the correlation of each component of $\hat{\mathbf{s}}$ with the overall spreading code of every user, the estimated symbol stream of each user can be identified.

4.3.2 Simulation Example (Constant Modulus)

In this section, a simulation example is provided to illustrate the proposed approach. Uplink CDMA systems with four receive antennas and two users were considered. Each user transmitted QPSK symbols with equal power. The spreading sequences and scrambling sequences were randomly generated. The processing gain of the basic

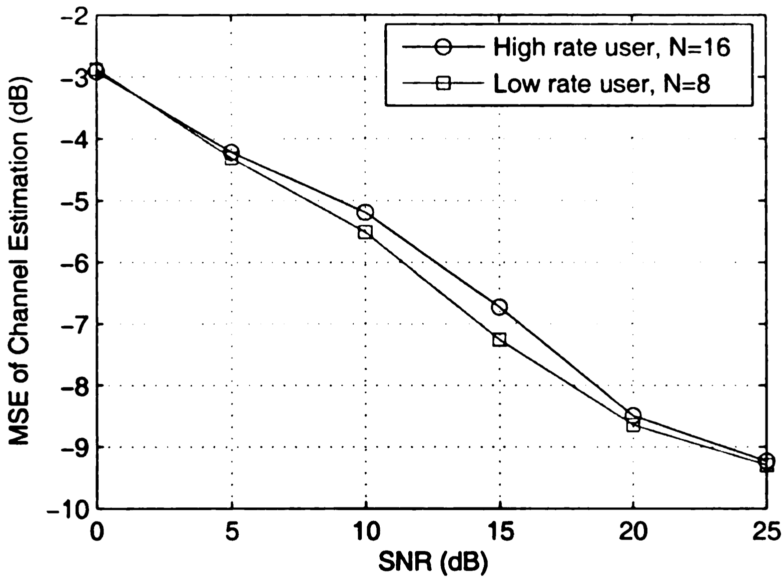

Figure 4.11. MSE of channel estimation, two users, $N = 16$ for the low rate user and $N = 8$ for the high rate user, 100 Monte Carlo runs and 1024 symbols per run.

rate user is $N = 16$. Each subchannel has four paths, which are uniformly distributed in one basic-rate symbol period. In this example, the additive noise is white Gaussian. SNR refers to chip level signal-to-noise ratio with respect to the desired user. The equalizers were designed based on 256 symbols, and were applied to 1024 symbols to calculate the normalized symbol mean square error SMSE. SMSE and MSE of channel estimation (CHMSE) were further averaged over 100 Monte Carlo runs. In this example, one user transmitted at basic symbol rate, and the other user transmitted at two times the basic rate. The estimation and equalization results are shown in Figure 4.11-4.13. Table 4.2 shows the average time in seconds per Monte Carlo run to extract the low rate user for both with and without matrix pencil approach.

Channel Order	15		7	
Number of receive antennas	4	3	4	3
Average time per run (s)	3.95	2.18	1.59	1.19

Table 4.2. Average time per run using MSLP+JADE approach.

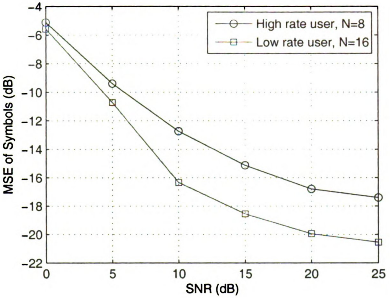

Figure 4.12. MSE of symbol estimation, two users, $N = 16$ for the low rate user and $N = 8$ for the high rate user, 100 Monte Carlo runs and 1024 symbols per run.

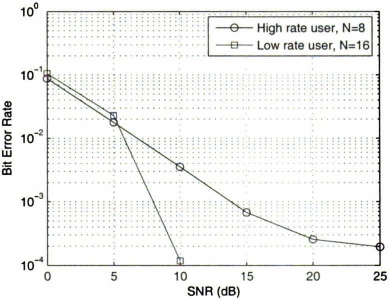

Figure 4.13. Bit error rate, $N = 16$ for the low rate user and $N = 8$ for the high rate user, 100 Monte Carlo runs and 1024 symbols per run.

4.4 Summary

In this chapter, multistep linear prediction based methods are proposed to perform blind channel estimation and equalization for long-code CDMA. Both uplink and downlink are considered:

- **Downlink** First, chip-rate equalization is performed to recover the scrambled signal. Secondly, after descrambling, the descrambled signal is regarded as the channel output of a short-code CDMA system with unknown channel parameters, and SEA method is applied to recover the signal of the desired user. The simulation results show that, the approach with SEA enhancement delivers much better performance than the approach that perform direct despreading after the descrambling procedure. It also can be observed that, when the receiver is equipped with multiple antennas, the performance can be improved significantly.

- **Uplink** In the uplink, if the spreading codes are nonconstant modulus, the transmission induced cyclostationarity make it possible to conduct blind channel estimation based on the second-order statistics (SOS) of the received signal. In this chapter, two SOS approaches are developed. One is based on the Fourier analysis and strict spreading code design, and the other one is based on the matrix pencil method. It was shown that the matrix pencil approach can relax the conditions on the spreading codes, and can deliver significantly better performance. If the spreading codes are constant modulus, higher-order statistics have to be exploited. In this chapter, the JADE (joint approximate diagonalization of eigen-matrices) algorithm proposed in [114] was applied for blind channel estimation. Compared to the methods exploiting transmission induced cyclostationarity, the MSLP+JADE approach developed for the system with constant modulus spreading codes has better performance, since higher-order statistics are exploited.

As chip level channel modeling and equalization are performed, the proposed approach can be extended to multirate CDMA systems in a straight forward manner.

CHAPTER 5

Blind Equalization of Space-time Block Coded DS-CDMA

This chapter considers blind channel estimation and signal detection in space-time block coded CDMA systems. Because of the size and complexity limitation of the mobile devices, it is more practical and economic to apply multiple antennas at the base station. Therefore space-time coding is only considered for downlink systems in this chapter. First, in order to achieve *maximum transmission diversity gain*, after spreading and scrambling, time-reversal space-time block coding (TR-STBC) [81–83] is applied to formulate a two-branch transmission. Only one spreading code is assigned to each user, and the time-reversed blocks can be regarded as spread spectrum signals whose spreading code is in the reversed order as the regular block in the same coding block. Secondly, motivated by [65], a blind channel estimation approach is developed based on the principal component algorithm. *The major advantage of this approach is that it can mitigate all the interference items (including multipath interference, multiuser interference, and the noise) simultaneously and effectively, and can achieve good channel estimation even at low SNR levels.* Finally, after the channel estimation, MMSE equalizer was applied to the matched filter output to recover the transmitted information symbols.

5.1 Transmission Scheme

In this chapter, TR-STBC technique is applied to achieve maximum transmission diversity. The transmission scheme is illustrated in Figure 5.1. Similar transmission

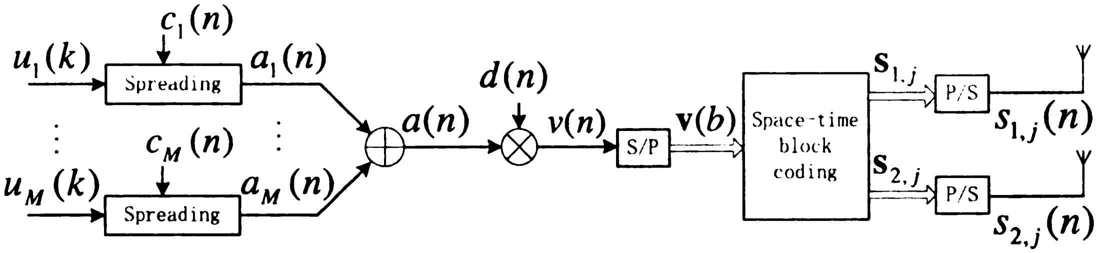

Figure 5.1. Downlink Transmission Scheme

scheme can be found in [83] and [84].

Consider a long code DS-CDMA downlink system with M users. The base station has two transmission antennas, and each mobile station has K ($K = 1$ or 2) receive antennas. Let $u_m(k)$ denote the kth symbol of user m, then the spreading result is given by

$$a_m(n) := \sum_{k=-\infty}^{\infty} u_m(k)c_m(n - kN), \tag{5.1}$$

where $c_m(n), n = 0, \ldots, N-1$, is the spreading code of user m. The summation of the spread spectrum signals $a(n) = \sum_{m=1}^{M} a_m(n)$ is *scrambled* by a pseudo-random sequence $d(n)$:

$$v(n) = a(n)d(n). \tag{5.2}$$

Collect PN consecutive scrambled chips to a $1 \times PN$ block $\mathbf{v}(b)$:

$$\mathbf{v}(b) = [v_b(0), v_b(1), \ldots, v_b(PN-1)], \tag{5.3}$$

where $v_b(i) = v(bPN + i), i = 0, \ldots, PN-1$. After prefix and postfix insertion, the resulting block can be represented as:

$$\mathbf{v}'(b) = [\mathbf{v}_p(b), \mathbf{v}(b), \mathbf{v}_o(b)], \tag{5.4}$$

where $\mathbf{v}_p(b)$ and $\mathbf{v}_o(b)$ are vectors that denote the prefix and postfix of the bth block, respectively. Let L represent the maximum length of the channels, $\mathbf{v}_p(b)$ and $\mathbf{v}_o(b)$

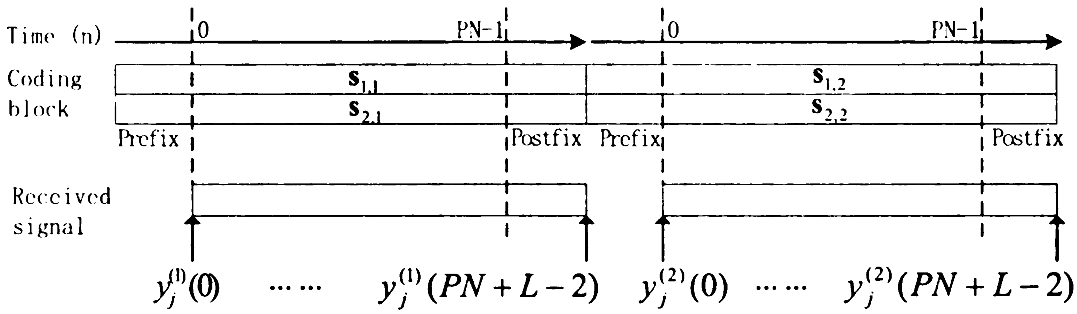

Figure 5.2. Data Structure of the Transmitted Signal

are chosen to be $1 \times [L-1]$ vectors to remove inter-block interference completely.

Next, two consecutive vectors $\mathbf{v}'(2b)$ and $\mathbf{v}'(2b+1)$ are used to form a space-time coding block given by:

$$\begin{bmatrix} \mathbf{s}_{1,1} & \mathbf{s}_{1,2} \\ \mathbf{s}_{2,1} & \mathbf{s}_{2,2} \end{bmatrix} = \begin{bmatrix} \mathbf{v}'(2b) & -\mathbf{v}'^{*}(2b+1)\mathbf{T}_{PN} \\ \mathbf{v}'(2b+1) & \mathbf{v}'^{*}(2b)\mathbf{T}_{PN} \end{bmatrix}, \tag{5.5}$$

where * denotes complex conjugate, and

$$\mathbf{T}_{PN} = \begin{bmatrix} 0 & 0 & \cdots & 1 \\ 0 & \cdots & 1 & 0 \\ \vdots & \vdots & \vdots & \vdots \\ 1 & 0 & \cdots & 0 \end{bmatrix}_{PN \times PN} \tag{5.6}$$

is a permutation matrix, which performs a time reversal of the $1 \times PN$ vector $\mathbf{v}'^{*}(b)$ through the operation $\mathbf{v}'^{*}(b)\mathbf{T}_{PN}$. The two rows of the coding block in (5.5) are transmitted from the two antennas respectively. Here and in the subsequent discussions, b is omitted from the notation for simplicity. In order to discriminate the information chip sequence from the prefix and postfix, the entries of $\mathbf{s}_{i,j}$ is denoted by

$$\mathbf{s}_{i,j} = [s_{i,j}(-L+1), s_{i,j}(-L+2), \ldots, s_{i,j}(PN+L-2)], \tag{5.7}$$

where $s_{i,j}(n), 0 \leq n \leq PN-1$, is the original information chip sequence before adding

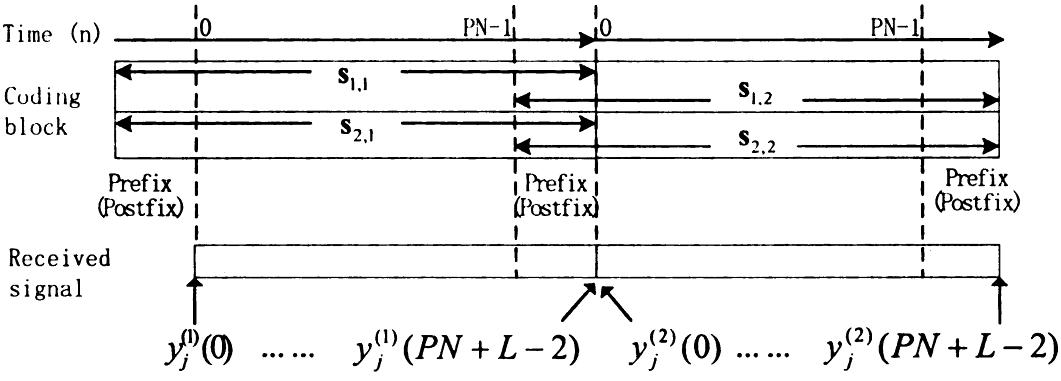

Figure 5.3. Data Structure of the Transmitted Signal using Shortened Prefix (Postfix)

the prefix and the postfix. The data structure of the space-time coded block is further illustrated in Figure 5.2.

In general cases, the length of both the prefix and the postfix should be no less than the channel order to avoid inter-block interference. For the channel estimation method presented in the next section, in order to approximate the correlation matrices using time average without edge effect, the prefix and postfix should be chosen to have the same second-order statistical properties as the chips that bearing information bits. One simple method is to use cyclic prefix and postfix. That is, the prefix $\mathbf{v}_p(b)$ is chosen to be the last $L-1$ symbols of $\mathbf{v}(b)$, and the postfix $\mathbf{v}_o(b)$ is chosen to be the first $L-1$ symbols of $\mathbf{v}(b)$. The total length of the chip sequence inserted between two information blocks is $2(L-1)$ as illustrated in Figure 5.2.

If no special statistical property is required for the prefix and the postfix, shorter prefix and postfix can be applied. It is mentioned in [115] that, when the prefix and the postfix possess certain conjugate symmetry properties, they can be merged into one sequence of length $L-1$. The coding structure with totally $L-1$ chips inserted between two information chip sequences is illustrated in Figure 5.3. The coding block should still satisfy:

$$\mathbf{s}_{1,2} = -\mathbf{s}_{2,1}^{*}\mathbf{T}_{PN} \tag{5.8}$$

$$\mathbf{s}_{2,2} = \mathbf{s}_{1,1}^{*}\mathbf{T}_{PN} \tag{5.9}$$

Therefore, we have

$$\begin{aligned}
& [s_{1,2}(-L+1), s_{1,2}(-L+2), \cdots, s_{1,2}(-1)] \\
= \; & -[s_{2,1}^*(PN+L-2), s_{2,1}^*(PN+1), \cdots, s_{2,1}^*(PN)] \qquad (5.10) \\
& [s_{2,2}(-L+1), s_{2,2}(-L+2), \cdots, s_{2,2}(-1)] \\
= \; & [s_{1,1}^*(PN+L-2), s_{1,1}^*(PN+1), \cdots, s_{1,1}^*(PN)]. \qquad (5.11)
\end{aligned}$$

From Figure 5.3, $[s_{1,2}(-L+1), \cdots, s_{1,2}(-1)]$ and $[s_{1,1}(PN), \cdots, s_{1,1}(PN+L-2)]$ represent the same sequence, which is the overlapped part of $\mathbf{s}_{1,1}$ and $\mathbf{s}_{1,2}$, then it can be obtained from (5.10) and (5.11) that

$$\begin{aligned}
& [s_{2,1}(PN), s_{2,1}(PN+1), \cdots, s_{2,1}(PN+L-2)] \\
= \; & -[s_{2,2}(-L+1), s_{2,2}(-L+2), \cdots, s_{2,2}(-1)]. \qquad (5.12)
\end{aligned}$$

Because $[s_{2,1}(PN), \cdots, s_{2,1}(PN+L-2)]$ and $[s_{2,2}(-L+1), \cdots, s_{2,2}(-1)]$ also represent the same sequence, the only choice of the overlapped chips (prefix/postfix) are zeros. That is , *zero padding* is the only way to reduce the length of the postfix/prefix, and satisfy (5.8-5.9) strictly at the same time.

For a fixed mobile device, let $\{g_i^{(p)}(l)\}_{l=0}^{L-1}, i = 1,2$ denote the channel between the ith transmit antenna and the pth receive antenna, then the received signal corresponding to block b at the pth antenna is given by

$$\begin{aligned}
y_p^{(j)}(k) \; &= \; \sum_{i=1}^{2} \sum_{l=0}^{L-1} g_i^{(p)}(l) s_{i,j}(k-l) + w_p^{(j)}(k), \\
& \quad (0 \leq k \leq PN+L-2, \; j = 1,2), \qquad (5.13)
\end{aligned}$$

where $w_p^{(j)}(k)$ is the additive white Gaussian noise at the pth receive antenna. Define the received signal array as:

$$\begin{aligned}
\mathbf{y}^{(j)}(k) \; &:= \; [y_1^{(j)}(k), y_2^{(j)}(k), \ldots, y_K^{(j)}(k)]^T \\
& \quad (0 \leq k \leq PN+L-2), \qquad (5.14)
\end{aligned}$$

and define the channel vector

$$\mathbf{g}_i(l) := [g_i^{(1)}(l), g_i^{(2)}(l), \ldots, g_i^{(K)}(l)]^T, \tag{5.15}$$

then we have

$$\mathbf{y}^{(j)}(k) = \sum_{i=1}^{2}\sum_{l=0}^{L-1} \mathbf{g}_i(l) s_{i,j}(k-l) + \mathbf{w}^{(j)}(k), \tag{5.16}$$

where $\mathbf{w}^{(j)}(k)$ is defined in the same way as $\mathbf{y}^{(j)}(k)$.

5.2 Blind Channel Estimation

In this section, based on the principal component algorithm [65], a blind channel estimation approach is developed for space-time coded long-code DS-CDMA system. The basic idea can be summarized as: (i) The time reversed chip sequence is still a spread spectrum signal, which implies that after space-time block coding, the transmitted signal from each antenna can be regarded as a DS-CDMA signal with aperiodic spreading codes. (ii) For DS-CDMA signals, the auto-covariance matrices of the received signal before and after despreading differ only by a rank one matrix, which is completely determined by the channel impulse response vector. The channel impulse response, therefore, can be estimated by calculating the principal eigenvector of this rank one matrix.

For simplicity, in the following discussions, we use $c_{i,j}^{(m)}(k,n), n = 0, \ldots, N-1$ to represent the overall spreading code for the kth symbol of user m carried by the sequence $\mathbf{s}_{i,j}$. Despread $\mathbf{y}^{(j)}(k)$ at different delays:

$$\mathbf{x}_{i,j}^{(m)}(k) = \begin{bmatrix} \sum_{n=0}^{N-1} \mathbf{y}^{(j)}(kN+n+L-1) c_{i,j}^{(m)}(k,n) \\ \vdots \\ \sum_{n=0}^{N-1} \mathbf{y}^{(j)}(kN+n+1) c_{i,j}^{(m)}(k,n) \\ \sum_{n=0}^{N-1} \mathbf{y}^{(j)}(kN+n) c_{i,j}^{(m)}(k,n) \end{bmatrix}. \tag{5.17}$$

Define

$$\begin{aligned}\mathbf{y}_L^{(j)}(n) &:= [(\mathbf{y}^{(j)}(n))^T, (\mathbf{y}^{(j)}(n-1))^T, \ldots, (\mathbf{y}^{(j)}(n-L+1))^T]^T, \\ &\quad (L-1 \leq n \leq PN+L-2) \qquad (5.18)\\ \mathbf{Y}^{(j)}(k) &:= [\mathbf{y}_L^{(j)}(kN+L-1), \mathbf{y}_L^{(j)}(kN+L), \ldots, \mathbf{y}_L^{(j)}(kN+N+L-2)], \qquad (5.19)\end{aligned}$$

then the despreading result can be represented as

$$\mathbf{x}_{i,j}^{(m)}(k) = \mathbf{Y}^{(j)}(k)\mathbf{c}_{i,j}^{(m)}(k), \qquad (5.20)$$

where

$$\mathbf{c}_{i,j}^{(m)}(k) = [c_{i,j}^{(m)}(k,0), c_{i,j}^{(m)}(k,1), \ldots, c_{i,j}^{(m)}(k,N-1)]^T. \qquad (5.21)$$

Define

$$\mathbf{H}_p := \begin{bmatrix} \mathbf{g}_p(0) & \mathbf{g}_p(1) & \cdots & \mathbf{g}_p(L-1) & 0 & \cdots & 0 \\ 0 & \mathbf{g}_p(0) & \mathbf{g}_p(1) & \cdots & \mathbf{g}_p(L-1) & \cdots & 0 \\ \vdots & \vdots & \ddots & \ddots & \ddots & \ddots & \vdots \\ 0 & \cdots & 0 & \mathbf{g}_p(0) & \mathbf{g}_p(1) & \cdots & \mathbf{g}_p(L-1) \end{bmatrix} \qquad (5.22)$$

and

$$\bar{\mathbf{s}}_{i,j}(n) = [s_{i,j}(n), s_{i,j}(n-1), \ldots, s_{i,j}(n-2L+2)]^T, \qquad (5.23)$$

then it can be obtained that

$$\mathbf{y}_L^{(j)}(n) = \sum_{i=1}^{2} \mathbf{H}_i \bar{\mathbf{s}}_{i,j}(n) + \mathbf{w}_L^{(j)}(n), \qquad (5.24)$$

where $\mathbf{w}_L^{(j)}(n)$ is defined in the same way as $\mathbf{y}_L^{(j)}(n)$. To further analyze the received signal, let $s_{i,j}^{(m)}(n)$ and $\bar{\mathbf{s}}_{i,j}^{(m)}(n)$ denote the contribution of user m to $s_{i,j}$ and $\bar{\mathbf{s}}_{i,j}(n)$ respectively, then $\mathbf{y}_L^{(j)}(n)$ can be decomposed as

$$\begin{aligned}\mathbf{y}_L^{(j)}(n) &= s_{i,j}^{(m)}(n-L+1)\tilde{\mathbf{g}}_i + \\ & \underbrace{\sum_{k\neq L} s_{i,j}^{(m)}(n-k+1)\mathbf{h}_{i,k} + \sum_{k\neq m}\sum_{q\neq i}\mathbf{H}_q\bar{\mathbf{s}}_{q,j}^{(k)}(n) + \mathbf{w}_L^{(j)}(n)}_{\mathcal{I}(n)}, \end{aligned} \tag{5.25}$$

where

$$\tilde{\mathbf{g}}_i = [\mathbf{g}_i^T(L-1), \mathbf{g}_i^T(L-2), \ldots, \mathbf{g}_i^T(0)]^T, \tag{5.26}$$

$\mathbf{h}_{i,k}$ represents the kth column of matrix $\mathbf{H}_i$, and $\mathcal{I}(n)$ stands for the inter-chip interference, multiuser interference and the noise.

Calculate the covariance matrix of the received signal before despreading, we get

$$\mathbf{R}_{yy} = E\{\mathbf{y}_L^{(j)}(n)(\mathbf{y}_L^{(j)}(n))^H\} = \tilde{\mathbf{g}}_i\tilde{\mathbf{g}}_i^H + \mathbf{R}_{\mathcal{I}\mathcal{I}}, \tag{5.27}$$

where $\mathbf{R}_{\mathcal{I}\mathcal{I}} = E\{\mathcal{I}(n)\mathcal{I}^H(n)\}$, and $(\cdot)^H$ represents complex conjugate transpose. From (5.19), the covariance matrix of $\mathbf{Y}^{(j)}(k)$ is given by

$$\begin{aligned}\mathbf{R}_{YY} &= E\{\mathbf{Y}^{(j)}(k)[\mathbf{Y}^{(j)}(k)]^H\} \\ &= N\mathbf{R}_{yy} \\ &= N\tilde{\mathbf{g}}_i\tilde{\mathbf{g}}_i^H + N\mathbf{R}_{\mathcal{I}\mathcal{I}}. \end{aligned} \tag{5.28}$$

From (5.20) and (5.25), it follows that the despread signal can be decomposed as

$$\mathbf{x}_{i,j}^{(m)}(k) = Nu_{i,j}^{(m)}(k)\tilde{\mathbf{g}}_i + \sum_{l=0}^{N-1}\mathcal{I}(KN+L-1+l)c_{i,j}^{(m)}(k,l), \tag{5.29}$$

where $u_{i,j}^{(m)}(k)$ denotes the kth symbol of user m in block $\mathbf{s}_{i,j}^{(m)}$. Therefore, we have

$$\mathbf{R}_{xx} = E\{\mathbf{x}_{i,j}^{(m)}(k)(\mathbf{x}_{i,j}^{(m)}(k))^H\} = N^2\tilde{\mathbf{g}}_i\tilde{\mathbf{g}}_i^H + N\mathbf{R}_{\mathcal{I}\mathcal{I}}. \tag{5.30}$$

The difference between $\mathbf{R}_{xx}$ and $\mathbf{R}_{YY}$ is given by

$$\mathbf{R}_{xx} - \mathbf{R}_{YY} = N(N-1)\tilde{\mathbf{g}}_i\tilde{\mathbf{g}}_i^H. \tag{5.31}$$

From (5.31), clearly, the channel impulse response $\tilde{\mathbf{g}}_i$ can be estimated up to a scalar through eigen-value decomposition.

5.3 Signal Detection

In this section, an equivalent system model is derived based on the time-reversal coding structure, and the MIMO matched filter is used to decouple the two chip sequences contained in one coding block. After space-time decoding, the MIMO system is transformed into two SIMO systems, and MMSE equalizer is designed to recover the signal.

5.3.1 Space-Time Decoding

Since the TR-STBC scheme is applied at the transmitter end, at the receiver, the signals transmitted from the two antennas can be decoupled by the MIMO matched filter. Define the received signal block corresponding to coding block b as

$$\begin{aligned}
\mathbf{r}_1(n) &= \mathbf{y}^{(1)}(n) \\
\mathbf{r}_2(n) &= \mathbf{y}^{*(2)}(PN+L-2-n) \\
&\quad (n = 0, 1, \ldots, PN+L-2).
\end{aligned} \tag{5.32}$$

From (5.16), the z–transform of $\mathbf{r}_1(k)$ is given by

$$\mathbf{r}_1(z) = \mathbf{g}_1(z)s_{1,1}(z) + \mathbf{g}_2(z)s_{2,1}(z) + \mathbf{w}^{(1)}(z). \tag{5.33}$$

For a causal sequence $\alpha(k)$, the z-transform is defined as $\alpha(z) = \sum_{k=0}^{\infty} \alpha(k) z^{-k}$, then the z–transform of $\alpha^*(k)$ is given by

$$\alpha^*(z) = \sum_{k=0}^{\infty} \alpha^*(k) z^{-k}. \tag{5.34}$$

Therefore the z–transform of $\mathbf{r}_2(k)$ can be deduced as

$$\begin{aligned}
& \mathbf{y}^{(2)}(k) \longrightarrow \mathbf{y}^{(2)}(z) \\
\Longrightarrow\ & \mathbf{y}^{(2)}(-k) \longrightarrow \mathbf{y}^{(2)}(z^{-1}) \\
\Longrightarrow\ & \mathbf{y}^{(2)}(PN + L - 2 - k) \longrightarrow z^{-PN-L+2}\mathbf{y}^{(2)}(z^{-1}) \\
\Longrightarrow\ & \mathbf{r}_2(k) = \mathbf{y}^{*(2)}(PN + L - 2 - k) \\
& \longrightarrow \mathbf{r}_2(z) = z^{-PN-L+2}\mathbf{y}^{*(2)}(z^{-1}).
\end{aligned} \tag{5.35}$$

From (5.16) and (5.5), it follows that

$$\begin{aligned}
\mathbf{y}^{(2)}(z) &= \mathbf{g}_1(z)s_{1,2}(z) + \mathbf{g}_2(z)s_{2,2}(z) + \mathbf{w}^{(2)}(z) \\
&= -z^{-PN+1}\mathbf{g}_1(z)s_{2,1}^*(z^{-1}) + z^{-PN+1}\mathbf{g}_2(z)s_{1,1}^*(z^{-1}) + \mathbf{w}^{(2)}(z).
\end{aligned} \tag{5.36}$$

Finally, $\mathbf{r}_2(z)$ has following expression

$$\mathbf{r}_2(z) = z^{-L+1}[-\mathbf{g}_1^*(z^{-1})s_{2,1}(z) + \mathbf{g}_2^*(z^{-1})s_{1,1}(z)] + z^{-PN-L+2}\mathbf{w}^{(2)*}(z^{-1}). \tag{5.37}$$

Define $\mathbf{r}(k) = [\mathbf{r}_1^H(k), \mathbf{r}_2^H(k)]^H$, then we have

$$\mathbf{r}(z) = \begin{bmatrix} \mathbf{r}_1(z) \\ \mathbf{r}_2(z) \end{bmatrix} = \tilde{\mathbf{H}}(z) \begin{bmatrix} s_{1,1}(z) \\ s_{2,1}(z) \end{bmatrix} + \tilde{\mathbf{w}}(z), \tag{5.38}$$

where

$$\tilde{\mathbf{H}}(z) = \begin{bmatrix} \mathbf{g}_1(z) & \mathbf{g}_2(z) \\ z^{-L+1}\mathbf{g}_2^*(z^{-1}) & -z^{-L+1}\mathbf{g}_1^*(z^{-1}) \end{bmatrix} \tag{5.39}$$

$$\tilde{\mathbf{w}}(z) = \begin{bmatrix} \mathbf{w}^{(1)}(z) \\ z^{-PN-L+2}\mathbf{w}^{(2)*}(z^{-1}) \end{bmatrix}. \tag{5.40}$$

Because $w_p^{(j)}(k)$ is white gaussian, from the definition of $\mathbf{w}^{(j)}(k), j = 1, 2$, we have $\mathbf{R}_{ww}(k) = E\{\tilde{\mathbf{w}}(n)\tilde{\mathbf{w}}^H(n-k)\} = \sigma_n^2\mathbf{I}\delta(k)$, and $\mathbf{R}_{ww}(z) = \sigma_n^2\mathbf{I}$. From (5.39), the MIMO matched filter is given by

$$\tilde{\mathbf{H}}^H(z^{-1}) = \begin{bmatrix} \mathbf{g}_1^H(z^{-1}) & z^{L-1}\mathbf{g}_2^T(z) \\ \mathbf{g}_2^H(z^{-1}) & -z^{L-1}\mathbf{g}_1^T(z) \end{bmatrix}. \tag{5.41}$$

It can be observed that $\tilde{\mathbf{H}}(z)$ has the following orthogonal properties:

$$\tilde{\mathbf{H}}^H(z^{-1})\tilde{\mathbf{H}}(z) = [\mathbf{g}_1^H(z^{-1})\mathbf{g}_1(z) + \mathbf{g}_2^H(z^{-1})\mathbf{g}_2(z)]\mathbf{I}_2, \tag{5.42}$$

where $\mathbf{I}_2$ denotes the 2×2 identical matrix. Thus, the signals can be decoupled using the MIMO matched filter $\tilde{\mathbf{H}}^H(z^{-1})$, that is

$$\mathbf{q}(z) = \begin{bmatrix} q_1(z) \\ q_2(z) \end{bmatrix} = \tilde{\mathbf{H}}^H(z^{-1})\mathbf{r}(z) = \tilde{h}(z)\begin{bmatrix} s_{1,1}(z) \\ s_{2,1}(z) \end{bmatrix} + \tilde{\mathbf{w}}'(z), \tag{5.43}$$

where

$$\begin{aligned} \tilde{h}(z) &:= \mathbf{g}_1^H(z^{-1})\mathbf{g}_1(z) + \mathbf{g}_2^H(z^{-1})\mathbf{g}_2(z) && (5.44) \\ \tilde{\mathbf{w}}'(z) &:= \begin{bmatrix} w_1'(z) \\ w_2'(z) \end{bmatrix} = \tilde{\mathbf{H}}^H(z^{-1})\tilde{\mathbf{w}}(z). && (5.45) \end{aligned}$$

From the fact $\mathbf{R}_{ww}(z) = \sigma_n^2\mathbf{I}$, we have

$$\begin{aligned} \mathbf{R}'_{ww}(z) &= \sum_{k=-\infty}^{\infty} E\{\tilde{\mathbf{w}}'(n)[\tilde{\mathbf{w}}'(n-k)]^H\}z^{-k} \\ &= \tilde{\mathbf{H}}^H(z^{-1})\mathbf{R}_{ww}(z)\tilde{\mathbf{H}}(z) \\ &= \sigma_n^2\tilde{\mathbf{H}}^H(z^{-1})\tilde{\mathbf{H}}(z) \\ &= \sigma_n^2\tilde{h}(z)\mathbf{I}. \end{aligned} \tag{5.46}$$

Therefore, $w_1'(z)$ and $w_2'(z)$ are uncorrelated, and the detection problems are completely decoupled.

5.3.2 MMSE Equalization

After decoupling, the transmitted signals, $\mathbf{s}_{1,1}$ and $\mathbf{s}_{2,1}$, have been separated from each other, while the decoupled results are still distorted by a linear filter $\tilde{h}(z)$. Based on the channel estimation result, ML detectors can be applied to estimate the original input. Considering the complexity of the ML approach, in this section, an MMSE equalizer is designed to recover the information chip sequences. Since $s_{1,1}(k)$ and $s_{2,1}(k)$ have the same statistical properties, from (5.43), both of them can be estimated using the same equalizer. Let $f(k), k = 0, \ldots, L_e - 1$ denote the equalizer coefficients, the equalization output is then given by:

$$\hat{s}_{i,1}(k-\tau) = \sum_{l=0}^{L_e-1} f^*(l) q_i(k-l) \qquad (i = 1, 2), \tag{5.47}$$

where τ is the equalization delay. Define

$$\mathbf{f} = [f(0), f(1), \ldots, f(L_e - 1)]^T, \tag{5.48}$$

and

$$\mathbf{q}_i(n) = [q_i(n), q_i(n-1), \ldots, q_i(n - L_e + 1)]^T, \tag{5.49}$$

then the MMSE equalizer is given by

$$\mathbf{f} = \mathbf{R}_{qq}^{\#} \tilde{\mathbf{h}}_\tau, \tag{5.50}$$

where $\mathbf{R}_{qq} = \mathbf{E}\{\mathbf{q}_i(n)\mathbf{q}_i^H(n)\}$, $\tilde{\mathbf{h}}_\tau = [\tilde{h}(\tau), \ldots, \tilde{h}(0), 0, \ldots, 0]^T$, and $\mathbf{R}_{qq}^{\#}$ represents the pseudoinverse of matrix $\mathbf{R}_{qq}$.

After equalization, the information chip sequence $\mathbf{v}(2b)$ and $\mathbf{v}(2b+1)$ can be recovered, and the symbol sequence of the desired user can be estimated through descrambling and despreading.

5.4 Simulation Examples

In this section, simulation examples are provided to illustrate the proposed approach. We consider a downlink CDMA system with 8 users. The spreading gain is selected to be $N = 16$. The mobile stations with both one and two receive antennas are considered. QPSK signals are transmitted from the base station. Each space-time coding block contain 16 information symbols ($P = 8$). Two kinds of prefix and postfix are tested. One is simply zero padding. For the other one, the prefix $\mathbf{v}_p(b)$ is chosen to be the last $L - 1$ symbols of $\mathbf{v}(b)$, and the postfix $\mathbf{v}_o(b)$ is chosen to be the first $L - 1$ symbols of $\mathbf{v}(b)$. 256 symbols are used to perform blind channel estimation, and the equalization is carried out for 1024 symbols. The MSE of the channel estimation and the BER are averaged over 100 Monte Carlo runs for different SNR levels. The channels are generated randomly and independently for each run. Each multiple channel has 3 rays, which are uniformly distributed over 5 chip periods. The performance of the proposed approach is compared with the approach without space-time coding. For the later case, only one transmission antenna is used, and the same channel estimation method is applied.

The simulation results are shown in Figure 5.4 and Figure 5.5. It can be observed that, by introducing transmission space diversity, the proposed scheme delivers much better performance compared with conventional single transmit antenna scheme. Two kinds of prefix and postfix have similar channel estimation results, but the transmission scheme using zero padding delivers better BER performance, as less interference is introduced in this case.

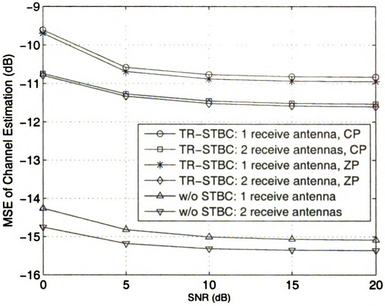

Figure 5.4. MSE of channel estimation. Spreading gain $N = 16$, and number of users $M = 8$.

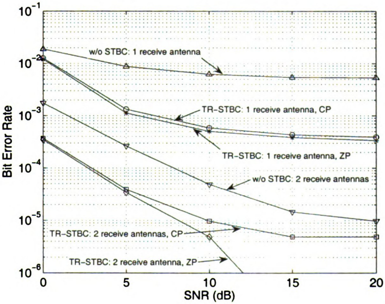

Figure 5.5. Bit error rate. Spreading gain $N = 16$, and number of users $M = 8$.

5.5 Summary

In this chapter, a blind signal detection approach based on the principal component algorithm is presented for TR-STBC DS-CDMA systems with aperiodic spreading codes. Compared with the scheme without space-time coding, significant gain can be obtained by introducing transmission diversity. Both cyclic prefix/postfix and zero padding were discussed and tested with simulation. While similar performance can be observed using both kinds of prefix/postfix, it is more spectral efficient to use zero padding. It is shown that the proposed approach is not only very effective in mitigating multipath interference and multiuser interference, but is also robust to additive noise.

CHAPTER 6

Conclusions and Future Works

6.1 Conclusions

The research focus of this dissertation is blind signal detection for DS-CDMA over frequency selective channels. Statistics based methods are designed for both short-code and long-code CDMA systems. A fast HOS based approach – MR-CSEA is proposed for multi-rate short-code systems, and MSLP based chip-rate equalizers are designed for long-code systems. Blind equalization approaches have been developed for space-time coded downlink long-code CDMA with maximum transmission diversity. Based on the theoretical analysis and simulation results, we have the following conclusions:

- *Characterization of CDMA systems*

  When modelling with symbol-level inputs and chip-level outputs, the short-code DS-CDMA can be characterized with an MIMO time invariant model, while the long-code DS-CDMA can only be characterized by time variant model because of the time variant nature of the spreading code. By taking the chip-rate scrambled signal as the input, the long-code DS-CDMA can also be modelled as a time invariant system.

- *Equalizer design for multirate short-code systems*

  - For both MC and VSL schemes, the signal of a high-rate user can be regarded as the sum of the signals of several virtual users.
  - The code structure can be exploited to recover the symbol-rate signal

blindly, and only the spreading code of the desired user is assumed to be known.

  - By using proper initialization, the signals of different virtual users can be recovered in correct order, which is necessary for restoring the sequence of the corresponding high-rate user.
  - The proposed MR-CSEA approach has fast convergence speed and superior performance. The simulation results show that, when the chip SNR is larger than 15dB, the proposed approach has much better performance, and converges much faster than existing blind approaches. It can be observed that, at high SNR, the proposed method converges to the MMSE equalizer with known channel information.

- *Two-stage blind channel estimation and signal detection for long-code systems*

  MSLP based blind channel identification methods have been developed for both uplink and downlink long-code CDMA. First, convolutive mixtures are converted to instantaneous mixtures. Secondly, both second-order-statistics based and higher-order-statistics based approaches can be developed for blind signal detection.

  - *Blind signal detection for downlink long-code systems*

    After chip-rate equalization, the descrambled signal can be modelled as the output of a short-code CDMA system. By using this method, the performance can be improved significantly.

  - *Blind signal detection for uplink long-code systems*

    * When the spreading codes are nonconstant modulus, the cyclostationarity introduced by the transmitted signal can be exploited to perform blind channel estimation based only on the second-order statistics (SOS) of the observed data.
    * By choosing the spreading codes that have special properties in frequency domain, Fourier analysis method can be used to perform blind

channel estimation. This method is relatively simple, but additional constraint is required.

* By introducing a random linear transform, the matrix pencil approach can remove the extra constraint on the code sequences. Simulation results show that the matrix pencil based approach delivers much better result than the one relying on the Fourier transform.

* If the spreading codes are constant modulus, higher-order statistics based methods have to be applied to exploit the phase information. In this research, JADE algorithm is applied to identify the channels blindly.

* As chip level channel modeling and equalization are performed, the proposed approach can be extended to multirate CDMA systems in a straight forward manner.

- *Blind equalizer design for space-time coded downlink CDMA*

  - After space-time coding, the two chip sequences assigned to the two transmission antennas can be treated as two long-code CDMA sequence with prefix/postfix inserted. In the time interval between two consecutive prefixes/pofixes, the spreading sequences of the two transmission antennas are independent. Based on this observation, statistical method can be developed to perform blind channel estimation.

  - Both cyclic prefix/postfix and zero padding can be used to suppress interblock interference, and similar performances have been observed. However, using zero padding is more spectrally efficient, as the length of the prefix/postfix could be reduced by half.

  - Significant improvement can be achieved by introducing transmission diversity.

6.2 Related Future Works

In this section, possible future research directions are discussed.

- *Further discussions on blind channel estimation of downlink CDMA with TR-STBC scheme.*

  In this thesis, the blind channel estimation is performed for downlink CDMA with TR-STBC scheme. While the signal components of all active users share the same channel impulse responses between the base-station and the received antennas of a given mobile device, only the signal component of the desired user is analyzed to perform blind channel estimation. The performance can be improved by exploiting the statistical properties of all signal components. Because two transmission antennas are applied to the TR-STBC scheme, the MSLP algorithm developed for conventional downlink systems can not be applied directly for blind channel estimation, since there are two channels need to be estimated. Because each antenna can be treated as a virtual user, algorithms designed for uplink systems may be extended to this case, and simulations need to be carried out for performance analysis.

- *Blind signal detection for space-time spreading scheme*

  Applying spacial diversity is a trend in next generation wireless communication systems. Alamouti space-time block coding scheme has been specified in W-CDMA standardization, while space-time spreading (STS) scheme [116], which includes the STBC scheme as a special case, has been adopted in IS-2000 standard. So far, *blind signal detection methods designed for STS scheme has rarely been observed.* Consider a CDMA system with STS transmission scheme. Let $u(k)$ denote the kth symbol of the transmitted stream, then the signal transmitted from one antenna is given by

$$\mathbf{s}_1(k) = \frac{1}{\sqrt{2}}(u(2k)\mathbf{c}_1 + u(2k+1)\mathbf{c}_2), \tag{6.1}$$

and the signal transmitted from the other antenna is given by

$$\mathbf{s}_2(k) = \frac{1}{\sqrt{2}}(u(2k+1)\mathbf{c}_1 - u(2k)\mathbf{c}_2), \tag{6.2}$$

where $\mathbf{c}_1$ and $\mathbf{c}_2$ are $1 \times 2N$ spreading sequences. It can be observed that every symbol is spread by both spreading sequences. Therefore, it is difficult to perform blind signal detection by exploiting the code structure. Blind signal detection of STS scheme should be considered from a totally new viewpoint.

APPENDICES

APPENDIX A

List of Abbreviations and Acronyms

ANMSE	Asymptotic Normalized Mean Square Error
AMPS	Advanced Mobile Phone Service
CDMA	Code Division Multiple Access
CM	Constant Modulus
CMA	Constant Modulus Algorithm
CSEA	Code Constrained Super Exponential Algorithm
DS-CDMA	Direct Sequence Code Division Multiple Access
FDMA	Frequency Division Multiple Access
FIR	Finite Impulse Response
GSM	Global System for Mobile Communications
HOS	Higher-Order Statistics
IFC	Inverse Filter Criterion
IIR	Infinite Impulse Response
ISI	Inter-Symbol Interference
JADE	Joint Approximate Diagonalization of Eigen-Matrices
JOSC	Joint Optimization with Subspace Constraints
LCM	Least Common Multiple
MC	Multiple Code
MIMO	Multiple-Input Multiple-Output
ML	Maximum-Likelihood
MMSE	Minimum Mean Square Error

MR-CC-IFC	Multi-rate Code Constrained Inverse Filter Criterion
MR-CSEA	Multi-rate Code Constrained Super Exponential Algorithm
MSE	Mean Square Error
MSLP	Multistep Linear Prediction
MUI	Multi-User Interference
QPSK	Quadrature Phase-Shift Keying
SEA	Super Exponential Algorithm
SIC	Serial Interference Cancellation
SIMO	Single-Input Multiple-Output
SISO	Single-Input Single-Output
SNR	Signal-to-Noise Ratio
SOS	Second-Order Statistics
STBC	Space-Time Block Coding
STS	Space-Time Spreading
STTC	Space-Time Trellis Codes
TDMA	Time Division Multiple Access
TR-STBC	Time-Reversal Space-Time Block Coding
VSL	Variable Sequence Length

APPENDIX B

Definitions of Higher-Order Statistics

Let $x_1, x_2, \ldots, x_n$ be a set of random variables. Their joint characteristic function is given by

$$\phi(\omega_1, \ldots, \omega_n) = E\left\{e^{j\sum_{i=1}^{n}\omega_i x_i}\right\} \tag{B.1}$$

The joint cumulant of $x_{n_1}, x_{n_2}, \ldots, x_{n_m}$, $n_i \in \{1, 2, \ldots, n\}$ is defined by

$$\text{cum}\{x_{n_1}, x_{n_2}, \ldots, x_{n_m}\} = (-j)^m \left.\frac{\partial^m \ln\phi(\omega_1, \ldots, \omega_n)}{\partial\omega_{n_1}\cdots\partial\omega_{n_m}}\right|_{\omega_{n_1}=\omega_{n_2}=\cdots=\omega_{n_m}=0} \tag{B.2}$$

The mth order joint cumulant $\text{cum}\{x_{n_1}, x_{n_2}, \ldots, x_{n_m}\}$ is related to the moments of $x_{n_1}, \ldots, x_{n_m}$ up to order m. For example, if x_1, x_2, x_3, x_4 are zero-mean random variables, then

$$\begin{aligned}
\text{cum}(x_1) &= 0 \\
\text{cum}(x_1, x_2) &= E\{x_1x_2\} \\
\text{cum}(x_1, x_2, x_3) &= E\{x_1x_2x_3\} \\
\text{cum}(x_1, x_2, x_3, x_4) &= E\{x_1x_2x_3x_4\} - E\{x_1x_2\}E\{x_3x_4\} \\
&= -E\{x_1x_3\}E\{x_2x_4\} - E\{x_1x_4\}E\{x_2x_3\}
\end{aligned} \tag{B.3}$$

The *kurtosis* of x_1 is defined as

$$\text{cum}_4\{x_1\} \triangleq \text{cum}\{x_1, x_1, x_1^*, x_1^*\} = E\{|x_1|^4\} - 2\{E\{|x_1|^2\}\}^2 - |E\{x_1^2\}|^2. \tag{B.4}$$

The mth order joint cumulant $\mathrm{cum}\{x_{n_1}, x_{n_2}, \ldots, x_{n_m}\}$ has the following important property: if $x_{n_1}, x_{n_2}, \ldots, x_{n_m}$ are jointly Gaussian, then their joint cumulant is zero whenever $m > 2$. For the convenience of notation, we denote

$$\mathrm{cum}\{x_1 : p_1, x_2 : p_2 \ldots\} = \mathrm{cum}\{\underbrace{x_1, x_1, \ldots, x_1}_{p_1 terms}, \underbrace{x_2, x_2, \ldots, x_2}_{p_2 terms} \ldots\} \tag{B.5}$$

APPENDIX C

Convergence Analysis of the CSEA Approach

In this appendix, the equivalent combined channel-equalizer domain representation of both CSEA and MR-CSEA is given in Section C.1, then the convergence analysis of both algorithms is presented in Section C.2.

C.1 Equivalent Representation in the Combined Response Domain

Let $\tilde{\mathbf{f}}^{(m_0)}$ denote the equalizer to extract the desired user m_0 in a single-rate system, or the desired virtual user (i_0, j_0, m_0) in a multirate system, then the combined response in the code-constrained case is given by (see (3.60) and (3.87))

$$\Theta = (\tilde{\mathbf{H}}\Pi^{\perp}_{\mathcal{A}^{(m_0)}})\tilde{\mathbf{f}}^{(m_0)}. \tag{C.1}$$

Let $\theta(n)$ denote the nth component of Θ, and $\Theta^{\odot(p,q)}$ stands for the Hadamard power in complex case , whose nth component is given by

$$\Theta^{\odot(p,q)}(n) = \theta(n)^p \theta^*(n)^q. \tag{C.2}$$

For the unconstrained case, $\Theta = \tilde{\mathbf{H}}\tilde{\mathbf{f}}^{(m_0)}$. It can be seen that $\Theta \in range(\tilde{\mathbf{H}})$.

Define space $\mathcal{S}_A \triangleq range(\tilde{\mathbf{H}})$, the orthogonal projection operator onto $\mathcal{S}_A$ is given by

$$\mathcal{P}_A = \tilde{\mathbf{H}}(\tilde{\mathbf{H}}^H\tilde{\mathbf{H}})^{\#}\tilde{\mathbf{H}}^H. \tag{C.3}$$

If $\mathcal{P}_A = I$, then it is called the sufficent order case. Otherwise, it is called undermodeled case, in which $\tilde{\mathbf{H}}$ is not of full rank.

Compared with (3.29) and (3.30), we have

- *Unconstrained super-exponential algorithm:*

$$\begin{aligned} \Theta' &= \tilde{\mathbf{H}}(\tilde{\mathbf{H}}^H\tilde{\mathbf{H}})^{\#}\tilde{\mathbf{H}}^H\Theta^{\odot(p,q)} = \mathcal{P}_A\Theta^{\odot(p,q)} && \text{(C.4)} \\ \Theta'' &= \frac{\Theta'}{\parallel \Theta' \parallel_2} && \text{(C.5)} \end{aligned}$$

For code constrained case, Define space $\mathcal{S}_{CA} = range(\tilde{\mathbf{H}}\Pi^{\perp}_{\mathcal{A}(m_0)})$. From (C.1), we can see that $\Theta \in \mathcal{S}_{CA}$. The orthogonal projection operator on to $\mathcal{S}_{CA}$ is given by

$$\begin{aligned} \mathcal{P}_{CA} &= \tilde{\mathbf{H}}E((\tilde{\mathbf{H}}E)^H\tilde{\mathbf{H}}E)^{\#}(\tilde{\mathbf{H}}E)^H \\ &= \tilde{\mathbf{H}}E(\tilde{\mathbf{H}}E)^{\#} = \tilde{\mathbf{H}}(\tilde{\mathbf{H}}E)^{\#} && \text{(C.6)} \\ & \quad (since\ E(\tilde{\mathbf{H}}E)^{\#} = (\tilde{\mathbf{H}}E)^{\#}) \end{aligned}$$

where $E = \Pi^{\perp}_{\mathcal{A}(m_0)}$. Therefore, the equivalent algorithm of CSEA in the combined response domain can be obtained as

- *Code Constrained super-exponential algorithm:*

$$\begin{aligned} \Theta' &= (\tilde{\mathbf{H}}E)(\tilde{\mathbf{H}}E)^{\#}\Theta^{\odot(p,q)} = \mathcal{P}_{CA}\Theta^{\odot(p,q)} && \text{(C.7)} \\ \Theta'' &= \frac{\Theta'}{\parallel \Theta' \parallel_2} && \text{(C.8)} \end{aligned}$$

Since $\tilde{\mathbf{H}}E$ is not of full rank, constrained algorithm is corresponded to a special undermodel case.

C.2 Convergence Analysis

In this section, we prove that the CSEA approach is equivalent to a gradient search algorithm which maximizes the cost function

$$\mathbf{F}_{2p}(\Theta) = \left\{ \frac{\| \Theta \|_{2p}}{\| \Theta \|_2} \right\}^{2p}, \tag{C.9}$$

with the constraint $\Theta \in \mathcal{S}_{CA}$, where $p = 2, 3, \ldots, \infty$.

Proposition C.1 *The super-exponential algorithm (C.7) (C.8) is equivalent to the gradient search algorithm defined by*

$$\begin{aligned} \Theta' &= \Theta^{(n)} + \frac{1}{p\mathbf{F}_{2p}(\Theta^{(n)})} \mathcal{P}_{CA} \nabla_{\Theta^*} \mathbf{F}_{2p}(\Theta^{(n)}) & \text{(C.10)} \\ \Theta^{(n+1)} &= \frac{\Theta'}{\|\Theta'\|_2}, & \text{(C.11)} \end{aligned}$$

For the convenience of calculation, we prove that the following algorithm is equivalent to (C.7) (C.8)

$$\begin{aligned} \Theta' &= \Theta^{*(n)} + \frac{1}{p\mathbf{F}_{2p}(\Theta^{(n)})} \mathcal{P}_{CA} \nabla_{\Theta} \mathbf{F}_{2p}(\Theta^{(n)}) & \text{(C.12)} \\ \Theta^{*(n+1)} &= \frac{\Theta'}{\|\Theta'\|_2}, & \text{(C.13)} \end{aligned}$$

Proof:

Define: $u = \|\Theta\|_{2p}^{2p}$, $v = \|\Theta\|_2^{2p}$, then

$$\mathbf{F}_{2p}(\Theta) = \frac{\|\Theta\|_{2p}^{2p}}{\|\Theta\|_2^{2p}} = \frac{u}{v}. \tag{C.14}$$

Therefore

$$\begin{aligned} \nabla_{\Theta} u &= \nabla_{\Theta} \sum_n |\theta(n)|^{2p} = \nabla_{\Theta} \sum_n \theta^p(n)(\theta^p(n))^* = [p\theta^{p-1}(n)(\theta^p(n))^*]_{n=0}^{\infty} \\ &= p\Theta^{\odot(p-1,p)} & \text{(C.15)} \end{aligned}$$

and

$$\begin{aligned}
\nabla_{\Theta} v &= \nabla_{\Theta}(\sum_n |\theta(n)|^2)^p = p(\sum_n |\theta(n)|^2)^{p-1}\Theta^* \\
&= p\|\Theta\|_2^{2(p-1)}\Theta^* \qquad (C.16)
\end{aligned}$$

From (C.14) to (C.16), we have

$$\begin{aligned}
\nabla_{\Theta}\mathbf{F}_{2p}(\Theta) &= \frac{v \cdot \nabla_{\Theta} u - u \cdot \nabla_{\Theta} v}{v^2} \\
&= \frac{p \cdot \Theta^{\odot(p-1,p)} \cdot \|\Theta\|_2^{2p} - p\|\Theta\|_2^{2(p-1)}\Theta^* \cdot \|\Theta\|_{2p}^{2p}}{(\|\Theta\|_2^{2p})^2}. \qquad (C.17)
\end{aligned}$$

For (C.12), $\|\Theta^{(n)}\|_2 = 1$, then we have

$$\begin{aligned}
\Theta' &= (\Theta^{(n)})^* + \frac{1}{p \cdot \mathbf{F}_{2p}(\Theta^{(n)})} \cdot \mathcal{P}_{CA} \cdot \nabla_{\Theta}\mathbf{F}_{2p}(\Theta^{(n)}) \\
&= (\Theta^{(n)})^* + \frac{1}{p\|\Theta^{(n)}\|_{2p}^{2p}} \cdot \mathcal{P}_{CA} \cdot p\left[\frac{\Theta^{(n)\odot(p-1,p)} - \Theta^{(n)*}\|\Theta^{(n)}\|_{2p}^{2p}}{(\|\Theta^{(n)}\|_2^{2p})^2}\right] \\
&= \Theta^{(n)*} - \mathcal{P}_{CA} \cdot \Theta^{(n)*} + \frac{\mathcal{P}_{CA} \cdot \Theta^{(n)\odot(p-1,p)}}{\|\Theta^{(n)}\|_{2p}^{2p}} \qquad (C.18)
\end{aligned}$$

If $\Theta^{(0)} \in \mathcal{S}_{CA}$, then $\Theta^{(k)} \in \mathcal{S}_{CA} \Rightarrow \mathcal{P}_{CA}\Theta^{(k)} = \Theta^{(k)}$. Thus from (C.18), we get

$$\Theta' = \frac{\mathcal{P}_{CA} \cdot \Theta^{(n)\odot(p-1,p)}}{\|\Theta^{(n)}\|_{2p}^{2p}} \qquad (C.19)$$

Notice that $\|\Theta^{(n)}\|_{2p}^{2p}$ is a scalar, so (C.12) (C.13) are equivalent to (C.7) (C.8) after we add the normalization step.

□ *End of proof*

Define $\alpha_n \triangleq \|\mathcal{P}_{CA}\Theta^{(n)\odot(p-1,p)}\|_2$, and $\lambda_n \triangleq \mathbf{F}_{2p}(\Theta^{(n)})$. From (C.12) (C.13) and (C.19), we have

$$\alpha_n\Theta^{*(n+1)} = \lambda_n\Theta^{*(n)} + \mathbf{x}^{*(n)}, \qquad (C.20)$$

where

$$\mathbf{x}^{*(n)} = \frac{1}{p}\mathcal{P}_{CA}\nabla\mathbf{F}_{2p}(\Theta^{(n)}). \tag{C.21}$$

or equivalently:

$$\begin{aligned} \alpha_n\Theta^{(n+1)} &= \lambda_n\Theta^{(n)} + \mathbf{x}^{(n)} && \text{(C.22)} \\ \Longrightarrow \Theta^{(n+1)} &= \frac{\lambda_n}{\alpha_n}\Theta^{(n)} + \frac{1}{\alpha_n}\mathbf{x}^{(n)} \\ &= \Theta^{(n)} + \tilde{\mathbf{x}}^{(n)} && \text{(C.23)} \end{aligned}$$

where

$$\tilde{\mathbf{x}}^{(n)} = \frac{1}{\alpha_n}\mathbf{x}^{(n)} + \frac{\lambda_n - \alpha_n}{\alpha_n}\Theta^{(n)}. \tag{C.24}$$

Proposition C.2 *With $\{\alpha_n\}_{n\geq 0}$, $\{\lambda_n\}_{n\geq 0}$ defined as above, we have*

$$0 < \lambda_n < \alpha_n < \lambda_{n+1} < 1 \tag{C.25}$$

$$\textit{and } \lambda_{n+1} - \lambda_n > p(\alpha_n - \lambda_n). \tag{C.26}$$

Proof:

(a) *orthogonal property*: $\langle\Theta^*, \nabla\mathbf{F}_{2p}(\Theta)\rangle = 0$ for any $\|\Theta\|_2 = 1$.
For $\|\Theta\|_2 = 1$, from (C.17), we have

$$\begin{aligned} \langle\Theta^*, \nabla\mathbf{F}_{2p}(\Theta)\rangle &= p\langle\Theta^*, \Theta^{\odot(p-1,p)}\rangle - p\mathbf{F}_{2p}(\Theta)\langle\Theta^*, \Theta^*\rangle \\ &= p\|\Theta\|_{2p}^{2p} - p\mathbf{F}_{2p}(\Theta) = 0 && \text{(C.27)} \\ &\quad (\text{Here } \langle\mathbf{x}, \mathbf{y}\rangle \triangleq \sum_n \mathbf{x}(n)\mathbf{y}^*(n).) \end{aligned}$$

(b) $\langle\Theta^{*(n)}, \mathbf{x}^{*(n)}\rangle = 0$
Since $\mathcal{P}_{CA} = \mathcal{P}_{CA}^H$, $\langle\mathbf{x}, \mathcal{P}_{CA}\mathbf{y}\rangle = \langle\mathcal{P}_{CA}\mathbf{x}, \mathbf{y}\rangle$. Thus, from (C.21)

$$\langle\Theta^{*(n)}, \mathbf{x}^{*(n)}\rangle = \frac{1}{p}\langle\mathcal{P}_{CA}\Theta^{*(n)}, \nabla\mathbf{F}_{2p}(\Theta^{(n)})\rangle = 0 \tag{C.28}$$

(c) From (a) and (b), it follows from (C.22) that

$$\begin{aligned}
&& \alpha_n^2\|\Theta^{(n+1)}\|_2^2 = \lambda_n^2\|\Theta^{(n)}\|_2^2 + \|\mathbf{x}^{(n)}\|_2^2. & \\
&& \texttt{(Note that } \|\Theta^{(k+1)}\|_2 = \|\Theta^{(n)}\|_2 = 1\texttt{)} & \\
\Longrightarrow && \alpha_n^2 = \lambda_n^2 + \|\mathbf{x}^{(n)}\|_2^2 & \\
\Longrightarrow && \alpha_n \geq \lambda_n,\ \forall n. & \qquad (C.29)
\end{aligned}$$

$\alpha_n = \lambda_n$ if and only if $\mathbf{x}^{(n)} = 0$, i.e. $\Theta^{(n)}$ is a stationary point.

(d) Since function $\|\cdot\|_{2p}^{2p}$ is convex, we have

$$\begin{aligned}
&& \|\Theta^{(n+1)}\|_{2p}^{2p} - \|\Theta^{(n)}\|_{2p}^{2p} \ \geq \ |\langle\nabla\|\Theta^{(n)}\|_{2p}^{2p},\ \tilde{\mathbf{x}}^{(n)}\rangle| & \qquad (C.30) \\
\Longleftrightarrow && \|\Theta^{(n+1)}\|_{2p}^{2p} \ \geq \ \|\Theta^{(n)}\|_{2p}^{2p} + |\langle\nabla\|\Theta^{(n)}\|_{2p}^{2p},\ \tilde{\mathbf{x}}^{*(n)}\rangle| & \\
\Longleftrightarrow && \lambda_{n+1} \ \geq \ \lambda_n + |\langle p\Theta^{(n)\odot(p-1,p)},\ \tfrac{1}{\alpha_n}\mathcal{P}_{CA}(\Theta^{(n)\odot(p-1,p)} - \lambda_n\Theta^{*(n)})\rangle & \\
&& +\langle p\Theta^{(n)\odot(p-1,p)},\ \tfrac{\lambda_n-\alpha_n}{\alpha_n}\Theta^{*(n)}\rangle| & \\
\Longleftrightarrow && \lambda_{n+1} \geq \lambda_n + |p\alpha_n + p\lambda_k(\tfrac{\lambda_n}{\alpha_n} - 1) - p\tfrac{\lambda_n^2}{\alpha_k}| & \\
\Longleftrightarrow && \lambda_{n+1} \geq \lambda_n + |p(\alpha_n - \lambda_n)| = \lambda_n + p(\alpha_n - \lambda_n)\ \texttt{(Since } \alpha_n \geq \lambda_n\texttt{)} & \\
\Longleftrightarrow && \lambda_{n+1} \geq \alpha_n - (p-1)\lambda_n + (p-1)\alpha_n & \\
\Longleftrightarrow && \lambda_{n+1} \geq \alpha_n + (p-1)(\alpha_n - \lambda_n) & \\
\Longrightarrow && \lambda_{n+1} \geq \alpha_n & \qquad (C.31)
\end{aligned}$$

□ *End of proof*

The proof of (C.30):

From [117], we have

$$\sum_n |q(n)|^{2p} - \sum_n |\theta(n)|^{2p} \geq 2p \cdot Re\langle\Theta^{\odot(p-1,p)}, (\mathbf{q} - \Theta)^*\rangle \qquad (C.32)$$

i.e.

$$\|\mathbf{q}\|_{2p}^{2p} - \|\Theta\|_{2p}^{2p} \geq 2p \cdot Re\langle\Theta^{\odot(p-1,p)}, (\mathbf{q} - \Theta)^*\rangle \qquad (C.33)$$

for any two vectors $\mathbf{q}, \Theta \in l_2$, with restrict inequality whenever $\mathbf{q} \neq \Theta$. Apply this to $\Theta^{(n+1)}$ and $\Theta^{(n)}$, we obtain

$$\|\Theta^{(n+1)}\|_{2p}^{2p} - \|\Theta^{(n)}\|_{2p}^{2p} \;\geq\; 2p \cdot Re\langle \Theta^{(n)\odot(p-1,p)}, (\Theta^{(n+1)} - \Theta^{(n)})^*\rangle \tag{C.34}$$

Note that

- $\nabla\|\Theta^{(n)}\|_{2p}^{2p} = p \cdot \Theta^{(n)\odot(p-1,p)}$
- $\langle \nabla\|\Theta^{(n)}\|_{2p}^{2p},\ \tilde{\mathbf{x}}^{(n)}\rangle \geq 0$, `is real`

Thus, we have

$$\|\Theta^{(n+1)}\|_{2p}^{2p} - \|\Theta^{(n)}\|_{2p}^{2p} \;\geq\; |\langle \nabla\|\Theta^{(n)}\|_{2p}^{2p},\ \tilde{\mathbf{x}}^{(n)}\rangle| \tag{C.35}$$

Proposition C.3 *Assume $\{\Theta^{(n)}\}_{n=0}^{\infty}$ is defined as (C.7)(C.8) or (C.10)(C.11), then $\{\Theta^{(n)}\}_{n=0}^{\infty}$ converges.*

Proof:

Since $0 < \lambda_n < \alpha_n < \lambda_{n+1} < 1$,

$$\lim_{n\to\infty} \lambda_n = \lim_{n\to\infty} \alpha_n = C_0 > 0 \tag{C.36}$$

for some constant C_0. From (C.23) and (C.28),

$$\begin{aligned}
& \lim_{n\to\infty} \langle \Theta^{(n+1)}, \Theta^{(n)}\rangle = \lim_{n\to\infty} \frac{\lambda_n}{\alpha_n} \langle \Theta^{(n)}, \Theta^{(n)}\rangle = 1 \\
\Longrightarrow\ & \lim_{n\to\infty} \|\Theta^{(n+1)} - \Theta^{(n)}\|_2^2 \\
& = \lim_{n\to\infty} \langle \Theta^{(n+1)} - \Theta(n),\ \Theta^{(n+1)} - \Theta(n)\rangle \\
& = \lim_{n\to\infty} [\|\Theta^{(n+1)}\|_2^2 + \|\Theta^{(n)}\|_2^2 - \langle \Theta^{(n)}, \Theta^{(n+1)}\rangle - \langle \Theta^{(n+1)}, \Theta^{(n)}\rangle] \\
& = 0 \\
\Longrightarrow\ & \{\Theta(n)\}_{n=0}^{\infty} \texttt{ converges}
\end{aligned} \tag{C.37}$$

□ *End of proof*

BIBLIOGRAPHY

BIBLIOGRAPHY

[1] T. S. Rappaport, *Wireless Communications: Principles and Practice*, Prentice-Hall, 1996.

[2] Tero Ojanperä and Ramjee Prásad, Eds., *WCDMA: Towards IP Mobility and Mobile Internet*, Artech House, 2000.

[3] Harri Holma and Antti Toskala, Eds., *WCDMA for UMTS*, John Wiley & Sons, Ltd, England, 2nd edition, 2002.

[4] L. Tong and S. Perreau, "Multichannel blind identification: From subspace to maximum likelihood methods," in *Proceedings Of The IEEE*, Oct. 1998, vol. 86, pp. 1951–1968.

[5] L. Tong, G. Xu, and T. Kailath, "Blind identification and equalization based on second-order statistics: A time domain approach," *IEEE Transactions on Information Theory*, vol. 40, pp. 340–349, Mar. 1994.

[6] L. Tong, G. Xu, B. Hassibi, and T. Kailath, "Blind identification and equalization based on second-order statistics: A frequency domain approach," *IEEE Transactions on Information Theory*, vol. 41, pp. 329–334, Jan. 1995.

[7] E. Serpedin and G. B. Giannakis, "Blind channel identification and equalization with modulation-induced cyclostationarity," *IEEE Transactions on Signal Processing*, vol. 46, pp. 1930–1944, July 1998.

[8] S.D. Halford and G.B. Giannakis, "Direct blind equalization for transmitter induced cyclostationarity," in *1997 First IEEE Signal Processing Workshop on Signal Processing Advances in Wireless Communications*, Paris, April 1997, pp. 117–120.

[9] Hui Liu, Guanghan Xu, Lang Tong, and Thomas Kailath, "Recent developments in blind channel equalization: from cyclostationarity to subspaces," *Signal Processing*, vol. 50(1-2), pp. 83–99, Apr. 1996.

[10] J. K. Tugnait and Bin Huang, "On direct blind equalization of simo iir channels with common zeros using second-order statistics," in *Proc. IEEE Asilomar Conf. on Signals, Systems, and Computers*, Nov. 1997, vol. 2, pp. 1614–1618.

[11] G. B. Giannakis and S. D. Halford, "Blind fractionally spaced equalization of noisy FIR channels: direct and adaptive solutions," *IEEE Transactions on Signal Processing*, vol. 45, pp. 2277–2292, Sept. 1997.

[12] C.B. Papadias and A. D. Gesbert, ; Paulraj, "Direct second-order blind equalization of polyphase channels based on a decorrelation criterion," in *Proc. IEEE ICASSP 1999*, Mar. 1999, vol. 5, pp. 2503–2506.

[13] Xiaohua Li and H. Fan, "Direct estimation of blind zero-forcing equalizers based on second-order statistics," *IEEE Transactions on Signal Processing*, vol. 48, pp. 2211–2218, Aug. 2000.

[14] E. Moulines, P. Duhamel, J. F. Cardoso, and S. Mayrargue, "Subspace methods for the blind identification of multichannel FIR filters," *IEEE Transactions on Signal Processing*, vol. 43, pp. 516–525, Feb. 1995.

[15] K. Abed-Meraim, J. Cardoso, A. Y. Gorokhov, P. Loubaton, and E. Moulines, "On subspace methods for blind identification of single-input multiple-output fir systems," *IEEE Transactions on Signal Processing*, vol. 45, no. 1, pp. 42–55, Jan. 1997.

[16] G. B. Giannakis and S. D. Halford, "Asymptotically optimal blind fractionally spaced channel estimation and performance analysis," *IEEE Transactions on Signal Processing*, vol. 45, no. 7, pp. 1815–1830, July 1997.

[17] L. Tong and H. Zeng, "Blind channel identification using cyclic spectra," in *Proc. 26th Conf. Information Sciences and Systems*, Princeton, NJ, Mar 1994, pp. 711–716.

[18] H. Zeng and L. Tong, "Blind channel estimation using the second-order statistics: Algorithms," *IEEE Transactions on Signal Processing*, vol. 45, pp. 1919–1930, Aug. 1997.

[19] D. Gesbert and P. Duhamel, "Robust blind channel identification and equalization based on multi-step predictors," in *Proc. IEEE ICASSP 1997*, Apr. 1997, vol. 5, pp. 3621–3624.

[20] J. K. Tugnait, "Multistep linear predictors-based blind equalization of FIR/IIR single-input multiple-output channels with common zeros," *IEEE Transactions on Signal Processing*, vol. 47, pp. 1689–1700, Jun. 1999.

[21] C. L. Nikias and J. M. Mendel, "Signal processing with higher-order sprectra," *IEEE Signal Processing Magazine*, vol. 10, pp. 10–37, July 1993.

[22] D. Donoho, "On minimum entropy deconvolution," in *Applied Time Series Analysis, II*, D. F. Findley, Ed. New York: Academic, 1981.

[23] R. A. Wiggins, "Minimum entropy deconvolution," *Geoexploration*, vol. 16, pp. 21–35, Mar. 1978.

[24] O. Shalvi and E. Weinstein, "New criteria for blind deconvolution of nonminimum phase systems (channels)," *IEEE Transactions on Information Theory*, vol. 36, no. 2, pp. 312–321, Mar. 1990.

[25] J. K. Tugnait, "Identification and deconvolution of multichannel linear nongaussian processes using higher order statistics and inverse filter criteria," *IEEE Transactions on Signal Processing*, vol. 45, no. 3, pp. 658–872, Mar. 1997.

[26] Chong-Yung Chi, Ching-Yung Chen, Chil-Horng Chen, and Chih-Chun Feng, "Batch processing algorithms for blind equalization using higher-order statistics," *IEEE Signal Processing Magazine*, vol. 20, pp. 25–49, Jan. 2003.

[27] D. Godard, "Self recovering equalization and carrier tracking in two-dimensional data communication systems," *IEEE Transactions on Communications*, vol. 28, pp. 1867–1875, Nov. 1980.

[28] C. R. Johnson, P. Schniter, T. J. Endres, J. D. Behm, D. R. Brown, and R. A. Casas, "Blind equalization using the constant modulus criterion: a review," in *Proceedings of the IEEE*, Oct. 1998, vol. 86, pp. 1927–1950.

[29] O. Shalvi and E. Weinstein, "Super-exponential methods for blind deconvoluation," *IEEE Transactions on Information Theory*, vol. 39, pp. 504–519, Mar. 1993.

[30] Y. Inouye and K. Tanebe, "Super-exponential algorithms for multichannel blind deconvolution," *IEEE Transactions on Signal Processing*, vol. 48, pp. 881 – 888, Mar. 2000.

[31] Mamadou Mboup and Phillip A. Regalia, "A gradient search interpretation of the super-exponential algorithm," *IEEE Transactions on Information Theory*, vol. 46, no. 7, pp. 2731–2734, November 2000.

[32] Ming Gu and Lang Tong, "Geometrical characterizations of constant modulus receivers," *IEEE Transactions on Signal Processing*, vol. 47, pp. 2745–2756, Oct. 1999.

[33] Mamadou Mboup and Phillip A. Regalia, "On the equivalence between the super-exponential algorithm and a gradient search method," in *Proc. IEEE ICASSP 1999*, March 2000, vol. 5. pp. 2643–2646.

[34] Phillip A. Regalia, "On the equivalence between the godard and shalvi-weinstein schemes of blind equalization," *Signal Processing (Elsevier)*, vol. 73, pp. 185–190, Feb. 1999.

[35] Sergio Verdú, *Multiuser Detection*, Cambridge University Press, Aug. 1998.

[36] M. Honig, U. Madhow, and S. Verdù, "Blind Adaptive Multiuser Detection," *IEEE Transactions on Information Theory*, vol. 41, July 1995.

[37] M.K. Tsatsanis, "Inverse Filtering Criteria for CDMA Systems," *IEEE Transactions on Signal Processing*, vol. 45, no. 1, pp. 102–112, Jan. 1997.

[38] M. K. Tsatsanis and Zhengyuan Xu, "Performance analysis of minimum variance cdma receivers," *IEEE Transactions on Signal Processing*, vol. 46, pp. 3014–3022, Nov. 1998.

[39] E. G. Strom, S. Parkvall, S. L. Miller, and B. E. Ottersten, "Propagation delay estimation in asynchronous direct-sequence code-division multiple access systems," *IEEE Transactions on Communications*.

[40] S. E. Bensley and B. Aazhang, "Subspace-based channel estimation for code division multiple access communication systems," *IEEE Transactions on Communications*.

[41] M. Torlak and G. Xu, "Blind multiuser channel estimation in asynchronous CDMA systems," *IEEE Transactions on Signal Processing*, vol. 45, pp. 137–147, Jan. 1997.

[42] Xiaodong Wang and H. V. Poor, "Blind equalization and multiuser detection in dispersive CDMA channels," *IEEE Transactions on Communications*, vol. 46, pp. 91–103, Jan. 1998.

[43] Yu Song and S. Roy, "Subspace blind detection of asynchronous CDMA signals in multipath channels," in *1999 2nd IEEE Workshop on Signal Processing Advances in Wireless Communications*, Annapolis, MD, May 1999, pp. 21–24.

[44] Xiaodong Wang and H. Vincent Poor, "Blind Multiuser Detection: A Subspace Approach," *IEEE Transactions on Information Theory*, vol. 44, no. 2, pp. 677–690, Mar. 1998.

[45] D. Gesbert, J. Sorelius, and A. Paulraj, "Blind multi-user MMSE detection of CDMA signals," in *Proc. IEEE ICASSP 1998*, May 1998, vol. 6, pp. 3161–3164.

[46] H. Yan and S. Roy, "Blind channel identification for multirate CDMA systems," in *Proc. IEEE ICASSP 2000*, June 2000, vol. 5, pp. 2509–2512.

[47] Zhengyuan Xu, "Asymptotically near-optimal blind estimation of multipath CDMA channels," *IEEE Transactions on Signal Processing*, vol. 49, pp. 2003–2017, Sept. 2001.

[48] Ping Liu and Zhengyuan Xu, "Correlation matching in channel estimation for multirate DS/CDMA," in *Proc. IEEE ICASSP 2002*, May 2002, vol. 3, pp. 2581–2584.

[49] J. K. Tugnait and Tong tong Li, "A multistep linear prediction approach to blind asynchronous CDMA channel estimation and equalization," *IEEE Journal on Selected Areas in Communications*, vol. 19, no. 6, pp. 1090–1102, JUNE 2001.

[50] J. K. Tugnait and Tong tong Li, "Blind detection of asynchronous CDMA signals in multipath channels using code-constrained inverse filter criterion," *IEEE Transactions on Signal Processing*, vol. 49, pp. 1300–1309, July 2001.

[51] Chong-Yung Chi and Chii-Horng Chen, "Cumulant-based inverse filter criteria for MIMO blind deconvolution: properties, algorithms, and application to DS/CDMA systems in multipath," *IEEE Transactions on Signal Processing*, vol. 49, pp. 1282–1299, July 2001.

[52] Chong-Yung Chi, Chi-Horng Chen, and Ching-Yung Chen, "Blind MAI and ISI suppression for DS/CDMA systems using HOS-based inverse filter criteria," *IEEE Transactions on Signal Processing*, vol. 50, pp. 1368–1381, June 2002.

[53] J. K. Tugnait and Tongtong Li, "Blind asynchronous multiuser CDMA receivers for ISI channels using code-aided CMA," *IEEE Journal on Selected Areas in Communications*, vol. 19, pp. 1520–1530, Aug. 2001.

[54] P. Arasaratnam, S. Zhu, and A. G. Constantinides, "Stochastic conjugate gradient based multi-user constant modulus algorithm for use in multiuser DS-CDMA environment," in *Proc IEEE GLOBECOM 2002*, Nov. 2002, vol. 1, pp. 458–462.

[55] Ping He, T. T. Tjhung, and L. K. Rasmussen, "Constant modulus algorithm (CMA) for CDMA communications systems," in *Proc. IEEE 48th Veh. Technol. Conf.*, May. 1998, vol. 2, pp. 949–953.

[56] J. Miguez and L. Castedo, "A linearly constrained constant modulus approach to blind adaptive multiuser interference suppression," *IEEE Communications Letters*, vol. 2, pp. 217–219, Aug. 1998.

[57] Tongtong Li and J. K. Tugnait, "Further results on blind detection of asynchronous CDMA signals using code-constrained super-exponential algorithm," in *Proc. IEEE ICASSP 2002*, May 2002, vol. 3, pp. 2229–2232.

[58] Tongtong Li and J. K. Tugnait, "Super-exponential methods for blind detection of asynchronous cdma signals over multipath channels," in *Proc. IEEE ICC 2001*, June 2001, vol. 3, pp. 816–820.

[59] Tongtong Li and J. K. Tugnait, "Super-exponential methods for blind detection of asynchronous CDMA signals over multipath channels," *IEEE Transactions on Wireless Communications*, vol. 3, no. 5, pp. 1379–1385, Sept 2004.

[60] S. Bhashyam and B. Aazhang, "Multiuser channel estimation and tracking for long-code CDMA systems," *IEEE Transactions on Communications*, vol. 50, pp. 1081–1090, July 2002.

[61] Stefano Buzzi and H. Vincent Poor, "Channel estimation and multiuser detection in long-code DS/CDMA systems," *IEEE Journal On Selected Areas In Communications*, vol. 19, no. 8.

[62] S. Buzzi and H.V. Poor, "A Multipass Approach to Joint Data and Channel Estimation in Long-Code CDMA Systems," *IEEE Transactions on Wireless Communications*, vol. 3, pp. 612–626, Mar. 2004.

[63] Y. Chen, M. Zoltowski, J. Ramos, C.Chatterjee, and V. Roychowdhury, "Reduced-dimension blind space-time 2D Rake receivers for DS-CDMA communication systems," *IEEE Transactions on Signal Processing*, vol. 48, pp. 1521–1536, June 2000.

[64] C.J. Escudero, U. Mitra, and D.T.M. Slock, "A Toeplitz displacement method for blind multipath estimation for long code DS/CDMA signals," *IEEE Transactions on Signal Processing*, vol. 49, pp. 654 –665, Mar. 2001.

[65] Hui Liu and M.D. Zoltowski, "Blind equalization in antenna array CDMA systems," *IEEE Transactions on Signal Processing*, vol. 45, no. 1, pp. 161–172, Jan. 1997.

[66] Lang Tong, Alle-Jan van der Veen, Patrick Dewilde, and Youngchul Sung, "Blind decorrelating rake receivers for long-code wcdma," *IEEE Transactions on Signal Processing*, vol. 51, pp. 1642–1655, June 2003.

[67] B. Evans M. Torlak and G. Xu., "Blind estimation of FIR channels in CDMA systems with aperiodic spreading sequences," in *Proc. IEEE Asilomar Conf. on Signals, Systems, and Computers*, Oct. 1997, pp. 495–499.

[68] Z. Xu and M.K. Tsatsanis, "Blind Channel Estimation for Long Code Multiuser CDMA Systems," *IEEE Transactions on Signal Processing*, vol. 48, no. 4, pp. 988–1001, Apr. 2000.

[69] Z. Xu, "Low-complexity multiuser channel estimation with aperiodic spreading codes," *IEEE Transactions on Signal Processing*, vol. 49, pp. 2813–2822, Nov. 2001.

[70] Zigang Yang and Xiaodong Wang, "Blind multiuser detection for long-code multipath CDMA," in *Proc. IEEE Asilomar Conf. on Signals, Systems, and Computers*, 2000, vol. 2, pp. 1148–1152.

[71] A.J. Weiss and B. Friedlander, "Channel estimation for DS-CDMA downlink with aperiodic spreading codes," *IEEE Transactions on Communications*, vol. 47, pp. 1561–1569, Oct. 1999.

[72] Y. Sung and L. Tong, "Tracking of Fast-Fading Channels in Long-Code CDMA," *IEEE Transactions on Signal Processing*, vol. 52, no. 3, pp. 786–795, Mar. 2004.

[73] C. D. Frank, E. Visotsky, and U. Madhow, "Adaptive interference suppression for the downlink of a direct sequence cdma system with long spreading sequences," *Journal of VLSL Signal Processing.*

[74] T. P. Krauss, W. J. Hillery, and M. D. Zoltowski., "Downlink specific linear equalization for frequency selective cdma cellular systems," *Journal of VLSI Signal Processing Systems*, vol. 30, pp. 143–161, 2002.

[75] Tongtong Li, J. K. Tugnait, and Zhi Ding, "Channel estimation of long-code CDMA systems utilizing transmission induced cyclostationarity," in *Proc. IEEE ICASSP 2003*, April 6-10 2003, vol. 4, pp. 105–108.

[76] D. Gesbert, M. Shafi, D. Shiu, P. J. Smith, and A. Naguib, "From Theory to Practice: An Overview of MIMO Space-Time Coded Wireless Systems," *IEEE Journal on Selected Areas in Communications*, vol. 21, no. 3, pp. 281–302, Apr. 2003.

[77] Vahid Tarokh, Nambi Seshadri, and A. R. Calderbank, "Space-Time Codes for High Data Rate Wireless Communication: Performance Criterion and Code Construction," *IEEE Transactions on Information Theory*, vol. 44, no. 2, pp. 744–765, Mar. 1998.

[78] S. M. Alamouti, "A simple transmit diversity technique for wireless communications," *IEEE Journal on Selected Areas in Communications*, vol. 16, no. 8, pp. 1451–1458, Oct. 1998.

[79] Vahid Tarokh, Hamid Jafarkhani, and A. R. Calderbank, "Space-Time Block Codes from Orthogonal Designs," *IEEE Transactions on Information Theory*, vol. 45, no. 5, pp. 1456–1467, 1999.

[80] W.-J. Choi and J. M. Cioffi, "Space-time block codes over frequency selective Rayleigh fading channels," in *Proc. IEEE Veh. Technol. Conf.*, Nov. 1999, pp. 2541–2545.

[81] E. Lindskog and A. Paulraj, "A transmit diversity scheme for channels with intersymbol interference," in *Proc. IEEE ICC 2000*, June 2000, vol. 1, pp. 307–311.

[82] E.G. Larsson, P. Stoica, E. Lindskog, and Jian Li;, "Space-time block coding for frequency-selective channels," in *Proc. IEEE ICASSP 2002*, May 2002, vol. 3, pp. 2405–2408.

[83] S. Zhou and G. B. Giannakis, "Single-Carrier Space-Time Block-Coded Transmissions Over Frequency-Selective Fading Channels," *IEEE Transactions on Information Theory*, vol. 49, no. 1, pp. 164–179, Jan. 2003.

[84] G. Leus, F. Petré, and M. Moonen, "Space-Time Chip Equalization for Maximum Diversity Space-Time Block Coded DS-CDMA Downlink Transmission," *EURASIP Journal on Applied Signal Processing*, vol. 2004, no. 5, pp. 740–750, May 2004.

[85] F. Petré, G. Leus, L. Deneire, M. Engels, M. Moonen, and H. D. Man, "Space-Time Block Coding for Single-Carrier Block Transmission DS-CDMA Downlink," *IEEE Journal on Selected Areas in Communications*, vol. 21, no. 3, pp. 350–361, Apr. 2003.

[86] J. Ma and J.K. Tugnait, "Blind Multiuser Receiver for Space-Time Coded CDMA Signals in Frequency-Selective Channels," in *Proc. IEEE Asilomar Conf. on Signals, Systems, and Computers*, Nov. 3-6, 2002, vol. 2, pp. 1647–1652.

[87] D. Reynolds, X. Wang, and H. V. Poor, "Blind Adaptive Space-Time Multiuser Detection With Multiple Transmitter and Receiver Antennas," *IEEE Transactions on Signal Processing*, vol. 50, no. 6, pp. 1261–1276, June 2002.

[88] Y. Sung and L. Tong, "Semiblind channel estimation for space-time coded wcdma," in *Proc. IEEE ICC 2003*, May 2003, vol. 5, pp. 3297–3301.

[89] Weiguo Liang and Tongtong Li, "Blind detection of multirate asynchronous CDMA signals using super-exponential methods," in *ICSP'04*, Beijing, China, Aug. 2004.

[90] Tongtong Li, Weiguo Liang, Zhi Ding, and Jitendra K. Tugnait, "Blind multiuser detection for long code cdma systems with transmission induced cyclostationarity," *accepted to EURASIP Journal on Wireless Communications and Networking.*

[91] Weiguo Liang and Tongtong Li, "Blind multiuser detection for uplink CDMA systems with aperiodic spreading codes," in *Proceeding of CISS 2004*, University of Princeton, Princeton, NJ, Mar. 2004.

[92] O. Shalvi and E. Weinstein, *Blind Deconvolution*, chapter Universal methods for blind deconvolution, pp. 121–180, Prentice Hall, Englewood Cliffs, NJ, 1994.

[93] Yujiro Inouye and Kazuaki Tanebe, "Super-exponential algorithms for multichannel blind deconvolution," *IEEE Transactions on Signal Processing*, vol. 48, no. 3, pp. 881–888, March 2000.

[94] Y. Li and Z. Ding, "Global convergence of fractionally spaced godard (CMA) adaptive equalizers," *IEEE Transactions on Signal Processing*, vol. 44, pp. 818–826, Apr. 1996.

[95] H. H. Zeng, L. Tong, and Jr. C. R. Johnson, "Relationships between the constant modulus and wiener receivers," *IEEE Transactions on Information Theory*, vol. 44, pp. 1523–1538, July 1998.

[96] P. E. Caines, *Linear Stochastic Systems*, Wiley Series in Probability and Mathematical Statistics. John Wiley & Sons, New York, 1988.

[97] J. Ma and J. K. Tugnait, "Blind detection of multirate asynchronous CDMA signals in multipath channels," *IEEE Transactions on Signal Processing*, vol. 50, pp. 2258–2272, Sept. 2002.

[98] P. Liu and Z. Xu, "A globally convergent cma-based approach to blind multiuser detection," in *Proc. IEEE Asilomar Conf. on Signals, Systems, and Computers*, Nov 2002, vol. 2, pp. 634–638.

[99] I. Ghauri and D. T. M. Slock, "Linear receivers for the DS-CDMA downlink exploiting orthogonality of spreading sequences," in *Proc. IEEE Asilomar Conf. on Signals, Systems, and Computers*, Nov. 1998, vol. 1, pp. 650–654.

[100] Kemin Li and Hui Liu, "A new blind receiver for downlink DS-CDMA communications," *IEEE Communications Letters*, vol. 3, no. 7, pp. 193–195, July 1999.

[101] K. Hooli, M. Latva-aho, and M. Juntti, "Multiple access interference suppression with linear chip equalizers in wcdma downlink receivers," in *Global Telecommunications Conference 1999*, Dec. 1999, vol. 1a, pp. 467–471.

[102] S. Mudulodu and A. Paulraj, "A blind multiuser receiver for the CDMA downlink," in *Proc. IEEE ICASSP 2000*, June 2000, vol. 5, pp. 2933–2936.

[103] T. P. Krauss, M. D. Zoltowski, and G. Leus, "Simple MMSE equalizers for CDMA downlink to restore chip sequence: comparison to zero-forcing and RAKE," in *Proc. IEEE ICASSP 2000*, June 2000, vol. 5, pp. 2865–2868.

[104] J. K. Tugnait and Bin Huang, "Multistep linear predictors-based blind identification and equalization of multiple-input multiple-output channels," *IEEE Transactions on Signal Processing*, vol. 48, pp. 26–38, Jan. 2000.

[105] Gene H. Golub and Charles F. Van Loan, *Matrix Computations*, chapter 5. Orthogonalization and Least Squares, pp. 256–258, The Johns Hopkins University Press, Baltimore, Maryland, third edition, 1996.

[106] Simon Haykin, *Adaptive Filter Theory*, Prentice Hall, Inc, Upper Saddle River, New Jersey 07458, 3rd edition, 1996.

[107] D. Slock, "Blind joint equalization of multiple synchronous mobile users using oversampling and/or multiple antennas," in *Proc. IEEE Asilomar Conf. on Signals, Systems, and Computers*, Oct. 1994, vol. 3, pp. 1154–1158.

[108] N. Delfosse and P. Loubaton, "Adaptive blind separation of convolution mixtures," in *Proc. IEEE ICASSP 1996*, Atlanta, GA, May 1996, vol. 5, pp. 2940–2943.

[109] Z. Ding, "Matrix outer-product decomposition method for blind multiple channel identification," *IEEE Transactions on Signal Processing*, vol. 45, pp. 3053–3061, Dec. 1997.

[110] P. Loubaton A. Gorokhov and E. Moulines, "Second-order blind equalization in multiple input multiple output FIR systems: A weighted least square approach," in *Proc. IEEE ICASSP 1996*, May 1996, vol. 5, pp. 2415–2418.

[111] Chunqi Chang, Zhi Ding, Sze Fong Yau, and F.H.Y. Chan, "A matrix-pencil approach to blind separation of colored nonstationary signals," *IEEE Transactions on Signal Processing*, vol. 48, pp. 900–907, March 2000.

[112] Jing Liang and Zhi Ding, "Nonminimum-phase FIR channel estimation using cumulant matrix pencils," *IEEE Transactions on Signal Processing*, vol. 51, pp. 2310–2320, Sept 2003.

[113] Tongtong Li, Zhi Ding, J. K. Tugnait, and Weiguo Liang, "Channel identification and signal separation for long-code CDMA systems using multistep linear prediction method," in *Proc. IEEE ICC 2004*, June 2004.

[114] J.F. Cardoso and A. Souloumiac, "Blind beamforming for non-gaussian signals," in *IEE Proceedings-F*, Dec. 1993, vol. 140, pp. 362–370.

[115] Erik G. Larsson and Petre Stoica, *Space-Time Block Coding for Wireless Communications*, Cambridge University Press, Cambridge, UK, 2003.

[116] B. Hochwald, T. L. Marzetta, and C. B. Papadias, "A Transmitter Diversity Scheme for Wideband CDMA Systems Based on Space-Time Spreading," *IEEE Journal on Selected Areas in Communications*, vol. 19, no. 1, pp. 48–60, Jan. 2001.

[117] Phillip A. Regalia and Mamadou Mboup, "Undermodeled equalization: A characterization of stationary points for a family of blind criteria," *IEEE Transactions on Signal Processing*, vol. 47, no. 3, pp. 760–770, March 1999.